NATIONAL TECHNICAL UNIVERSITY OF ATHENS

SCHOOL OF ELECTRICAL AND COMPUTER ENGINNERING

DEPARTMENT OF COMMUNICATION, ELECTRONIC AND INFORMATION ENGINEERING

Optimal Power Allocation in the uplink of Two-Tier Wireless Femtocell Networks

A DISSERTATION

by

JOHN ZOBOLAS

Supervisor: Symeon Papavassiliou, Associate Professor, NTUA

Approved by the three - member committee:

.....	.....	.....
Symeon Papavassiliou	Efstathios Sykas	Michael Theologou
Associate Professor NTUA	Professor NTUA	Professor Emeritus NTUA

Athens, May 2013

.....

JOHN ZOBOLAS

Graduate Electrical and Computer Engineer from NTUA

© 2013 - All rights reserved

It is forbidden to copy, store and distribute this work, in whole or in part, for commercial purposes. Reproduction, storage and distribution may be permitted for non-profit, educational or research purposes, provided that the source of origin is indicated and this message is retained. Questions concerning the use of work for profit should be addressed to the author. The views and conclusions contained in this document express the author and should not be interpreted as representing the official positions of the National Technical University of Athens.

Abstract

In this thesis, the problem of efficient power allocation in the uplink of two-tier closed-access femtocell networks is addressed. Specifically, a single CDMA macrocell is assumed, where *N* femtocells reside within the macrocell. Within the proposed framework, which supports multiple services, appropriate utility functions are adopted to reflect users' degree of satisfaction with respect to their actual throughput requirements and the corresponding power consumption. The overall problem is formulated as a non-cooperative game where users aim selfishly at maximizing their utility-based performance while taking into account the interference caused by both the CDMA macrocell and the neighbouring femtocells.

The existence and uniqueness of a Nash equilibrium point of the proposed Multi Service Two-Tier Power Control Game with Pricing (*MTTPG*) is proven, at which all users have achieved a targeted SINR threshold value or transmit with their maximum power, leading essentially to an SINR-balanced system. Moreover, a distributed iterative algorithm for reaching *MTTPG* game's equilibrium is provided. Finally, the operational effectiveness of the proposed approach is evaluated through modeling and simulation, while its superiority is illustrated via presenting various scenarios of the proposed framework.

Keywords: << Two-tier femtocell networks, Power allocation, utility function, real-time and non-real time services, Nash equilibrium >>

Acknowledgments

I would like to give my sincere thanks to my supervisor Professor, Mr. Symeon Papavassiliou, for trusting and believing in me. Many thanks also go to the Doctoral candidates Ms. Tsiropoulou Eirini Eleni and Mr. Katsini Giorgo for the time that they dedicated to overseeing my work (by stealing time from their own academic tasks) and for all the useful discussions we had regarding this thesis. Lastly, I would like to thank all my friends for being there for me after an exhausting day of work. This thesis is dedicated to all who improvise and want something more out of their lives!

Table of Contents

Table of Figures

1. Introduction

1.1 About Femtocells

The surest way to increase the system capacity of a wireless link is by getting the transmitter and receiver closer to each other, which creates the dual benefits of higher quality links and more spatial reuse. In a network with nomadic users, this inevitably involves deploying more infrastructure, typically in the form of microcells, hotspots, distributed antennas, or relays. A less expensive alternative is the recent concept of femtocells – also called home base-stations (HBS), home node-stations (HNB) or FAPs (Femto Access Points) – which are data access points installed by home users to get better indoor voice and data coverage (Chandrasekhar & Andrews, 2008).

The demand for higher data rates in wireless networks is unrelenting, and has triggered the design and development of new data-minded cellular standards such as WiMAX (802.16e), 3GPP's High Speed Packet Access (HSPA) and LTE standards, as well as the 3GPP2's EVDO and UMB standards. Moreover, Wi-Fi networks are nowadays the de facto standard in wireless data communications since they can provide the high transmission rates demanded by the consumers in indoor buildings for Internet services. Although the Wi-Fi networks will not be able to support the same level of mobility and coverage as the cellular standards, to be competitive for home and office use, cellular data systems will need to provide service roughly comparable to that offered by the Wi-Fi networks. Studies on wireless usage show that more than 50 percent of all voice calls and more than 70 percent of data traffic originate indoors and thus, cellular networks must meet the expectations of both kinds of user services (Chandrasekhar & Andrews, 2008).

The growth in wireless capacity is exemplified by this observation from Martin Cooper of Arraycomm: "*The wireless capacity has doubled every 30 months over the last 104 years*". This translates into an approximately million-fold capacity increase since 1957. Breaking down these gains shows a *25x* improvement from wider spectrum, a *5x* improvement by dividing the spectrum into smaller slices, a *5x* improvement by designing better modulation schemes, and a whopping *1600x* gain through reduced cell sizes and transmit distance. This reduction of the cell boundaries was done gradually, starting from the microcells (with a radius of a few hundred meters), then the relays that functioned as small base stations which provided service for places where the central macrocell could not have satisfactory cover and reaching the femtocells today (Andrews, Claussen, Dohler, Rangan, & Reed, 2012).

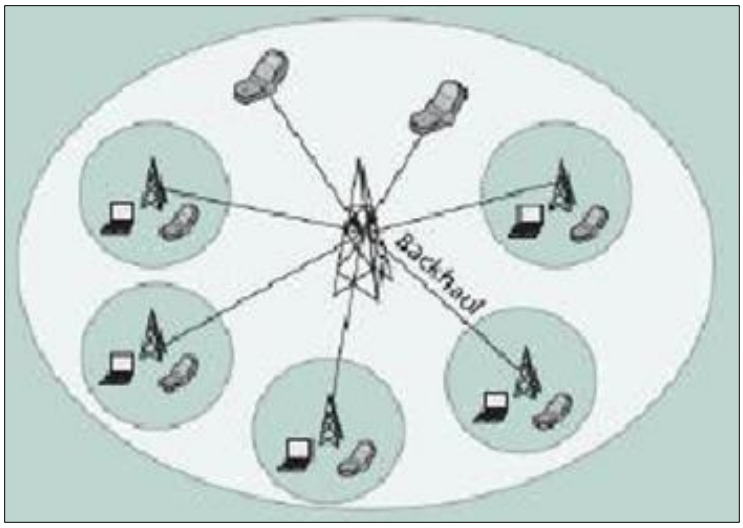

Figure 1: A macrocell deployed with 5 femtocells for better network coverage

While the femtocells can be installed easily by the home users, have a low transmission power and can cover a small-radius distance, they also allow the network provider to greatly improve the indoors coverage, especially in places such as apartments, metro stations, company offices, etc. Moreover, by assigning the indoor users to femtocells, the macrocell can distribute its resources to less users and thus improve their service quality. So, not only can femtocells contribute to the improvement of the network's indoor coverage but also to its overall throughput (see Figure 1). Regarding the communication of the femtocells with the rest of the cellular network, this can be done over an existing broadband connection such as the digital subscriber line (DSL), via the cable modem (IP backhaul) or by a separate radio frequency (RF) backhaul channel (see Figure 2).

Femtocells are compatible with cell phones, personal computers and generally every 3G-enabled device. Due to their short transmit-receive distance, femtocells can greatly lower transmit power, prolong handset battery life, and achieve a higher signal-to-interference-plus-noise ratio (SINR). All these translate into improved reception – the so-called *five-bar* coverage – and higher capacity. Because of the reduced interference, more users can be packed into a given area in the same region of spectrum, thus increasing the area spectral efficiency, or equivalently, the total number of active users per Hz per unit area. Lastly, the cost benefit of deploying femtocells is huge because it reduces the operating and capital expenditure costs for the network operators. A typical urban macrocell costs upwards of *$1000/month* in site lease, and additional costs for electricity and backhaul. In the future, the macrocell network will be stressed by the operating expenses, especially when the subscriber growth does not match the increased demand for data traffic. The deployment of femtocells will reduce the need for adding macro-BS towers. Recent studies

show that the operating expenses scale from *$60,000/year/macrocell* to just *$200/year/femtocell* (Chandrasekhar & Andrews, 2008).

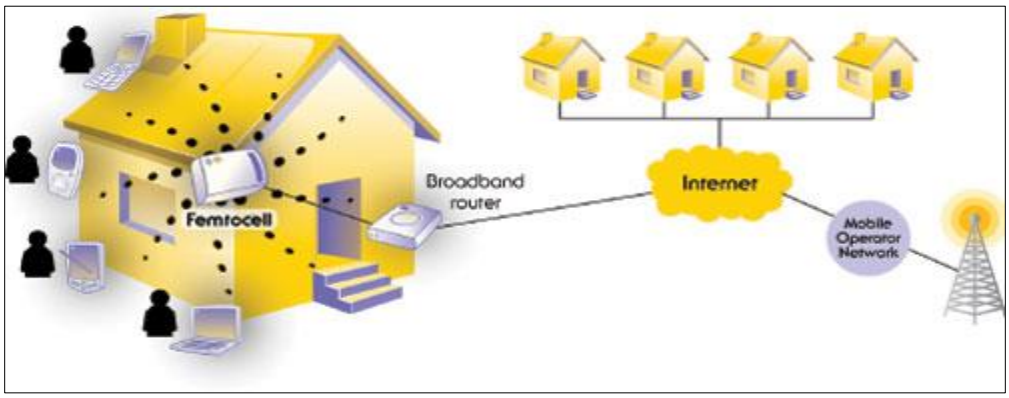

Figure 2: Communication of the FAP device with the ISP via DSL and cable broadband connections

1.2 Spectrum Assignment Policies and Interference in Femtocells

Femtocells have critical effects on the performance of mobile networks. While adding femtocells will produce huge benefits for both the operators and the users, a careful preparation should take place regarding the spectrum allocation because without unique spectrum for the femtocell or very careful spectrum planning in the network, femtocells could suffer from severe interference problems (Abdulrahman & Ahmad, 2012). In a Two-Tier Cellular Network (one that has both macrocells and femtocells deployed) there exist two types of interference:

1. **Cross-Tier interference**: This type of interference is caused between different tier users – that is between a femto-user and a macro-user.
2. **Co-Tier interference**: This type of interference is caused between users of the same kind of cell – that is between two macro-users or between neighboring femtocells.

Considering the above categorization, three different approaches – spectrum assignment policies – have been proposed to solve the issue of spectrum allocation in Two-Tier Networks (Mesodiakaki, 2011):

1. **Dedicated Spectrum**: In this case, different frequencies are assigned to femtocells and macrocell. Thus, the cross-tier interference is completely avoided, since the two tiers operate in different channels. On the other hand, this policy results in smaller spectral efficiency since the cells of a tier can only have access to a subset of the total available bandwidth.
2. **Shared Spectrum**: In this case, maximum spectrum allocation is achieved since all cells (femto and macro) share the same bandwidth and thus have access to all available network resources. However, in such an implementation, the cross-tier interference could degrade the overall performance of the system if it is not effectively addressed. There exist two sub-policies regarding the channel assignment between femtocells and macrocell when we have a shared spectrum policy:
    a. **Orthogonal assignment:** The frequency channel that a macro-user uses is orthogonal with the one assigned to a femto-user (OFDMA) and thus, while sharing the same spectrum, there is no interference between the two users.
    b. **Co-channel assignment:** Every user can be assigned any frequency channel simultaneously and the separation of the users' signals is done by code-division (simple CDMA).

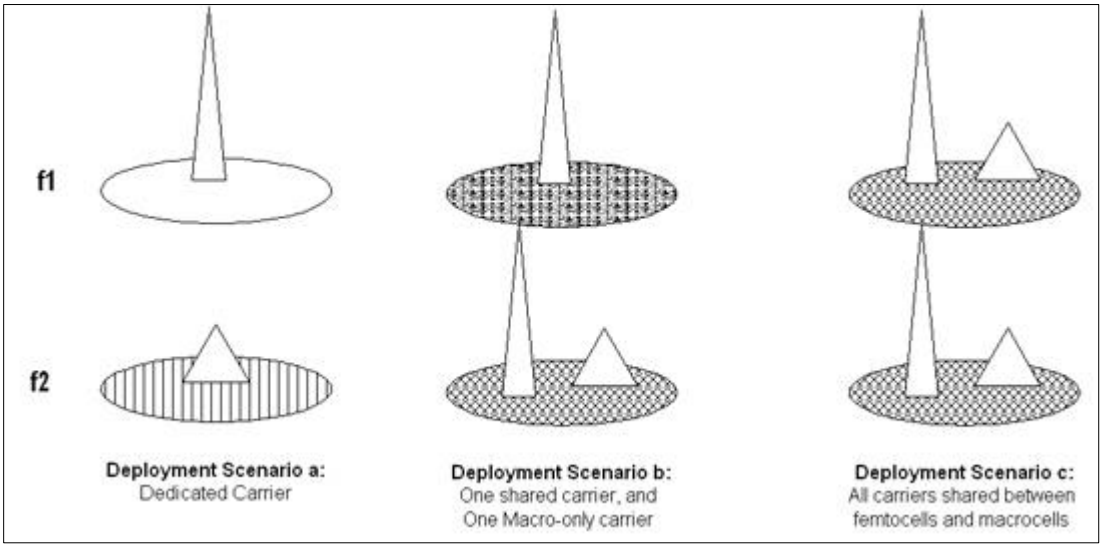

Figure 3: The 3 Spectrum Assignment Policies: Dedicated Spectrum, Partially Shared Spectrum and Shared Spectrum

3. **Partially Shared Spectrum**: This case is considered a middle ground solution between the previous 2 policies since the macrocell has access to all the spectrum while the femtocells operate only on a subset of it. It is considered the best spectrum assignment policy because:

a. The spectral efficiency achieved is even better than the one from the shared spectrum case and
b. It is possible to reduce the cross-tier interference since the macro-users that suffer (or even cause) such interference can use the exclusively dedicated to the macrocell bandwidth – something which the macro-users in the shared spectrum policy simply cannot do (see Figure 3).

1.3 Access Policies in Femtocells

Another important matter that should be addressed is the access policy of the femto-users because it affects the behavior of the macro-users and consequently the performance of the network. We have three cases of access policies:

1. **Closed access or Closed Subscriber Group (CSG):** In this case, there is a group of users (2-5 usually) that represent the subscribers of a femtocell and thus are its exclusive users. No other user (femto or macro) can use the femtocell resources except than its subscribers. The subscriber list of a femtocell can be determined only by its owner which of course contributes to the security and privacy of its users. Problems arise when users that do not belong in a CSG come close to the closed group's femtocell. Since these users are not in the subscriber list, they continue to transmit to their own base station and thus causing interference in the uplink to the users of the CSG. In Figure 4, we can see two cases where users have minimum or none network coverage because of the huge cross-tier interference created in those areas – called Dead Zones. In both cases, a non-subscriber macro-user is within the range of a femtocell. In the uplink scenario, the macro-user transmits with high power towards the macrocell base station and thus causes interference to the subscribers of the nearby femtocell which translates to zero network coverage for them. Moreover, in the downlink scenario, the femtocell access point (FAP) transmits with power that exceeds the one that reaches the macro-user from its own base station, resulting in great interference for that user.

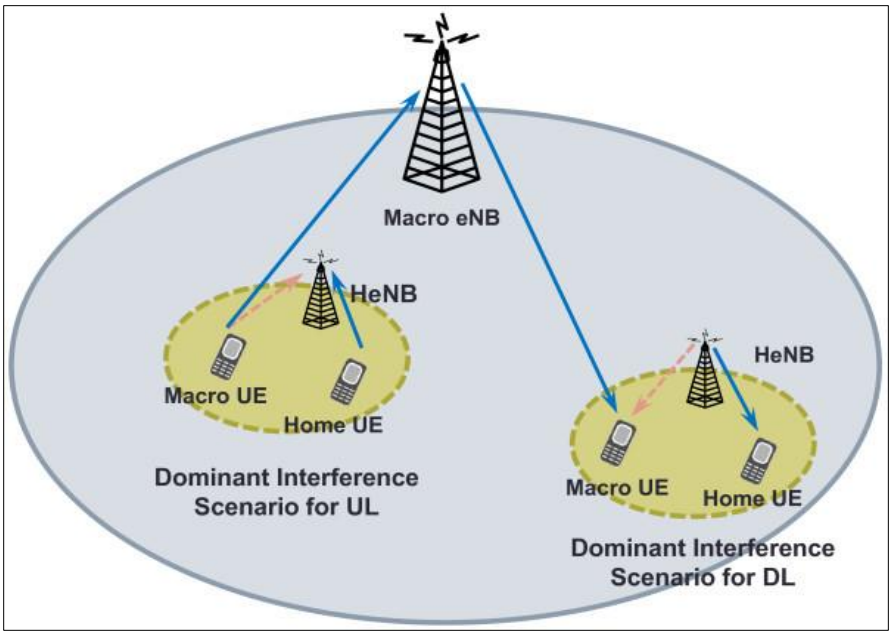

Figure 4: Dead Zones in the uplink (UL) and downlink (DL) of Two-Tier Cellular Networks

2. **Open access:** In this access policy, all users have access to the resources of a femtocell regardless of the tier they belong to or if they are subscribers or not. Specifically, the users connect to the base station with the larger transmission signal and hence the cross-tier interference is avoided as well as the dead zones created by the closed access policy, while a significant reduce in the load of the macrocell is achieved and the total network throughput increases by making use of a better resource management/sharing policy. Concluding, the problem that arises when a non-subscriber user approaches or enters the range of a femtocell does not exist in this case. However, the open-access policy has the following main disadvantages (Mesodiakaki, 2011):
    a. Since users pay for their femtocell devices, they are unwilling to accept non-registered users as users of their femtocell. In this case, in order to keep this product attractive to the subscribers, it is imperative to reduce the amount paid by subscribers to providers or to provide them with other benefits.
    b. Since all users can use the resources of the femtocells, the number of handover increases due to the mobility of the outdoor users. Also, there is an increased probability of a handover failure since the neighbor list may not be correctly created and/or updated (Roche, Valcarce, Lopez-Perez, & Zhang, 2010).

c. The open access policy creates an additional overhead to the network because of a greater demand for computational power from the mobile terminals which have to check every time the user is nearby a femtocell if they can use its resources or not.
d. A fully open access policy can also be problematic due to the loss in data rate resulting from the allocation of the limited bandwidth to a potentially large number of users (Choi, Monajemi, Kang, & Villasenor, 2008).

In the next table, we compare the main points of the two access policies we analyzed so far (Roche, Valcarce, Lopez-Perez, & Zhang, 2010):

Closed Access	Open Access
Higher interference	More handovers
Lower network throughput	Higher network throughput
Serves only indoor users	Increased outdoor capacity
Home Market	SMEs (Small to Medium-sized Enterprises), hotspots
Easier billing	Security needs

3. **Hybrid access:** This is a mix of the two previous access policies and its main characteristic is that a femtocell, in addition to serving its own CSG, it allows the use of its resources to 1 – N non-subscriber users (no more than that though). In other words, full access is offered to subscribers and limited to other users. This choice is the favorite among the network providers since:
    a. The service of registered users is always ensured.
    b. The number of users who suffer from outage (loss of connection to the network) is decreased.
    c. A significant reduce in the load of the macrocell occurs since users that cause strong interference are handovered to the nearby femtocell.

d. A significant reduce in the load and backhaul of the femtocell also occurs since only a limited number of users can connect to its station (in contrast to the open access policy which allows an unlimited number of users).

1.4 Current Research on Power Control for Two-Tier Cellular Networks

In this section, we present some of the main international research papers regarding power control on Two-Tier Cellular Networks. A small summary is given for each of those papers. Much of this research work is addressed to the issue of interference management which is logical considering that one way to mitigate the cross-tier interference is to use a power control scheme for the users.

- **Interference Mitigation Using Uplink Power Control for Two-Tier Femtocell Networks** (Jo, C. Mun, Moon, & Yook, 2009): This paper proposes two interference mitigation strategies that adjust the maximum transmit power of femtocell users to suppress the cross-tier interference at a macrocell base station (BS). The open-loop and the closed-loop control suppress the cross-tier interference less than a fixed threshold and an adaptive threshold based on the noise and interference (NI) level at the macrocell BS, respectively. Simulation results show that both schemes effectively compensate the uplink throughput degradation of the macrocell BS due to the cross-tier interference and that the closed-loop control provides better femtocell throughput than the open-loop control at a minimal cost of macrocell throughput.
- **Uplink Capacity and Interference Avoidance for Two-Tier Femtocell Networks** (Chandrasekhar & Andrews, 2009): This paper develops an uplink capacity analysis and interference avoidance strategy in a two-tier CDMA network. The authors evaluate a network-wide area spectral efficiency metric called the *operating contour (OC)* defined as the feasible combinations of the average number of active macrocell users and femtocell base stations (FAPs) per cell-site that satisfy a target outage constraint. The capacity analysis provides an accurate characterization of the uplink outage probability, accounting for power control, path loss and shadowing effects. Considering worst case interference at a corner femtocell, results reveal that interference avoidance through a time-hopped CDMA physical layer and sectorized antennas allows about a 7x higher femtocell density, relative to a split spectrum two-tier network with omnidirectional femtocell antennas. A femtocell exclusion region and a tier selection based handoff

policy offers modest improvements in the OCs. Lastly, these results provide guidelines for the design of robust shared spectrum two-tier networks.

- **Power Control in Two-Tier Femtocell Networks** (Chandrasekhar, Muharemovic, Shen, Andrews, & Gatherer, 2009): In a Two-Tier Cellular Network cross-tier interference limits overall capacity with universal frequency reuse. To quantify near-far effects with universal frequency reuse, this paper derives a fundamental relation providing the largest feasible cellular signal-to-interference-plus-noise ratio (SINR), given any set of feasible femtocells SINRs. The authors provide a link budget analysis which enables simple and accurate performance insights in a two-tier network. A distributed utility based SINR adaptation at femtocells is proposed to alleviate cross-tier interference at the macrocell from cochannel femtocells. Each femtocell maximizes their individual utility consisting of a SINR based reward less an incurred cost (interference to the macrocell). Numerical results show greater than *30%* improvement in mean femtocell SINRs relative to FM. If cross-tier interference prevents a cellular user from obtaining its SINR target, the authors propose an algorithm that reduces transmission powers of the strongest femtocell interferers. The algorithm ensures that a cellular user achieves its SINR target even with *100* femtocells/cell-site (with typical cellular parameters) and requires a worst case SINR reduction of only *16%* at femtocells. These results motivate design of power control schemes requiring minimal network overhead in two-tier networks with shared spectrum.
- **Distributed interference management in femtocell networks** (D. T. Ngo, Le, Le-Ngoc, Hossain, & Kim, 2012): This paper proposes distributed joint power and admission control algorithms for the management of interference in two-tier femtocell networks, where the newly-deployed femtocell users (FUEs) share the same frequency band with the existing macrocell users (MUEs) using code-division multiple access (CDMA). As the owner of the licensed radio spectrum, the MUEs possess strictly higher access priority over the FUEs; thus, their quality of service (QoS) performance, expressed in terms of the prescribed minimum signal-to-interference-plus-noise ratio (SINR), must be maintained at all times. For the lower-tier FUEs, the authors explicitly consider two different design objectives, namely, throughput-power tradeoff optimization and soft QoS provisioning. With an effective dynamic pricing scheme combined with admission control to indirectly manage the cross-tier interference, the proposed schemes lend themselves to distributed algorithms that mainly require local information to offer maximized net utility of individual users. The approach employed in this work is particularly attractive, especially in view of practical implementation under the limited backhaul network capacity available for femtocells. It is shown that the proposed algorithms robustly support all the prioritized MUEs with guaranteed QoS requirements whenever feasible, while allowing the FUEs to optimally exploit the remaining

network capacity. The convergence of the developed solutions is rigorously analyzed, and extensive numerical results are presented to illustrate their potential advantages.

- **Distributed Power Control for Spectrum-Sharing Femtocell Networks Using Stackelberg Game** (Xin, Liang, & Garg, 2011): In this paper, the authors investigate distributed power allocation strategies for a spectrum-sharing femtocell network, where a central macrocell is underlaid with several femtocells. Assuming that the macrocell protects itself by pricing the interference from the femtocells, a Stackelberg game is formulated to jointly consider the utility maximization of the macrocell and the femtocells. Then, the Stackelberg equilibrium for the proposed game is studied, and an effective distributed interference price bargaining algorithm with guaranteed convergence is proposed to achieve the equilibrium. Numerical examples are then presented to verify the proposed studies. It is shown that the algorithm is effective in distributed power allocation and macrocell protection requiring minimal network overhead for spectrum-sharing-based two-tier femtocell networks.
- **Distributed Pareto-Optimal Power Control for Utility Maximization in Femtocell Networks** (Ngo, Le, & Le-Ngoc, 2012): This paper proposes two Pareto-optimal power control algorithms for a two-tier network, where newly-deployed femtocell user equipments (FUEs) operate in the licensed spectrum owned by an existing macrocell. Different from homogeneous network settings, the inevitable requirement of robustly protecting the quality of service (QoS) of all prioritized macrocell user equipments (MUEs) here lays a major obstacle that hinders the successful application of any available solutions. Directly targeting at this central issue, the first algorithm jointly maximizes the total utility of both user classes. Specifically, the authors adopt the log-barrier penalty method to effectively enforce the minimum signal-to-interference-plus-noise ratios (SINRs) imposed by the macrocell, paving the way for the adaptation of load-spillage solution framework. On the other hand, the second algorithm is applied to the scenario where only the sum utility of all FUEs needs to be maximized. At optimality, the authors show that the MUEs' prescribed SINR constraints are met with equality in this case. With the search space for Pareto-optimal SINRs substantially reduced, the second algorithm features scalability, low computational complexity, short converging time, and stable performance. It is proved that the two developed algorithms converge to their respective global optima, and more importantly, they can be implemented in a distributive manner at individual links. Effective mechanisms are also available to flexibly designate the access priority to MUEs and FUEs, as well as to fairly share radio resources among users. Numerical results confirm the merits of the devised approaches.
- **A Distributed Cluster-Based Self-Organizing Approach to Resource Allocation in Femtocell Networks** (Ta-Sung & Wei-Sheng, 2012): In this paper, a distributed algorithm is proposed, which

uses a cluster-based self-organizing approach to managing the spectrum and power resources among femtocells. The aim of the proposed algorithm is to achieve an optimized throughput of the networks in a decentralized manner. The algorithm involves three phases: sensing phase, sniffer phase, and power control phase, and is performed in each femtocell. Simulation results indicate that the proposed algorithm improves the uplink throughput of the femtocell networks and effectively avoids interference with the conventional macro-cellular networks.

- **Per Cluster Based Opportunistic Power Control for Heterogeneous Networks** (Jin, Chae, & Kim, 2011): This paper proposes an opportunistic power control algorithm to mitigate the aggregate interference (AGGI) from active femtocells in the uplink transmission. The macrocell base station (MBS) decides the interference allowance per femtocell and femtocell users then allocate their transmit power within the allowance to suppress the cross-tier interference in heterogeneous networks. The power control algorithm should reflect the number of active femtocells per cluster to effectively control the AGGI, and thus the authors propose two sensing algorithms (centralized and distributed case respectively), to estimate the number of active femtocells. Moreover, the two sensing algorithms are compared in terms of the outage and throughput performance. The algorithms exploit large-scale channel information and shadowing variation to guarantee the macrocell uplink channel quality. Consequently, the authors suggest that the two sensing algorithms increase total cell throughput.

1.5 Summary and Outline of Thesis

The main subject of this thesis is to study the issue of power allocation in a Two-Tier Cellular Network. The network topology consists of one central macrocell with many femtocells/FAPs in it. We assume that there are four kinds of different users and this classification is based on the tier that the users belong to – and so we have femto-users or macro-users – and secondly on the type of service that they want to satisfy – real-time users need small data rates for voice services while non-real time users request high data rate services. All these users are then considered as players of a non-cooperative game where each user/player follows the best strategy that will allow him to lower the transmission power as much as possible while achieving maximum throughput. The solution of this game is a state called Nash Equilibrium, where each user has maximized their satisfaction from the use of the network's resources and the optimal power allocation in the network is achieved. To find the equilibrium point, we implement a power control algorithm in Multi Service Two-Tier Networks (*MTTPG* algorithm), which is then extensively studied in

various case scenarios. Lastly, many conclusions are reached regarding the satisfaction of the service requirements of the distinct types of users, the usefulness of the femtocells, the maximum number of network users that can receive satisfactory quality of service and the convergence speed of the *MTTPG* algorithm among others.

To summarize, in this first section we provided various introductory information about femtocells as well as modern research trends regarding power control in Two-Tier Cellular Networks. The rest of the thesis is organized as follows: in section 2 we describe the System Model which includes the types of users, the utility function that will be used in each distinct case, the quality of service requirements and the issue of pricing of the femto-users. In section 3, using Game Theory concepts, we formulate and solve the problem of power allocation in the Two-Tier Cellular Network, present the algorithm that finds the solution and prove the existence and uniqueness of the Nash Equilibrium which constitutes the solution state. In section 4, we study the above algorithm through various simulations and draw conclusions for the system which are then presented in section 5, along with directions for further research. Section 6 is the bibliography which lists all the sources used or consulted in writing this thesis.

2. System Model

2.1 Introduction

In this chapter, we present the necessary data and details that are needed to understand the network system in which the problem of power allocation is modeled and solved. These points are given below:

- The system model includes a CDMA (Code Division Multiple Access) macrocell and N femtocells or FAPs (Femto Access Points) located inside the macrocell. The service radius of the central base station (of the macrocell) is $R_c = 500m$ whereas for every femtocell is $R_f = 50m$.
- We consider a time-slotted CDMA system where every user can send or receive data in each of these time slots. A time slot is a small fixed time interval during which the transmission of packets takes place in the network. This is done to simplify the presentation and analyzation of the problem of power allocation in this Two-Tier network since by studying the users' behavior over one time slot, quantities such as the path gain, power and data transmission rate, remain constant for every user.
- This study concerns the network uplink (or reverse link) – namely the data transmission from the users' moving stations to the base stations ($MS^{Transmitter} \rightarrow BS^{Receiver}$). The base stations can either be the FAPs or the macrocell base station (MBS).
- Every FAP serves two femto-users that consist its CSG (Closed Subscriber Group) and only those two have access to the resources of the femtocell – so there exists a *closed access policy* (see section 1.3) to ensure the privacy and security of the femto-users.
- The femtocells use the same frequency spectrum as the macrocell which means that there is a *shared spectrum policy* between them (see section 1.2). Since in each time slot every user can transmit data to its serving base station, the interference received by an individual user on the network comes from all the other users, femto and macro respectively.
- We denote the set of all network users with $L = L_m + L_f$, where L_m is the set of all macro-users with $|L_m| = m$, while L_f is the set of all femto-users, with $|L_f| = 2N$ (N FAPs with two users/FAP). Consequently, we have that: $|L| = m + 2N$.

- We denote the set of all the network's base stations as $S = \{1,2,\dots,N+1\}$, where the first index corresponds to the MBS while the rest are the N FAPs.
- The users' classification is done not only based on the tier they belong to (femtocell or macrocell) but also regarding the kind of service they want to satisfy. Depending on the type of service the users request, we have the real-time users (RT users) and the non-real time users (NRT users). The first demand the satisfaction of real-time services such as voice transmission while the second category requests for non-real time services that require high data transmission rates. Thus, considering both factors (type of service and user's tier) we end up with four distinct kinds of users: non-real time macro-users, real-time macro-users, non-real time femto-users and real-time femto-users. We symbolize this as: $L = L_{m,NRT} \cup L_{m,RT} \cup L_{f,NRT} \cup L_{f,RT}$. This classification is of great importance since every different type of user corresponds a different utility function (see section 2.6). In every femtocell, we consider that there is one non-real time user and one real-time user (always two users/FAP).
- Each user $i \in L$ transmits power $p_i \in [0, P_i^{Max}]$, where P_i^{Max} is the maximum power that a user can utilize and equals 2 Watts. This specific power value is due to technical and physical limitations that have to do with the weight of the device (users ask for even smaller devices nowadays which also means smaller batteries with longer lifetime expectancies) and the percentage of the radiation which is transmitted by a wireless device and absorbed by the human body. The corresponding data transmission rate for user $i \in L$ is $R_i \in [0, R_i^{Max}]$, with $R_i^{Max} = 2.4\ Mbps$ being the maximum data rate a user can achieve in the network under consideration.
- In every time slot, the path or channel gain – which is defined as the reduction factor in the power density of a signal as it is transmitted in space – is considered constant and for the study of the network's system we ignored the Rayleigh fading and the phenomenon of log-normal channel shadowing. We used a simplified path loss model that is based on the IMT-2000 specification and it's also the one used by the authors of (Chandrasekhar, Muharemovic, Shen, Andrews, & Gatherer, 2009).
- Typically, the cellular network under consideration looks like the one in Figure 5:

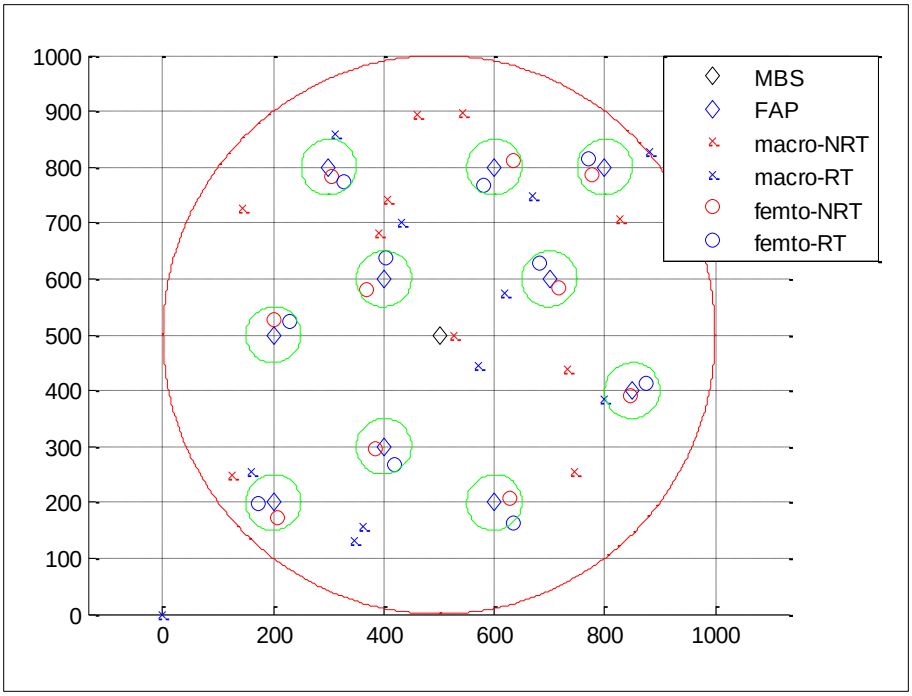

Figure 5: System Model

2.2 Types of Interference and Path Gain table

In a Two-Tier Cellular Network (like the one we study), there exist a total of five different kinds of interference. Generally, the interference that is experienced by a user is a quantity that is measured by the base station (MBS or FAP) that serves that particular user. By expanding on what we discussed in section 1.2, we have:

- **Co-tier Interference:**
    1. A macro-user causes interference to another macro-user that transmits to the MBS.
    2. A femto-user causes interference to the other femto-user of a particular FAP while the second transmits data to the common femtocell base station.
- **Cross-Tier Interference:**
    3. A macro-user causes interference to a femto-user since the signal that the first transmits, reaches the FAP that serves that femto-user (see case a in Figure 6).
    4. A femto-user causes interference to a macro-user since the signal that the first transmits reaches the MBS that serves the macro-user (see case b in Figure 6).

5. A femto-user causes interference to another femto-user that belongs to a different FAP (see case c in Figure 6).

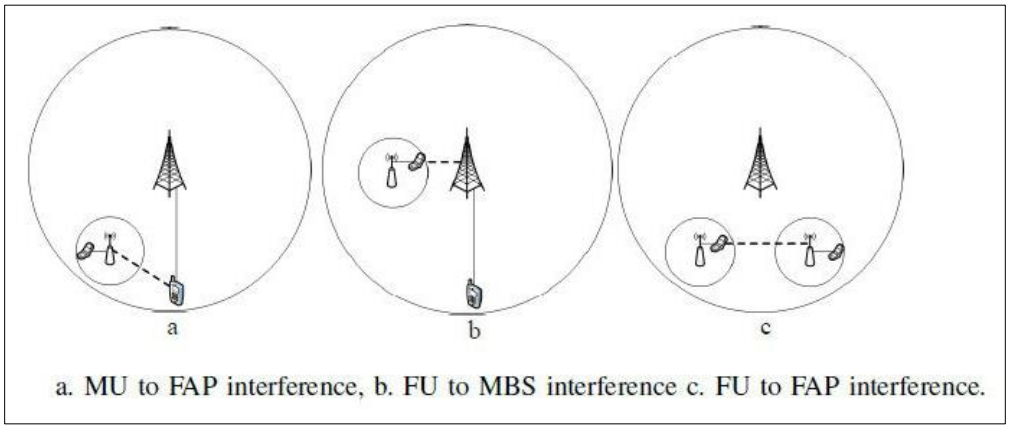

a. MU to FAP interference, b. FU to MBS interference c. FU to FAP interference.

Figure 6: The three case of cross-tier interference

Our goal is to calculate the path gain $g_{i,j}$ from user $j \in L$ to the base station $i \in S$, $\forall i,j$. For every kind of interference that is created (see the above five cases) there is a different formula that calculates the path gain in each situation, based on the model that we used (Chandrasekhar, Muharemovic, Shen, Andrews, & Gatherer, 2009):

$$g_{i,j} = \begin{cases} K_c d_{i,j}^{-a_c}, \ m \to MBS\,(1) \\ K_{f_i} d_{i,j}^{-b}, \ f \to FAP, f \in FAP\,(2) \\ K_c W d_{i,j}^{-a_c}, \ m \to FAP\,(3) \\ K_{f_0} W d_{i,j}^{-a_{f_0}}, \ f \to MBS\,(4) \\ K_{f_0} W^2 d_{i,j}^{-a_{f_0}}, \ f \to FAP, f \notin FAP\,(5) \end{cases} \quad (1)$$

Firstly, we note that $g_{i,j} = f(d_{i,j})$ which means that the path gain is a function of the distance of the user j to the base station i (in meters). Also, m stands for macro-user, f for femto-user, a_c, b, a_{f_0} respectively denote the cellular, indoor and indoor to outdoor femtocell path loss exponents (for practical reasons we set $a_c = a_{f_0} = a$), $K_{c,dB} = 30log_{10}(f_{c,Mhz}) - 71$ equals the fixed decibel propagation loss during cellular transmissions in free space, $f_{c,Mhz}$ is the carrier frequency in MHz (1900Mhz for a CDMA system), the term K_{f_i} is the fixed loss between femtocell user i and his own FAP i, K_{f_0}denotes the fixed loss between a femto-user and a base station different from the one that he transmits to (we assume that

$K_{f_0} = K_c$) and lastly, the term W explicitly models partition loss during indoor-to-outdoor propagation (that is whenever the signal has to pass through a "wall"). In case 5 of equation (1), the signal passes through two walls – as it leaves a house that has a femtocell installed and reaches another house's FAP – and so the term W^2 is used.

We can now use equation (1) to define the path gain table as: $G = \{g_{i,j}\}_{(N+1)\times(m+2N)}$, where $j \in L = \{1,2,\dots,m,m+1,m+2,\dots,m+(2N-1),m+2N\}$. The columns of G are the users, starting with the m macro-users and then putting the femto-users in groups of two in partial correspondence with the set $S = \{1,2,\dots,N+1\}$ while the rows of G are the base stations: $i \in S$. What we mean by partial correspondence between the sets L and S is that the first element of S (the "1" – first row of G) is the MBS that corresponds to the elements $\{1,2,\dots,m\}$ of L which represent the m macro-users, whereas the second element of S (the "2" – second row of G) is the first FAP which corresponds to the elements $\{m+1, m+2\}$ of L (the users of that FAP) and so on until the $(N+1)^{th}$ element of S, which is the N^{th} FAP that corresponds to the femto-users $\{m+(2N-1), m+2N\}$ of L. So, the general form of the table G is as follows:

$$G = \left(\begin{bmatrix} g_{1,1} & g_{1,2} & \cdots & g_{1,m} \\ \vdots & \vdots & \ddots & \vdots \\ g_{N+1,1} & g_{N+1,2} & \cdots & g_{N+1,m} \end{bmatrix} \begin{bmatrix} g_{1,m+1} & g_{1,m+2} & \cdots & g_{1,m+(2N-1)} & g_{1,m+2N} \\ \vdots & \vdots & \ddots & \vdots & \vdots \\ g_{N+1,m+1} & g_{N+1,m+2} & \cdots & g_{N+1,m+(2N-1)} & g_{N+1,m+2N} \end{bmatrix} \right)$$

The top-left matrix is composed of the path gains from all macro-users to the MBS (co-tier), the top-right matrix has the path gains from all femto-users to the MBS (cross-tier), the bottom-left matrix includes the path gains from all macro-users to all FAPs (cross-tier) – each line corresponds to a different FAP – and lastly, the bottom-right matrix accounts for all the path gains from every femto-user to every FAP in the network, including the one that they transmit to (co-tier and cross-tier).

2.3 Signal to Interference & Noise Ratio (SINR)

Since we described the path gain formula in every possible case (from every user to any base station), we can now define the signal-to-interference-plus-noise (SINR) for every user $i \in L$ as:

$$\gamma_i = \frac{W}{R_i} \frac{g_{s_i,i} p_i}{\sum_{\forall j \neq i} g_{s_i,j} p_j + \sigma_i} = G \frac{g_{s_i,i} p_i}{I_{s_i,-i}(\bar{p}_{-i})} \quad (2)$$

, where $G = {}^{W}/_{R_i}$, W is the system's spreading bandwidth, σ_i is the noise power (we assume AWGN), R_i the transmission rate of user i, $g_{i,j}$ is the path gain from user j to the base station i (as it was defined in section 2.2), s_i is the base station that serves user i, $\bar{p}_{-i}$ is a vector that includes all the users' powers excluding user i, while the term $I_{s_i,-i}(\bar{p}_{-i})$ denotes the network interference and background noise at the base station $s_i \in S$ when receiving data from its user i. Consequently, in the calculation of the SINR of a specific user, we consider all the different kinds of interference from all the network users (excluding the self-interference that a user causes to himself which is of course zero/non-existent).

2.4 Utility Function U and Actual Throughput Utility Function T

Because of the variety of services that the users require (see section 2.5) and the tier that they belong to (femto or macro) we introduce the concept of the *utility function* U_i for every user $i \in L$, which quantifies the degree of satisfaction resulting from the received quality of service (QoS) by the user and also measures the tradeoff between the user's utility-based actual uplink throughput performance and the corresponding energy consumption (p_i) per time slot. The general formula of the utility function is (Tsiropoulou, Kastrinogiannis, & Papavassiliou, 2009):

$$U\left(R_i^*, p_i, \bar{p}_{-i}\right) = \frac{T_i\left(R_i^*, p_i, \bar{p}_{-i}\right)}{p_i} = \frac{T_i\left(R_i^F f_i(\gamma_i), p_i, \bar{p}_{-i}\right)}{p_i} \quad (3)$$

, where $R_i^* \equiv R_i^F f_i(\gamma_i)$ denotes the user's i actual uplink transmission rate at the time slot under consideration, R_i^F is its fixed designed transmission rate, $\bar{p}_{-i}$ denotes the users' power allocation vector excluding user i, while $f_i(\gamma_i)$ denotes its *efficiency function.* The latter represents the probability of a successful packet transmission for user i and is an increasing function of his bit energy to interference ratio γ_i at any time slot. A user's efficiency function for the probability of a successful packet transmission at fixed data rates, depends on the transmission schemes (modulation and coding) being used (see Figure 7):

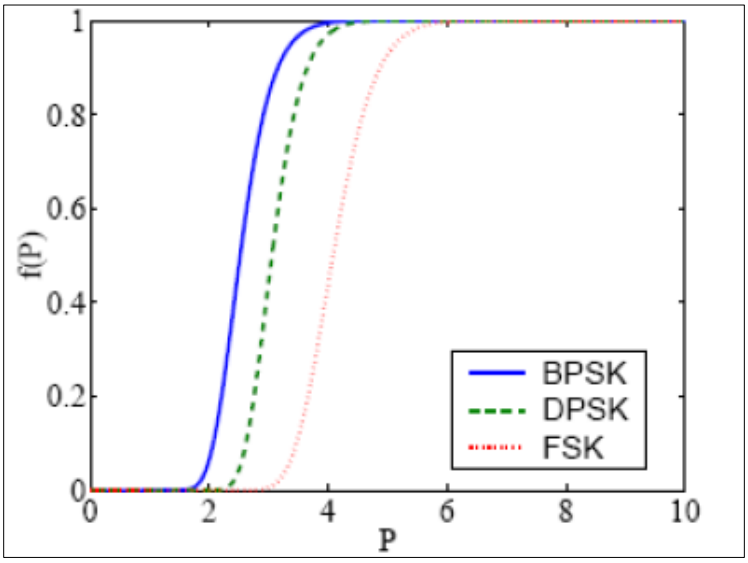

Figure 7: Probabilities of packet transmission success for BPSK, DPSK, and FSK modulation schemes

The efficiency function has the following four properties (Tsiropoulou, Kastrinogiannis, & Papavassiliou, 2009):

1) f_i is an increasing function of γ_i
2) f_i is a continuous, twice differentiable sigmoid function with respect to γ_i [1]
3) $f_i(0) = 0$ to ensure that $T_i|_{p_i=0} = 0$ and $\lim_{p_i \to 0^+} U_i = 0^+$
4) $f_i(\infty) = 1$

[1] A function $f(x)$ is defined as sigmoid if it has a unique inflection point x_{Infl} and the following inequalities are true: $\left.\frac{\partial^2 f}{\partial x^2}\right|_{x<x_{Infl}} > 0$ και $\left.\frac{\partial^2 f}{\partial x^2}\right|_{x>x_{Infl}} < 0$.

For the rest of this work we will assume that the efficiency function is the same for all users and we will write it as $f(\gamma_i)$. Moreover, the actual throughput utility function $T_i\left(R_i^*, p_i, \overline{p}_{-i}\right) \equiv T_i\left(R_i^*\right)$ is a function of user's i actual data rate R_i^* and reflects his degree of satisfaction in accordance to his service actual throughput expectations and QoS requirements fulfillment at every time slot. The general properties a throughput utility function should have are the following (Tsiropoulou, Kastrinogiannis, & Papavassiliou, 2009):

1) T_i is a strictly increasing function of R_i^*
2) T_i is a continuous, twice differentiable function with respect to R_i^*
3) $T_i(0) = 0$ to ensure that $\lim_{R_i \to 0^+} U_i = 0^+$
4) T_i is bounded above ($T_i\left(R_i^*\right) \leq 1$)
5) T_i is a sigmoid or strictly concave (convex respectively) function of R_i^*, with domain: $\left[0, R_i^{Max}\right]$, where $R_i^{Max} = 2.4Mbps$ is the maximum data rate a user can achieve in the network under consideration.

The usefulness of the 5th property above is illustrated in the next section, where we analyze and justify the proposed methodology for mirroring a real-time user's degree of satisfaction with respect to its corresponding service performance into a proper actual throughput utility function T_i.

2.5 Quality of Service (QoS)

As mentioned in section 2.1, there are four kinds of distinct users: $L = L_{m,NRT} \cup L_{m,RT} \cup L_{f,NRT} \cup L_{f,RT}$. If we consider the users' quality of service requirements independently of the tier they belong to (femtocell or macrocell), we can classify them as (Tsiropoulou, Kastrinogiannis, & Papavassiliou, 2009):

- **Real-time users (RT users)**, which demand short-term and strict QoS requirements as is the case with voice transmission and multimedia applications. We denote their set as: $L_{RT} = L_{m,RT} \cup L_{f,RT}$, meaning that there are some macro-users that are RT users as well as one femto-user from every FAP. RT users are also called voice users.

- **Non-real time users (NRT users)**, which want to achieve the highest throughput possible while having great tolerance for packet delay. We denote their set as: $L_{NRT} = L_{m,NRT} \cup L_{f,NRT}$, meaning that there are some macro-users that are NRT users as well as one femto-user from every FAP. NRT users are also called data users.

2.5.1 Real-Time users

Regarding RT services, since the users have small tolerance for packet delay and their requirements consist mainly of a constant target actual rate per time slot, we consider the throughput utility function T_i to be a sigmoid function of the user's actual data rate R_i^* (see Figure 8).

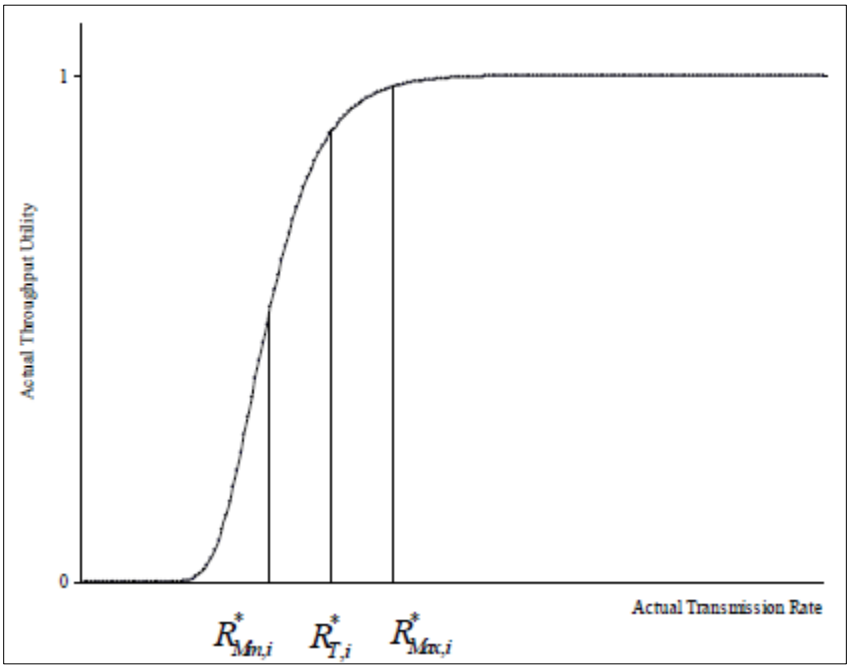

Figure 8: Actual Throughput Utility function for the RT users

We introduce the concept of the target uplink rate $R_{T,i}^*$, which indicates the ideal value of a RT user's actual transmission rate per time slot at which his service QoS requirements, the packet delay constraints as well as the need for short-term utility throughput are fulfilled. The permissible deviations from this target rate are expressed through the margin factor MF_i and thus we determine the lower and

upper bounds of the desired actual data rate as: $R^*_{Min,i} = R^*_{T,i} - MF_i$, $R^*_{Max,i} = R^*_{T,i} + MF_i$. This means that a RT user has his QoS requirements fulfilled when his actual transmission rate is inside the range $\left[R^*_{Min,i}, R^*_{Max,i} \right]$.

Specifically, we note that a RT user's margin factor determines the minimum acceptable levels of his expected actual throughput (i.e. $R^*_{Min,i} = R^*_{T,i} - MF_i$). Moreover, we argue that when the user's achieved actual transmission rate remains within the range of $\left[R^*_{Min,i}, R^*_{T,i} \right]$, his actual throughput utility must be a slowly decreasing function of his actual data rate. On the other hand, when $R^*_i < R^*_{Min,i}$, his actual throughput utility should be a rapidly decreasing function of R^*_i, indicating thus his priority to occupy additional system resources. Consequently, the value $R^*_{Min,i}$ should determine the unique inflection point of the sigmoid function $T_i, i \in L_{RT}$. The previous design option gives to a user's power and rate control mechanism, operating over fast fading channels environment, the enhanced flexibility of decreasing its actual uplink throughput up to a certain level ($R^*_{Min,i}$), if required due to its potentially bad instantaneous channel conditions, without however excluding him from transmitting data at that corresponding time slot. The later would occur, if a step function of a RT user's actual transmission rate was used to reflect his corresponding degree of satisfaction.

Furthermore, we argue that an additional increment of a RT user's actual data rate from its target one ($R^*_{T,i}$), must not contribute in an analogous increment of its actual throughput degree of satisfaction and thus, the latter should tend asymptotically to its maximum value, as $R_i \to \infty$. The previous argument is based on the observation that since a RT service's QoS prerequisites are fulfilled when the required target bit rate is achieved, an additional improvement of the user's actual throughput performance will not improve his degree of satisfaction further.

Moreover, by restricting up to a specific level ($R^*_{Max,i} = R^*_{T,i} + MF_i$) the achieved actual uplink data rates of RT users, that due to their temporarily good transmission environment can receive more recourses than required, we get the advantage of reallocating the excess system resources to the un-favored RT users (e.g. those with temporally bad transmission environment) in order to increase not only their performance satisfaction but also the overall number of RT users that can be simultaneously served. To conclude:

Definition 1: The throughput utility function for the real-time users is defined as: $T_i\left(R_i^*\right) \equiv T_i\left(\left(R_{T,i}^* + MF_i\right) f\left(\gamma_i\right)\right)$ (4.1), with $i \in L_{RT}$, $\gamma_i > 0$ and $R_i^* \in \left[0, R_{T,i}^* + MF_i\right]$. It is a sigmoid function with respect to R_i^* with unique inflection point $R_{Infl,i}^*$, defined as follows:

$$R_{Infl,i}^* = \left\{ R_i^* : \left. \frac{\partial^2 T_i\left(R_i^*\right)}{\partial\left(R_i^*\right)^2} \right|_{R_i^* = R_{Min,i}^*} = 0, R_{Min,i}^* = R_{T,i}^* - MF_i \right\} \quad (4.2)$$

Also: $T_i\left(R_{Max,i}^*\right) = T_i\left(R_{T,i}^* + MF_i\right) = 1$ (4.3).

2.5.2 Non-Real Time users

Concerning NRT data services, since the users have great tolerance for packet delays and they request for high throughput performance, we consider the throughput utility function T_i to be a strictly concave or convex function of the user's actual data rate R_i^* (see Figure 9 – red and green curves).

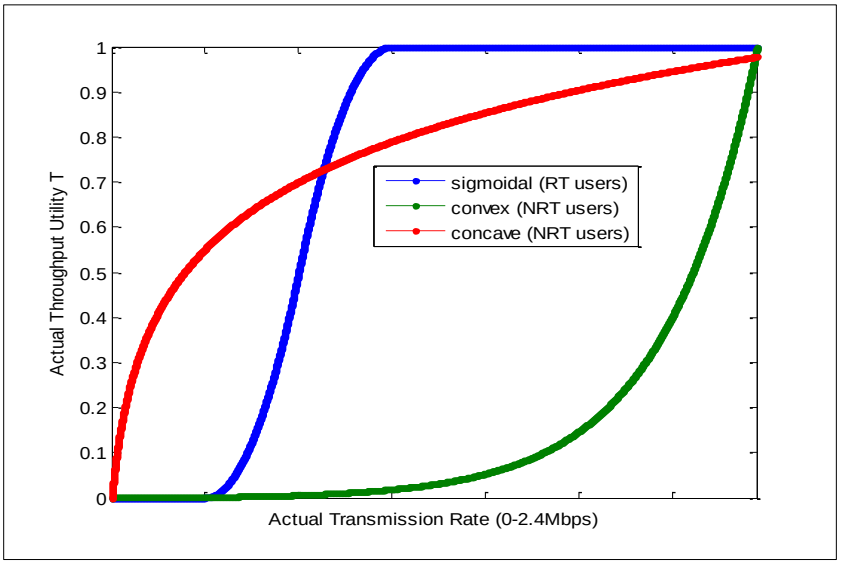

Figure 9: Throughput Utility function for NRT and RT users

Moreover, the maximum throughput that a NRT user can achieve is constrained by its transmitter's limitations and thus no NRT user can transmit with date rate greater than $R_i^{Max} = 2.4Mbps$ - this specific value also corresponds to the highest possible utility throughput: $T_i\left(R_{Max,i}^*\right) = T_i\left(R_i^{Max}\right) = 1$. To conclude:

Definition 2: The throughput utility function for the non-real time users is defined as: $T_i\left(R_i^*\right) \equiv T_i\left(R_i^{Max} f\left(\gamma_i\right)\right)$ (5.1), with $i \in L_{NRT}$, $\gamma_i > 0$, $R_i^* \in \left[0, R_i^{Max}\right]$ and it is a strictly concave or convex function with respect to R_i^*. Also: $T_i\left(R_{Max,i}^*\right) = T_i\left(R_i^{Max}\right) = 1$ (5.2).

If we look closely above at the two definitions as well as the equation (3), it is obvious that mathematically, the difference between the RT and NRT users (apart from the form of their respective T_i function) is the choice of the fixed transmission rate R_i^F. We used: $R_i^F = \begin{cases} R_{T,i}^* + MF_i, i \in L_{RT} \\ R_i^{Max}, i \in L_{NRT} \end{cases}$ and inserted that into: $T_i\left(R_i^*\right) = T_i\left(R_i^F f\left(\gamma_i\right)\right)$ for each case. The R_i^F value is the data rate R_i^* which maximizes the function $T_i\left(R_i^*\right)$ if $f\left(\gamma_i\right) \to 1$, which is true as we can verify from the equations (4.3) and (5.2) for the RT and NRT users respectively. So, by taking into account the two different kinds of services that the users request and the aforementioned remark, equation (3) becomes (Tsiropoulou, Kastrinogiannis, & Papavassiliou, 2009):

$$U_i\left(p_i, \bar{p}_{-i}\right) = \frac{T_i\left(R_i^*\right)}{p_i} = \begin{cases} \dfrac{T_i\left(R_i^{Max} f\left(\gamma_i\right)\right)}{p_i}, i \in L_{NRT} \\ \dfrac{T_i\left(\left(R_{T,i}^* + MF_i\right) f\left(\gamma_i\right)\right)}{p_i}, i \in L_{RT} \end{cases} \quad (6)$$

, where $R_i^* \in \left[0, R_i^{Max}\right], i \in L_{NRT}$ and $R_i^* \in \left[0, R_{T,i}^* + MF_i\right], i \in L_{RT}$, since $f\left(\gamma_i\right) \in [0,1], \forall \gamma_i \geq 0$. Intuitively, we consider that the function $U_i\left(p_i\right)$ is non-negative and bounded above (for normalization purposes only) and thus, $\lim_{p_i \to 0^+} U_i\left(p_i\right) = 0^+$, since if the user does not transmit data, then his satisfaction should be zero.

2.6 Pricing of the femto-users and Total Utility Function

In this section, we discuss the concept of pricing for the femto-users and therefore extend the utility function to include this pricing policy. The reasons why we would want to use such a taxation mechanism for the femto-users of the network are (D. T. Ngo, Le, Le-Ngoc, Hossain, & Kim, 2012), (Tsiropoulou, Katsinis, & Papavassiliou, 2012):

1. The macro-users are the main owners of the radio spectrum and since we have chosen a shared spectrum policy between them and the femto-users, it is only logical that the macro-users should be given higher priority in using the system's resources.
2. The macro-users' QoS requirements should always be satisfied (as higher priority users).
3. The pricing mechanism refers to a control signal that motivates users to adopt a *social behavior* – this means that the users care not only about their own QoS but for the other users too and so this mechanism betters overall system performance by encouraging efficient sharing of resources.
4. By using a cost function, we can decrease the cross-tier interference caused by the femto-users to the macro-users, thus making the former transmit with lower power so that the latter can meet their QoS requirements without difficulties.
5. Power, which is a limited and critical resource of the network, should be efficiently allocated and the use of a costing strategy that lowers the users' power helps in this direction since it reduces the interference to other users, increases the utility and hence the network's throughput performance.

To induce the pricing policy, we subtract a cost function $C_i\left(p_i, \bar{p}_{-i}\right)$ (increasing with regards to p_i) from the utility function $U_i\left(p_i, \bar{p}_{-i}\right)$ (see equation (6)) so that the more a femto-user increases his power, the more he will be penalized due to the greater interference he causes to the nearby users. Since for larger values of the transmission power p_i, the function $C_i\left(p_i, \bar{p}_{-i}\right)$ will also result in huge values, the total utility function of the network under consideration will decrease and consequently so will the total utility of the femto-user who is penalized (see equation (7)). As a result, the femto-user will want to limit his transmission power in order to maintain an acceptable level of utility and also impose less interference to the other users (Tsiropoulou, Katsinis, & Papavassiliou, 2012).

$$U_i^{net}\left(p_i,\bar{p}_{-i}\right)=U_i\left(p_i,\bar{p}_{-i}\right)-C_i\left(p_i,\bar{p}_{-i}\right) \quad (7)$$

In the recent literature, the usage-based pricing mechanisms that have been introduced are linear schemes of the user's transmission power p_i, where each user pays a price proportional to his transmission power. However, this simplified pricing mechanism is not realistic and does not well represent the actual system and user behavior, as the harm a user imposes on other users is not equivalent within the entire range of his transmission power (Tsiropoulou, Katsinis, & Papavassiliou, 2012). Analytically, if the transmission power of a user exceeds a predefined threshold, P_{thres}, the price increases more rapidly, considering a more realistic formulation and reflecting the criticality of this resource. Accordingly, a more realistic pricing scheme is represented by a convex function $C_i\left(p_i,\bar{p}_{-i}\right)$ with regards to the transmission power p_i (see Figure 10).

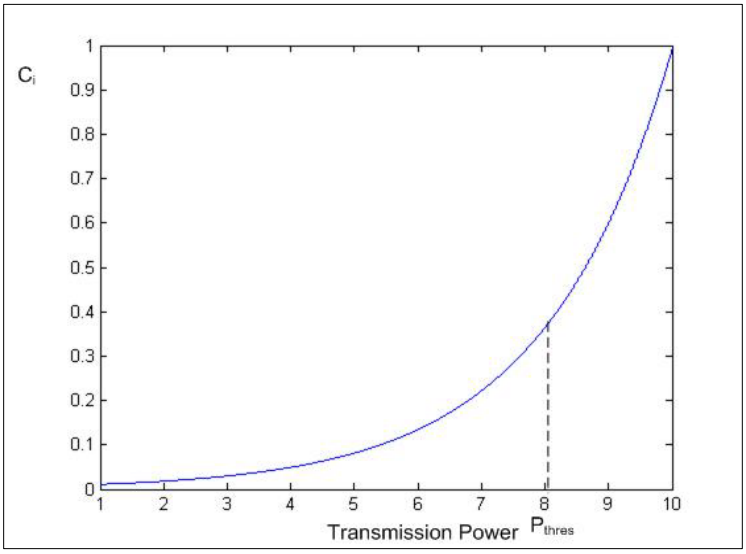

Figure 10: A convex pricing function

To conclude, we define the pricing function as:

$$C_i\left(p_i,\bar{p}_{-i}\right)=\begin{cases}0 & ,i\in L_m\\ c\left(e^{p_i}-1\right), & i\in L_f\end{cases},\ c\geq 0 \quad (8)$$

Finally, by combining the equations (6), (7) and (8), we can define the total utility function of a user $i \in L = L_{m,NRT} \cup L_{m,RT} \cup L_{f,NRT} \cup L_{f,RT}$, which correlates a different utility formula to each of the four kinds of users that exist in the network:

$$U_i^{net}\left(p_i, \overline{p}_{-i}\right) \overset{(7,6)}{=} \frac{T_i\left(R_i^*\right)}{p_i} - C_i\left(p_i, \overline{p}_{-i}\right) \overset{(6,8)}{=} \begin{cases} \dfrac{T_i\left(R_i^{Max} f\left(\gamma_i\right)\right)}{p_i} & , i \in L_{m,NRT} \\ \dfrac{T_i\left(\left(R_{T,i}^* + MF_i\right) f\left(\gamma_i\right)\right)}{p_i} & , i \in L_{m,RT} \\ \dfrac{T_i\left(R_i^{Max} f\left(\gamma_i\right)\right)}{p_i} - c\left(e^{p_i} - 1\right) & , i \in L_{f,NRT} \\ \dfrac{T_i\left(\left(R_{T,i}^* + MF_i\right) f\left(\gamma_i\right)\right)}{p_i} - c\left(e^{p_i} - 1\right), & i \in L_{f,RT} \end{cases} \quad (9)$$

For short, we will use the symbolism $U^{net}\left(p\right) = U\left(p\right) - C\left(p\right)$, considering that the reference is made to the functions themselves. The function $U\left(p\right)$ will keep its properties as defined after equation (6) – mainly that it is non-negative ($U\left(p\right) \geq 0, \forall p \geq 0$, $\lim_{p \to 0^+} U\left(p\right) = 0^+$) and bounded above (has a maximum).

3. Problem Formulation and Solution

3.1 A non-cooperative Multi Service Two-Tier Power Control Game with Pricing (MTTPG)

The main subject of this thesis is to present a way to achieve an optimal power allocation between the users of the Two-Tier Cellular Network (whose model is described in section 2). As the system starts operating (meaning that packets are being transferred in the network), an uplink power control algorithm is run at the beginning of each time slot, making decisions about the users' emitted power in order to maximize the satisfaction of the system's users – in terms of the use of network resources (power, throughput) – expressed by the total utility function corresponding to each user through the equation (9). Thus, each user is selfishly trying to transmit with power values that maximize his utility function without cooperating with the other users and thereby leading to an optimization of the system through an autonomous user operating environment where the goal is to achieve a total power allocation that provides high energy efficiency to that system.

So, by using concepts from Game Theory, we define the non-cooperative game $G=\left[L,\{P_i\},\{U_i^{net}(\cdot)\}\right]$, where L is the set of the players/users of the network (both femto-users and macro-users), $P_i=\left[0,P_i^{Max}\right]$ is the set of the users' strategies (the possible transmission power values) and $U_i^{net}(\cdot)$ is the total utility function of the user $i\in L$ as defined in equation (9). Every user chooses a strategy (transmission power) p_i such that: $p_i\in P_i$, in order to increase his utility – this translates into achieving the highest possible throughput (data rate) while consuming as low power as possible and thus increasing the battery life of his mobile phone. The utility of a user depends not only on the transmission power that he chooses but also on the strategy choices of the rest players/users (see the formula of SINR – equation (2)). So, in the power control game G, every player tries to maximize his total utility function U_i^{net} per time slot, considering that the other users' transmission power remains fixed. To summarize, the resulting non-cooperative game G can be expressed as the following optimization problem:

$$G \Leftrightarrow (MTTPG) \ \max_{p_i \in P_i} U_i^{net}\left(p_i, \bar{p}_{-i}\right), \forall i \in L \qquad (10)$$

, where $U_i^{net}(\cdot)$ is given from equation (9) and $P_i = \left[0, P_i^{Max}\right]$ is the strategy set of the user i.

Note: The name of the optimization problem (*MTTPG*) is an abbreviation of the phrase: Multi Service Two-Tier Power Control Game with Pricing.

3.2 Solving Methodology

3.2.1 Nash Equilibrium approach

In order to find the solution to the optimization problem stated in equation (10), we use the game theory concept of *Nash Equilibrium (NE)*. According to Nash, there is a solution-set of strategies – in this game this refers to a power vector $\bar{p} = (p_1, \ldots, p_{m+2N})$ – such that no user wishes to change his strategy (transmission power) since his total utility function cannot be maximized further, provided that the other users' powers do not change. The formal definition is given below (Saraydar, Mandayam, & Goodman, 2002):

Definition 3: The power vector $\bar{p} = (p_1, \ldots, p_L)$ consists a *NE* of the (*MTTPG*) game if $\forall i \in L$, the following applies: $U_i^{net}\left(p_i, \bar{p}_{-i}\right) \geq U_i^{net}\left(p_i', \bar{p}_{-i}\right), \forall p_i' \in P_i$.

The power that a non-cooperative user transmits can also be seen as the best response to the powers/strategies that the other users have chosen. So, we can define the *best response function* as (Saraydar, Mandayam, & Goodman, 2002):

Definition 4: The best response function $r_j : P_{-j} \to P_j$ is a mapping of the power vector $\bar{p}_{-j} \in P_{-j}$ to the set: $r_j\left(\bar{p}_{-j}\right) = \left\{p_j \in P_j : U_j^{net}\left(p_j, \bar{p}_{-j}\right) \geq U_j^{net}\left(p_j', \bar{p}_{-j}\right), \forall\, p_j' \in P_j\right\}$. This definition is the same as in (Tsiropoulou, Kastrinogiannis, & Papavassiliou, 2009): $r_j\left(\bar{p}_{-j}\right) = \max_{p_j \in P_j} U_j^{net}\left(p_j, \bar{p}_{-j}\right), \forall j \in L$.

Note: Using the best response function, we can define the *NE* of the G game as the power vector $\bar{p}_{NE} = \left(p_{NE,1}, \ldots, p_{NE,m+2N} \right)$, where $p_{NE,j} \in r_j \left(\bar{p}_{NE,-j} \right), \forall j \in L$. Moreover, if the system has reached its equilibrium state (all users' powers are now in *NE*) and we assume that $r_i \left(\bar{p}_{-i} \right)$ is the same as $r_i \left(\bar{p} \right)$, then in the *NE* the following will apply: $\bar{r} \left(\bar{p}_{NE} \right) = \bar{p}_{NE}$. The latter means that in the equilibrium state, the best response a user i can manage given the strategies of the rest of the players (which transmit with optimal powers), is to transmit with power equal to $p_{NE,i}$ and none other.

3.2.2 Properties of the Actual Throughput and Utility Functions

In this section, we will list various lemmas that will assist us in the proof of existence and uniqueness of the *NE* of the (*MTTPG*) game and thus to the existence of a unique solution to the problem of power allocation in the Two-Tier Cellular Network as stated in equation (10). These lemmas provide us with useful properties of the actual throughput utility function T_i and of the utility function U_i.

In section 2.5, we defined the formula of the throughput utility function T_i with respect to R_i^*, based on the various kinds of QoS requirements that the RT and NRT users have. Briefly, the general form of $T_i \left(R_i^* \right)$ is:

$$T_i(R_i^*) = \begin{cases} \text{sigmoid with respect to } R_i^*, i \in L_{RT} \\ \text{strictly concave (convex) with respect to } R_i^*, i \in L_{NRT} \end{cases}, R_i^* = R_i^F f(\gamma_i)$$

It is very important to prove that no matter the form of $T_i \left(R_i^* \right)$, it will always remain a sigmoid function of γ_i, i.e. $T_i \left(\gamma_i \right)$ is sigmoid $\forall i \in L$ (and so is $T_i \left(p_i \right)$, since from equation (2), $\gamma_i \sim p_i$). This is a necessary prerequisite to prove the *quasi-concaveness* of the utility function $U_i \left(p_i \right) = \dfrac{T_i \left(p_i \right)}{p_i}$ and thus the existence of its unique (global) maximum (which constitutes a *NE* for the macro-users since the pricing policy does not apply to them).

3.2.2.1 Lemma 1

For the RT users, given:

- The efficiency function $f\left(\gamma_i\right)$, which is sigmoid with respect to γ_i and has a unique inflection point $\gamma_{Infl,i}^{f}$ (2nd property of the efficiency function – see section 2.4)
- The actual throughput utility function $T_i\left(R_i^*\right)$, which is sigmoid with respect to R_i^* and has a unique inflection point $R_{Infl,i}^* \equiv R_{Min,i}^* = R_{T,i}^* - MF_i$ (see the first definition above), with $R_i^* \equiv R_{Max,i}^* f\left(\gamma_i\right) = \left(R_{T,i}^* + MF_i\right) f\left(\gamma_i\right), i \in L_{RT}$

, then the function $T_i\left(\gamma_i\right) = T_i\left(\left(R_{T,i}^* + MF_i\right) f\left(\gamma_i\right)\right)$ is also sigmoid with respect to γ_i ($\gamma_i \geq 0$) and has a unique inflection point $\gamma_{Infl,i}^{T}$, such that:

$$\gamma_{Infl,i}^{T}: \begin{cases} \gamma_{Infl,i}^{R^*} \leq \gamma_{Infl,i}^{T} \leq \gamma_{Infl,i}^{f}, \text{ when } \gamma_{Infl,i}^{R^*} \leq \gamma_{Infl,i}^{f} \\ \gamma_{Infl,i}^{f} \leq \gamma_{Infl,i}^{T} \leq \gamma_{Infl,i}^{R^*}, \text{ when } \gamma_{Infl,i}^{R^*} > \gamma_{Infl,i}^{f} \end{cases} \quad (11)$$

, where $\gamma_{Infl,i}^{R^*}$ is the mapping of the unique inflection point of $T_i\left(R_i^*\right)$ to the γ_i – axis:

$$R_{Infl,i}^* = R_{Max,i}^* f\left(\gamma_{Infl,i}^{R^*}\right) \Rightarrow \frac{R_{Infl,i}^*}{R_{Max,i}^*} = f\left(\gamma_{Infl,i}^{R^*}\right) \Rightarrow \gamma_{Infl,i}^{R^*} = f^{-1}\left(\frac{R_{Infl,i}^*}{R_{Max,i}^*}\right)$$

Proof: See Appendix A of (Tsiropoulou, Kastrinogiannis, & Papavassiliou, 2009). □

3.2.2.2 Lemma 2

For the NRT users, given:

- The efficiency function $f(\gamma_i)$, which is sigmoid with respect to γ_i and has a unique inflection point $\gamma_{Infl,i}^{f}$ (2nd property of the efficiency function – see section 2.4)
- The actual throughput utility function $T_i(R_i^*)$, which is strictly concave (convex) with respect to R_i^*, where $R_i^* \equiv R_{Max,i}^* f(\gamma_i) = R_i^{Max} f(\gamma_i)$, $i \in L_{NRT}$ (see second definition above)

, then the actual throughput utility function $T_i(\gamma_i) = T_i\left(R_i^{Max} f(\gamma_i)\right)$ is:

1. Sigmoid with respect to γ_i ($\gamma_i \geq 0$), with unique inflection point $\gamma_{Infl,i}^{T}$, such that $\gamma_{Infl,i}^{T} \leq \gamma_{Infl,i}^{f}$ ($\gamma_{Infl,i}^{f} \leq \gamma_{Infl,i}^{T}$), if $\lim_{\gamma_i \to 0^+} \frac{\partial^2 T_i(\gamma_i)}{\partial \gamma_i^2} = 0^+$ ($\lim_{\gamma_i \to \infty} \frac{\partial^2 T_i(\gamma_i)}{\partial \gamma_i^2} = 0^-$) (12)
2. Strictly concave (convex) with respect to γ_i ($\gamma_i \geq 0$), if $\lim_{\gamma_i \to 0^+} \frac{\partial^2 T_i(\gamma_i)}{\partial \gamma_i^2} = 0^-$ (in the convex case: $\lim_{\gamma_i \to \infty} \frac{\partial^2 T_i(\gamma_i)}{\partial \gamma_i^2} = 0^+$) (13)

Proof: See Appendix B of (Tsiropoulou, Kastrinogiannis, & Papavassiliou, 2009). □

According to Lemma (2), when $T_i(R_i^*)$ is strictly concave (convex) with respect to R_i^*, $i \in L_{NRT}$ and the equation (13) applies, then $T_i(\gamma_i)$ will also be strictly concave (convex) with respect to γ_i and p_i, since from equation (2), $\gamma_i \sim p_i$. In the next Lemma, we will prove that in these cases, the utility function $U_i(p_i) = \frac{T_i(p_i)}{p_i}$ has properties that contradict the basic assumptions we made (i.e. $U_i(p_i) \geq 0, \forall p_i \geq 0$, $\lim_{p_i \to 0^+} U_i(p_i) = 0^+$ and that it is bounded above) and therefore such cases become non-feasible in the problem under consideration.

3.2.2.3 Lemma 3

When the function $T_i\left(R_i^*\right), i \in L_{NRT}$ is strictly concave (convex) with respect to R_i^* and the equation (13) applies: $\lim_{\gamma_i \to 0^+} \frac{\partial^2 T_i(\gamma_i)}{\partial \gamma_i^{\,2}} = 0^-$ ($\lim_{\gamma_i \to \infty} \frac{\partial^2 T_i(\gamma_i)}{\partial \gamma_i^{\,2}} = 0^+$) – the second set of conditions of Lemma (2) – then either $\lim_{p_i \to 0^+} U_i(p_i) \neq 0^+$ or $U_i(p_i) < 0, \forall p_i \geq 0$ ($U_i(p_i)$ is not bounded above).

Proof: See Appendix C of (Tsiropoulou, Kastrinogiannis, & Papavassiliou, 2009). □

Corollary: Since equation (13), according to Lemma (3), does not apply because of the utility function that has been chosen (it does not satisfy its basic properties), then the equation (12) should be true: $\lim_{\gamma_i \to 0^+} \frac{\partial^2 T_i(\gamma_i)}{\partial \gamma_i^{\,2}} = 0^+$ ($\lim_{\gamma_i \to \infty} \frac{\partial^2 T_i(\gamma_i)}{\partial \gamma_i^{\,2}} = 0^-$) – the first set of conditions of Lemma (2). Consequently, along with Lemma (1) (see equation (11)) we have proven that $\forall i \in L = L_{NRT} \cup L_{RT}$, $T_i(\gamma_i)$ is a sigmoid function of γ_i and p_i, since from equation (2) we have that: $\gamma_i \sim p_i$.

We can now use the above corollary in order to prove the existence of a unique global maximum of the utility function $U_i\left(p_i, \bar{p}_i\right)$ of user i, provided that the other users' powers do not change and assuming that the femto-users are not under pricing policy (so U_i is given by equation (6)).

3.2.2.4 Lemma 4

For every user $i \in L$, the utility function $U_i\left(p_i, \bar{p}_i\right)$ is a *quasi-concave* function of its own power $p_i \in \left[0, P_i^{Max}\right]$. Moreover, considering that the other users' transmission powers are fixed, $U_i\left(p_i, \bar{p}_i\right)$ has a unique global maximization point p_i^*:

$$p_i^* = \begin{cases} \min\left\{ \dfrac{\gamma_i^* \left(R_{T,i}^* + MF_i \right) I_{s_i,-i}\left(\overline{p}_{-i} \right)}{Wg_{s_i,i}}, P_i^{Max} \right\}, i \in L_{RT} \\ \min\left\{ \dfrac{\gamma_i^* R_i^{Max} I_{s_i,-i}\left(\overline{p}_{-i} \right)}{Wg_{s_i,i}}, P_i^{Max} \right\}, i \in L_{NRT} \end{cases} \quad (14)$$

, where γ_i^* is the unique positive solution to: $\dfrac{\partial T_i(\gamma_i)}{\partial \gamma_i}\gamma_i - T_i(\gamma_i) = 0$ (15).

Proof: See also Appendix D of (Tsiropoulou, Kastrinogiannis, & Papavassiliou, 2009).

Using the corollary, we have that $T_i(p_i)$ is a sigmoid function of $p_i, \forall i \in L$. Also, for $T_i(\gamma_i) = T_i(p_i, \overline{p}_i)$ as a function of p_i with $p_i \geq 0$, the following are true:

1) Its domain is set of all positive real numbers, i.e. the interval $[0, \infty)$.
2) Its codomain is the half-open interval $[0,1)$ according to the properties 3 and 4 of the throughput utility function (see section 2.4).
3) It is an increasing function of $p_i, i \in L$ (since every sigmoid function is a monotonically increasing function).
4) It is strictly convex in the interval $\left(0, p_{Infl}^T\right]$, strictly concave in the interval $\left[p_{Infl}^T, P_i^{Max} \right]$ (from the definition of a sigmoid function with p_{Infl}^T the inflection point of $T(p)$ on the p–axis) and using equation (2), Lemma (1) and Lemma (2), the following applies:

$$p_{Infl,i}^T = \begin{cases} \dfrac{\gamma_{Infl,i}^T \left(R_{T,i}^* + MF_i \right) I_{s_i,-i}\left(\overline{p}_{-i} \right)}{Wg_{s_i,i}}, \forall i \in L_{RT} \\ \dfrac{\gamma_{Infl,i}^T R_i^{Max} I_{s_i,-i}\left(\overline{p}_{-i} \right)}{Wg_{s_i,i}}, \forall i \in L_{NRT} \end{cases}$$

, where $\gamma_{Infl,i}^T$ is the inflection point of $T_i(\gamma_i)$. Generally, we assume that $P_i^{Max} \geq p_{Infl,i}^T$.

5) It has a continuous derivative, since it is a composite function of $T_i\left(R_i^*\right)$ and $f(\gamma_i)$, which have continuous derivatives.

Since the conditions 1-5 above apply for the function $T_i(p_i, \bar{p}_i), \forall i \in L$, then the fraction $T_i(p_i, \bar{p}_i)/p_i, \forall i \in L$ is a quasi-concave function with respect to $p_i \in \left[0, P_i^{Max}\right]$, according to (Rodriguez, 2003). Consequently, since $U_i\left(p_i, \bar{p}_i\right)$ is a quasi-concave function of p_i, it must have a global maximum. Using the First Derivative Test in order to find the maximization point of $U_i\left(p_i, \bar{p}_i\right)$, we get:

$\frac{\partial U_i\left(p_i, \bar{p}_i\right)}{\partial p_i} = \frac{\partial\left(\frac{T_i\left(p_i\right)}{p_i}\right)}{\partial p_i} = \frac{\frac{\partial T_i\left(p_i\right)}{\partial p_i} p_i - T_i\left(p_i\right)}{p_i^2} = 0$, but using equation (2) we have: $\gamma_i = \mu p_i$, with $\mu = \frac{\partial \gamma_i}{\partial p_i} = \frac{\gamma_i}{p_i}$, and so: $\frac{\partial T_i\left(p_i\right)}{\partial p_i} p_i - T_i\left(p_i\right) = 0 \Rightarrow \frac{\partial T_i\left(\gamma_i\right)}{\partial \gamma_i} \gamma_i - T_i\left(\gamma_i\right) = 0$ which is equation (15). Furthermore, since $T_i\left(\gamma_i\right)$ is sigmoid, equation (15) has a unique solution (let's call it γ_i^*), as it is proved in (Rodriguez, 2003). Consequently, the unique value $\hat{p}_i$ that maximizes $U_i\left(p_i, \bar{p}_i\right)$ for $p_i \geq 0$, can be given using equation (2) from this formula:

$$\hat{p}_i = \begin{cases} \frac{\gamma_i^*\left(R_{T,i}^* + MF_i\right) I_{s_i,-i}\left(\bar{p}_{-i}\right)}{W g_{s_i,i}}, \forall i \in L_{RT} \\ \frac{\gamma_i^* R_i^{Max} I_{s_i,-i}\left(\bar{p}_{-i}\right)}{W g_{s_i,i}}, \forall i \in L_{NRT} \end{cases}$$

Finally, when the maximum permitted power value (P_i^{Max}) is smaller than $\hat{p}_i$, then the value $U_i\left(P_i^{Max}, \bar{p}_{-i}\right) = T_i\left(P_i^{Max}, \bar{p}_{-i}\right) \Big/ P_i^{Max}$ becomes the largest possible value of $U_i\left(p_i, \bar{p}_{-i}\right)$, since the utility function U_i is increasing in the closed interval $\left[0, \hat{p}_i\right]$ (see that: $\lim_{p_i \to 0^+} U_i\left(p_i\right) = 0^+$, $\hat{p}_i$ the global maximum point, $P_i^{Max} < \hat{p}_i$ and U_i is quasi-concave). Therefore, the smaller value of $\left\{\hat{p}_i, P_i^{Max}\right\}$ is the global maximization point of the utility function $U_i\left(p_i, \bar{p}_{-i}\right), p_i \in \left[0, P_i^{Max}\right]$, i.e. $p_i^* = \min\left\{\hat{p}_i, P_i^{Max}\right\}$ (which proves equation (14)). □

By considering Lemma 4 and assuming that no user is under pricing policy, we conclude that in order for the users to maximize their utility (expressed through the quasi-concave function U_i – see equation (6)) and thus their degree of satisfaction in terms of QoS-aware performance and corresponding energy consumption per time slot, they constantly attempt to meet specific SINRs (γ_i^*) at the base station, which eventually leads to an SINR-balanced network. Also, if a user's maximum transmission power is not

sufficient for reaching the targeted γ_i^*, due to its potentially bad channel conditions, then the best policy is to transmit with maximum power (P_i^{Max}), which corresponds to a SINR $\gamma_i' < \gamma_i^*$ and which constitutes the best response $r_i\left(\bar{p}\right)$ of user i.

3.2.3 Properties of The Total Utility Function

The next two lemmas help us to better understand some properties of the total utility function U_i^{net} (which includes pricing) as expressed in equation (7). Lemma (5) shows the relative position between two characteristic power values, mainly p_{Infl}^T (the unique inflection point of $T_i\left(p_i\right)$ – see corollary above) and p_i^* (the global maximization point of $U_i\left(p_i, \bar{p}_{-i}\right)$ – see equation (14)). In Lemma (6), we prove that there is a critical power value in U_i^{net} which helps us later in the proof of the existence and uniqueness of the *NE* for the femto-users.

3.2.3.1 Lemma 5

Given:

$\begin{cases} T(p) \equiv T\left(R_{max}^* f(\gamma)\right), \text{which is a sigmoid function of } p \text{ with unique inflection point } p_{Infl}^T \\ U(P) = \frac{T(p)}{p}, \text{ which is a quasi-concave function of } p \text{ (Lemma 4) with global maximum point } p^* \end{cases}$, it can be proved by contradiction that $p_{Infl}^T < p^*$.

Proof: See Appendix A of (Tsiropoulou, Katsinis, & Papavassiliou, 2012). □

3.2.3.2 Lemma 6

Given:

$\begin{cases} T(p) \equiv T\left(R_{max}^{*} f(\gamma)\right), \text{which is a sigmoid function of } p \text{ with unique inflection point } p_{Infl}^{T} \\ U(P) = \frac{T(p)}{p}, \text{ which is a quasi-concave function of } p \text{ (Lemma 4) with global maximum point } p^{*} \end{cases}$,

there exists a critical power value $p_{crit} \in \left[p_{Infl}^{T}, p^{*} \right)$ ($p_{Infl}^{T} < p^{*}$ from Lemma (5)) such that the function $U^{net}(p) = U(p) - C(p)$ is a monotonically decreasing function of p in the interval $p \in \left[p_{crit}, \infty \right)$.

Proof: See Appendix B of (Tsiropoulou, Katsinis, & Papavassiliou, 2012). □

By visualizing the result of Lemma (6), we now have a better image of the form of the function $U^{net}(p)$ with respect to the power p (considering both RT and NRT services). Specifically, we proved that if the function $U^{net}(p)$ has a global maximum point, this will reside in the interval $\left(0, p_{crit}\right]$, since for $p \geq p_{crit}$, $U^{net}(p)$ is decreasing. Let's call that point p_{net}^{*}. So, we have that: $p_{net}^{*} \in \left(0, p_{crit}\right]$ with $p_{crit} \in \left[p_{Infl}^{T}, p^{*} \right)$ and thus $p_{net}^{*} < p^{*}$, which shows that in order for the femto-users to maximize their utility $U^{net}(p)$ (which includes pricing), they transmit with a lower power value than what they would normally do without such policy (i.e. if their utility was $U(p)$ with a maximization point given in equation (14)) and as a result they succeed in limiting the cross-tier interference they would cause the macro-users which have higher priority in ensuring the satisfaction of their QoS requirements.

3.3 Existence and Uniqueness of the Nash Equilibrium

From the definition of the (*MTTPG*) game (see equation (10)) we can see that the users/players try independently from each other to maximize their utility $U_i^{net}\left(p_i,\bar{p}_{-i}\right)$ (see equation (9)) by choosing a strategy p_i that not only will satisfy their QoS needs but – provided that the other users' powers do not change – will also be the global maximization point of the function $U_i^{net}\left(p_i,\bar{p}_{-i}\right)$. The set of all the users' strategies will then be the unique *Nash Equilibrium* of the (*MTTPG*) game. However, the existence of a global maximum of $U_i^{net}\left(p_i\right)$ is related to its form and properties as a function of p_i: macro-users are not under pricing policy and so their total utility function is different from the one which we assigned to the femto-users (which are subject to such pricing schemes). Therefore, the proof of the existence of a global maximum of U_i^{net} will have two parts: one for the macro-users where $U_i^{net}\left(p_i\right)=U_i\left(p_i\right)$ and one for the femto-users where $U_i^{net}\left(p_i\right)=U_i\left(p_i\right)-C_i\left(p_i\right)$. Moreover, the proof takes into account the four different kinds of users that exist in the network under consideration, as it can immediately be seen from the $U_i^{net}\left(p_i,\bar{p}_{-i}\right)$ formula (see equation (9)).

Theorem 1 (Existence and Uniqueness of the *NE*): The function $U_i^{net}\left(p_i,\bar{p}_{-i}\right)$ (9) of the (*MTTPG*) game (10) has a global (unique) maximum, $p_{net,i}^{*}$, such that: $\begin{cases} p_{net,i}^{*}\equiv p_i^{*} & ,i\in L_m \\ p_{net,i}^{*}\in\left(0,p_{crit,i}\right] & ,i\in L_f \end{cases}$, where p_i^{*} is the global maximization point of the utility function $U_i\left(p_i,\bar{p}_{-i}\right)$ from Lemma (4) (see equation (14)), while $p_{crit,i}$ is the critical power value mentioned in Lemma (6). The power vector $\bar{p}_{net}^{*}=\left(p_{net,1}^{*},\ldots,p_{net,L}^{*}\right)$ is the unique *NE* of the (*MTTPG*) game and is given by:

$$p_{net,i}^{*}=\begin{cases} \min\left\{\dfrac{\gamma_i^{*}\left(R_{T,i}^{*}+MF_i\right)I_{s_i,-i}\left(\bar{p}_{-i}\right)}{Wg_{s_i,i}},P_i^{Max}\right\}, i\in L_{m,RT} & (16.1) \\ \min\left\{\dfrac{\gamma_i^{*}R_i^{Max}I_{s_i,-i}\left(\bar{p}_{-i}\right)}{Wg_{s_i,i}},P_i^{Max}\right\} \quad ,i\in L_{m,NRT} & (16.2) \\ \min\left\{\min_{p_{k,i}\in\Lambda_{k,i}}\left(\Lambda_{k,i}\right),P_i^{Max}\right\},\ i\in L_f=L_{f,RT}\cup L_{f,NRT} & (16.3) \end{cases} \qquad (16)$$

Notes on the formula above:

- $I_{s_i,-i}\left(\overline{p}_{-i}\right)$ is the total interference (plus noise) received at the base station $s_i \in S$, while its user i sends data on the uplink channel.
- P_i^{Max} is the maximum transmission power that a user can utilize.
- The SINR value γ_i^* is the unique positive solution to equation (15): $\frac{\partial T_i\left(\gamma_i\right)}{\partial \gamma_i}\gamma_i - T_i\left(\gamma_i\right) = 0$.
- $\Lambda_{k,i} = \left\{p_{1,i}^*, p_{2,i}^*, \ldots, p_{K,i}^*\right\},\ k = 1,2,\ldots,K,\ i \in L_f$ is the set of local maximum points of the function $U_i^{net}\left(p_i\right)$ with $p_{k,i}^* \in \left(0, p_{crit,i}\right]$. These points can be found using the Second Derivative Test: $\left.\frac{\partial U_i^{net}\left(p_i\right)}{\partial p_i}\right|_{p_i = p_{k,i}} = 0$ and $\left.\frac{\partial^2 U_i^{net}\left(p_i\right)}{\partial^2 p_i}\right|_{p_i = p_{k,i}} < 0$, with $U_i^{net}\left(p_i\right)$ given from equation (9) for $i \in L_{f,RT}$ and $i \in L_{f,NRT}$ respectively.

Proof:

Case 1: Macro-users $\left(i \in L_m = L_{m,NRT} \cup L_{m,RT}\right)$: From equation (9), we have that: $U_i^{net}\left(p_i, \overline{p}_{-i}\right) = U_i\left(p_i, \overline{p}_{-i}\right) = \frac{T\left(p_i\right)}{p_i}, \forall i \in L_m$ and so, using Lemma (4), $U_i^{net}\left(p_i\right)$ is quasi-concave with respect to p_i and since it is defined in a non-empty, convex and compact set – $\left(\left[0, P_i^{Max}\right]\right)$ – in which it is also continuous, there is a *NE* for the macro-users (for the proof see (Saraydar, Mandayam, & Goodman, 2002)). Using equation (14), we can find the global maximization point of $U_i^{net}\left(p_i\right)$ which corresponds to the macro-RT-users ($i \in L_{m,RT}$ – see equation (16.1)) and to the macro-NRT-users respectively ($i \in L_{m,NRT}$ – see equation (16.2)). The uniqueness of this maximization point (and thus of the corresponding *NE*) is ensured by the fact that the equation (15) has also a unique solution, due to $T_i\left(\gamma_i\right)$ being a sigmoid function with respect to γ_i, $\forall i \in L_m$ (see corollary of Lemma (3)). Thus, the significance of the sigmoidal form of the function $T_i\left(\gamma_i\right)$ is shown, since if instead of the conditions (12), the conditions (13) were true, then not only the function $T_i\left(\gamma_i\right), i \in L_{m,NRT}$ would lose its sigmoidal form and using Lemma (3) it would contradict

basic properties of the utility function, but the (*MTTPG*) game wouldn't have a unique *NE* for the macro-users, making the system unstable.

Case 2: Femto-users $\left(i \in L_f = L_{f,NRT} \cup L_{f,RT}\right)$: From equation (9), we have that: $U_i^{net}\left(p_i, \overline{p}_{-i}\right) = U_i\left(p_i, \overline{p}_{-i}\right) - C_i\left(p_i, \overline{p}_{-i}\right), \forall i \in L_f, L_f = L_{f,NRT} \cup L_{f,NRT}$. Since the femto-users' total utility function includes the cost function, it does not keep the quasi-concaveness property of the simple utility function. Thus, we cannot draw conclusions for the existence and uniqueness of the *NE* from that property as we did in the macro-users' case. In Lemma (6), we proved that there is a critical power value $p_{crit,i}$ such that U_i^{net} is a decreasing function of p_i, for $p_i \in \left[p_{crit}, \infty\right)$ – so if U_i^{net} has a global maximization point, it should lie in the interval $\left(0, p_{crit,i}\right]$.

Since $U_i^{net}\left(p_i, \overline{p}_{-i}\right) = U_i\left(p_i, \overline{p}_{-i}\right) - C_i\left(p_i, \overline{p}_{-i}\right), \forall i \in L_f$ (see equation (9)) is continuous on the closed interval $\left[0, p_{crit,i}\right]$[2] – using Weierstrass's Extreme Value Theorem (Goffman, 1971) we get the result that the function $U_i^{net}\left(p_i\right)$ has a global maximum in that interval and there is a point $p_{net,i}^*$, which is the unique *NE* of the (*MTTPG*) game for the femto-users. We can find this point using equation (16.3), which finds the smallest value from the set of local maximum points of $U_i^{net}\left(p_i\right)$ in the interval $\left(0, p_{crit,i}\right]$ (this set also includes the global maximum point), compares it with P_i^{Max} and chooses the smallest value of the two as the equilibrium power of the femto-user i. □

[2] $C_i\left(p_i, \overline{p}_{-i}\right)$ is an exponential continuous function and $U_i(p_i) = {T_i(p_i)}/{p_i}$ is continuous on the interval $(0, p_{crit,i}]$ using the quotient rule. Continuity of the function $U_i(p_i) = {T_i(p_i)}/{p_i}$ at 0^+ can be proven using L' Hospital's rule and the fact that $T_i(p_i)$ is sigmoid: $\lim_{\gamma \to 0^+} \frac{\partial T_i(p_i)}{\partial p_i} = 0^+$.

3.4 Remarks regarding the Local Maxima of the Total Utility Function

In this section, we perform an analysis regarding the local maximization points of the total utility function $U_i^{net}(p_i)$ in the interval $\left(0, p_{crit,i}\right]$ for $i \in L_f$. These points are the power values $p_{k,i} \in \Lambda_{k,i}$, $k = 1, 2, \ldots, K$ as we can see from equation (16.3) and can be found using the First Derivative Test:

$$\frac{\partial U_i^{net}(p_i)}{\partial p_i} = 0 \Rightarrow \frac{\partial U_i(p_i)}{\partial p_i} - \frac{\partial C_i(p_i)}{\partial p_i} = 0 \qquad (17)$$

In the case of the macro-users which are not under pricing policy, we have that: $C_i(p_i, \bar{p}_{-i}) = 0$ and so equation (17) simplifies to: $\frac{\partial U_i(p_i)}{\partial p_i} = 0 \Rightarrow \frac{\partial T_i(\gamma_i)}{\partial \gamma_i}\gamma_i - T_i(\gamma_i) = 0$, which is equation (15) and has a unique solution γ_i^* because of the sigmoidal form of the function $T_i(\gamma_i)$ (as it was proved in (Rodriguez, 2003)). On the other hand, in the case of the femto-users which are under a pricing scheme, using equation (8): $C(p_i, \bar{p}_{-i}) = c\left(e^{p_i} - 1\right),\ i \in L_f$, equation (17) now becomes:

$$\frac{\partial U_i^{net}(p_i)}{\partial p_i} = 0 \Rightarrow \frac{\partial}{\partial p_i}\left(\frac{T_i(p_i)}{p_i}\right) - \frac{\partial C_i(p_i)}{\partial p_i} = 0 \Rightarrow \frac{\frac{\partial T_i(p_i)}{\partial p_i}p_i - T_i(p_i)}{p_i^2} - ce^{p_i} = 0 \Rightarrow$$

$$\frac{\partial T_i(p_i)}{\partial p_i}p_i - T_i(p_i) = cp_i^2 e^{p_i} \xrightarrow{\text{General Form}} G(p) = F(c,p) \qquad (18)$$

Equation (18) shows that the local maximization points are precisely the intersection points of the functions $G(p)$ and $F(c,p)$. The solutions of equation (18) depend on the choice of the pricing factor c, making it impossible to analytically find them and draw conclusions regarding the number K of the elements of the set $\Lambda_{k,i}$. However, by further studying the functions G and F, we can make a qualitative graphical representation of their intersection points and thus better estimate the number of maximization points K.

1. Properties of function $F(c, p) = cp^2 e^p, c \geq 0$:

   a. $F(0) = 0$

   b. $F'(p) = cpe^p(2+p) > 0, \forall p > 0$, so F is a strictly increasing function.

   c. $F''(p) > 0, \forall p > 0$, so F is strictly convex.

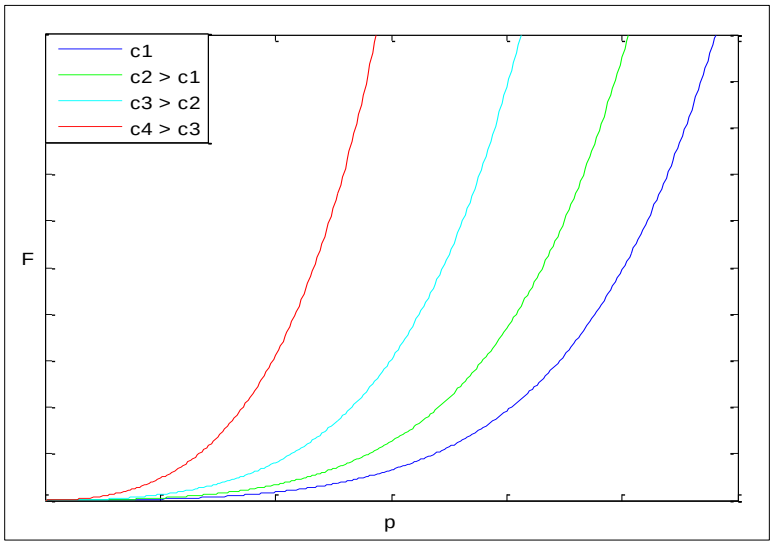

Figure 11: Graph of function F for different values of the pricing factor c

From Figure 11, we note that the larger the pricing factor c, the steeper the function F's curve is.

2. Properties of function $G(p) = \frac{\partial T(p)}{\partial p} p - T(p)$:

   a. $G(0) = \left.\frac{\partial T(p)}{\partial p}\right|_{p=0} * 0 - T(0) = 0$

   b. $G'(p) = \frac{\partial^2 T(p)}{\partial p^2}, p \geq 0$ which shows that the sign of $G'(p)$ depends on the sign of the term $\frac{\partial^2 T(p)}{\partial p^2}$.

c. Let p^* be the global maximization point of the quasi-concave utility function $U(p)$ such that: $\left.\frac{\partial U}{\partial p}\right|_{p=p^*} = 0$. From (Rodriguez, 2003) we have that for $p < p^*$, $U(p)$ is strictly increasing whereas for $p > p^*$, $U(p)$ is strictly decreasing. Also: $\frac{\partial U}{\partial p} = \frac{G(p)}{p^2}$, which means that if the sign of the function $\frac{\partial U}{\partial p}$ changes, so will the sign of $G(p)$, since the study is done for positive values of p. So, we have that:

$$\begin{cases} p < p^* \Rightarrow \left.\frac{\partial U}{\partial p}\right|_{p<p^*} > 0 \Rightarrow G(p) > 0 \\ p = p^* \Rightarrow \left.\frac{\partial U}{\partial p}\right|_{p=p^*} = 0 \Rightarrow \left.\frac{G(p)}{p^2}\right|_{p=p^*} = 0 \Rightarrow G(p^*) = 0 \\ p > p^* \Rightarrow \left.\frac{\partial U}{\partial p}\right|_{p>p^*} < 0 \Rightarrow G(p) < 0 \end{cases}$$

d. Since $T(p)$ is sigmoid with unique inflection point p_{Infl}^T, the following equations are true:

$$\begin{cases} p < p_{Infl}^T \Rightarrow \left.\frac{\partial^2 T(p)}{\partial p^2}\right|_{p<p_{Infl}^T} > 0 \Rightarrow G'(p) > 0 \Rightarrow G \text{ increasing} \\ p = p_{Infl}^T \Rightarrow \left.\frac{\partial^2 T(p)}{\partial p^2}\right|_{p=p_{Infl}^T} = 0 \Rightarrow G'(p) = 0 \Rightarrow \text{maximum point of } G \\ p > p_{Infl}^T \Rightarrow \left.\frac{\partial^2 T(p)}{\partial p^2}\right|_{p>p_{Infl}^T} < 0 \Rightarrow G(p) < 0 \Rightarrow G \text{ decreasing} \end{cases}$$

e. Lastly, using Lemma (5), we have that: $p_{Infl}^T < p^*$.

Based on the properties above, we made an approximate graph of the two functions under study (see Figure 12). Note that the blue point on the p-axis corresponds to the value p_{Infl}^T, while the red point to the value p^*. Also, the function $F(c,p)$ is drawn for three different values of the pricing factor c.

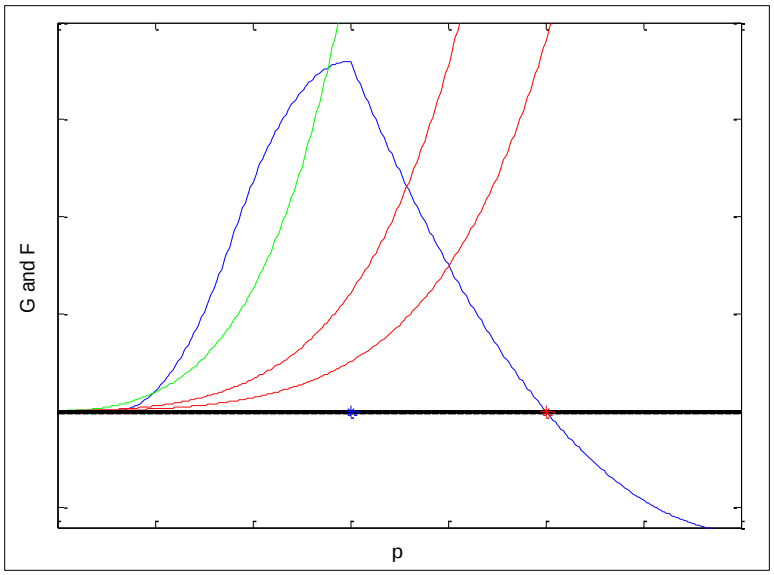

Figure 12: The plot of functions G(p) (blue) and F(c, p) (red, green)

Notes:

1. Since equation (18) always has a solution – the existence of the *NE* was proven in Theorem (1) – the intersection points of F, G are either one (see in Figure 12 that the two red curves intersect the blue curve one time each) and thus this unique point is chosen as the optimal equilibrium power p_{net}^{*}, or two (see in Figure 12 that the green curve intersects the blue curve twice), from which (see equation (16.3)) the smallest value is chosen. It is important to remember that the First Derivative Test is a necessary but not always sufficient condition to find the maximum of the total utility function: the second order derivative should also be calculated in order to verify that: $\left.\frac{\partial^2 U^{net}(p)}{\partial p^2}\right|_{p=p_{net}^{*}} < 0.$
2. Considering the above remark, we conclude that the set $\Lambda_{k,i}$ that contains all the local maximum points of $U^{net}(p)$ in the interval $\left(0, p_{crit}\right]$ (see Lemma (6)), has $K \leq 2$ elements (the corresponding intersection points of the functions F, G).
3. Whichever intersection point we choose from Figure 12 between the two functions under consideration, it corresponds to a power value $p_{net}^{*} < p^{*}$ (the red point on the p-axis), which is in agreement with the remark after Lemma (6), i.e. that the femto-users transmit at lower equilibrium powers under the pricing mechanism than what they would do without such a policy, limiting thus the interference they would otherwise cause to the other users of the network.

3.5 MTTPG Algorithm and Convergence to the Nash Equilibrium

In this section, based on the previous analysis, we introduce an iterative, distributed, slot-based, uplink power control algorithm that determines the optimal power allocation in the Two-Tier Cellular Network under consideration, which is also the unique Nash Equilibrium point of the (*MTTPG*) game. The algorithm consists of two parts:

1. **Network Part:** This part is executed at the macrocell base station (MBS). The MBS broadcasts the pricing factor c to the femto-users (the macro-users ignore this value since they are not under any pricing policy) and calculates the total utility from all the network users (femto and macro), expressed via their $U_i^{net}, \forall i \in L$. Finally, the MBS determines the best pricing factor (c_{best}) of the femto-users, which is a value that maximizes the total utility achieved in the network and brings the system to maximum efficiency/throughput.
2. **User part:** This part is executed individually on each user/player of the non-cooperative (*MTTPG*) game. After the user i receives the pricing factor c, he calculates the optimal transmission power (i.e. the Nash Equilibrium power) using one of the equations (16) based on what kind of user he is.

We will now present the two-part algorithm more analytically:

MTTPG Algorithm – Network Part:

1. Announce the initial pricing factor $c = 0$ to the femto-users.
2. Each user $i \in L$ determines (according to the MTTPG Algorithm – User Part) the equilibrium transmission power $p_{net,i}^{*}$ and calculates his total utility $U_i^{net}(\cdot)$.
3. Increase the pricing factor $c := c + \Delta c$ and announce it to the femto-users.
4. If the total utilities of the femto-users improve, i.e. $U_i^{net,c} \le U_i^{net,c+\Delta c}, \forall i \in L_f$ go to step (2). Otherwise, stop and set $c_{best} := c$ (Saraydar, Mandayam, & Goodman, 2002).

MTTPG Algorithm – User Part:

1. At the beginning of the time slot t, user i transmits with a randomly selected feasible power $p_{net,i}^{*}{}^{(0)}$, such that (for $k = 0$): $p_{net,i}^{*}{}^{(0)} \in \left[0, P_i^{Max}\right]$.

2. Every station s in the network (a FAP or the MBS) broadcasts to its users the value of the total interference that it receives from all the network users (femto and macro), which is the value $I_s^{(k)}\left(\bar{p}_{net}^{*\,(k)}\right), \forall s \in S$. The user i that is served by the station $s_i \in S$, calculates the value $I_{s_i,-i}^{(k)}\left(\bar{p}_{net,-i}^{*\,(k)}\right) = I_{s_i}^{(k)}\left(\bar{p}_{net}^{*\,(k)}\right) - g_{s_i,i}\, p_{net,i}^{*\,(k)}$ and then refines his power, computing the new value $p_{net,i}^{*\,(k+1)}$ using equation (16).
3. If the powers converge, i.e. $\left|p_{net,i}^{*\,(k+1)} - p_{net,i}^{*\,(k)}\right| \le 10^{-5}, \forall i \in L$ then stop, otherwise set $k := k+1$ and proceed to step (2).

Note that the MTTPG Algorithm is efficiently designed so as to reduce the need for heavy computations on the users' devices. This is demonstrated on the step (2) of the MTTPG Algorithm – User Part, where in order to compute the optimal transmission power, each user does not need the information of all the path gains g of the other users to his serving station and neither their power values. In this way, not only the complexity of the proposed algorithm is decreased, but also the signaling required for its execution on the wireless network. Moreover, since less computational power is required for the user's device, its battery life increases.

The next Theorem proves that the above MTTPG Algorithm – User Part does indeed converge to the unique *NE* of the corresponding (*MTTPG*) game, as it is given from equation (16):

Theorem 2 (MTTPG Algorithm Convergence): The MTTPG Algorithm converges to the unique Nash Equilibrium of the (*MTTPG*) game, as it was defined in equation (16) for every user/player, starting with any initial strategy ($p_{net,i}^{*\,(0)}$ – see step (1) above).

Proof: In Theorem 1, the existence and uniqueness of the *NE* – defined as the power vector $\bar{p}_{net}^{*} = \left(p_{net,1}^{*}, \ldots, p_{net,m+2N}^{*}\right)$ where each power $p_{net,i}^{*}$ is given using equation (16) – of the (*MTTPG*) game was proved. Considering the Definition (4) and the note afterwards, at the Nash Equilibrium the following will apply: $\bar{p}_{net}^{*} = \bar{r}\left(\bar{p}_{net}^{*}\right)$, where $\bar{r}\left(\bar{p}_{net}^{*}\right) = \left(r_1\left(\bar{p}_{net}^{*}\right), r_2\left(\bar{p}_{net}^{*}\right), \ldots, r_L\left(\bar{p}_{net}^{*}\right)\right)$ is the vector of best responses of all the users at the equilibrium, using the convection that $r_j\left(\bar{p}_{net}^{*}\right) \equiv r_j\left(\bar{p}_{net,-j}^{*}\right)$. In order to

prove the convergence of the MTTPG algorithm to the unique *NE* of the corresponding game, it is sufficient to prove that the best response function is a standard function (Saraydar, Mandayam, & Goodman, 2002). The function $\bar{r}\left(\bar{p}\right)$ is standard, if for every $\bar{p} \geq 0$, $\bar{p} = \left(p_1, p_2, \ldots, p_L\right)$, it satisfies the following three properties:

1. Positivity: $\bar{r}\left(\bar{p}\right) \geq 0$
2. Monotonicity: If $\bar{p}' \geq \bar{p}$, then $\bar{r}\left(\bar{p}'\right) \geq \bar{r}\left(\bar{p}\right)$
3. Scalability: $\forall a > 1$, then $a \cdot \bar{r}\left(\bar{p}\right) \geq \bar{r}\left(a \cdot \bar{p}\right)$

Using the fact that $\bar{p}_{net}^{*} = \bar{r}\left(\bar{p}_{net}^{*}\right)$ and for very user j the best response function is $r_j\left(\bar{p}_{net}^{*}\right) = p_{net,j}^{*}$, where the power value $p_{net,j}^{*}$ is defined in equation (16) for every user/player, we can easily prove that the best response function of the (*MTTPG*) game satisfies the three aforementioned properties and thus, it is a standard function. So, according to (Yates, 1995), the fixed point $\bar{p}_{net}^{*} = \bar{r}\left(\bar{p}_{net}^{*}\right)$ is unique and consequently the convergence of the MTTPG algorithm under the proposed response strategy (see equation (16)) is guaranteed.

4. Case Scenarios and Numerical Results

4.1 Simulation environment and parameter selection

In this section, we will present and analyze results regarding the system's efficiency under the proposed MTTPG algorithm for different case scenarios. These scenarios differ from one another with respect to the topology of the system (i.e. the corresponding position of the users and the FAPs inside the macrocell). Specifically, in each case scenario, we graphically present quantities such as the power consumption per user, the uplink data rate per user achieved, the users' SINR as well as the total utility of every user. These results are also distinguished based on the kind of services the users want (RT and NRT services) and/or the tier they belong to (femtocell or macrocell). The graphing plots and the source code that calculates the equilibrium power vector as well as the other quantities mentioned, were designed and implemented using the computing environment Matlab.

We will now present the simulation parameters used for the implementation of the MTTPG algorithm and the computation of functions such as the efficiency function $f(\gamma_i)$ and the actual throughput utility function $T_i(R_i^*)$ taking also into account the kind of service the users want to satisfy on each of the case scenarios. Regarding the propagation loss constants and the path loss exponents used in the propagation model (see equation (1)), we chose the values from the next table:

Propagation Parameter	**Value**
$K_{f_0} = K_c$	10 dB (0.1)
K_{f_i}	20 dB (0.01)
W	5 dB (0.32)
$a_c = a_{f_0} = a$	4
b	3

Furthermore, as discussed in section 2.4, we assume that the efficiency function is the same for all users during our simulations and we chose to use the sigmoid function: $f(\gamma_i) = \left(1 - e^{-3.7\gamma_i}\right)^{80}$

(Tsiropoulou, Katsinis, & Papavassiliou, 2012) which satisfies the four properties of the general efficiency function (again see section 2.4). Regarding the satisfaction of the different QoS user requirements (RT and NRT services – see section 2.5) which is reflected upon the choice of the form of the actual throughput utility function $T_i(R_i^*)$, we have that:

$$T_i\left(R_i^*\right)=\begin{cases}\log\left(b\cdot R_i^*+1\right), \forall i\in L_{NRT}=L_{m,NRT}+L_{f,NRT}\\ \left(1-e^{-\left(R_i^*-R_{Min,i}^*\right)}\right)^M, \forall i\in L_{RT}=L_{m,RT}+L_{f,RT}\end{cases}$$, where $R_i^*=R_i^F f\left(\gamma_i\right)$ (see equation (3)),

$R_i^F=\begin{cases}R_i^{Max}, i\in L_{NRT}\\ R_{Max,i}^*, i\in L_{RT}\end{cases}$ (see definition (1) and (2)) and $R_{Max,i}^*=R_{T,i}^*+MF_i$, $R_{Min,i}^*=R_{T,i}^*-MF_i$. The values used on the functions' parameters are presented in the next table (Tsiropoulou, Katsinis, & Papavassiliou, 2012):

Function Parameters	**Value**
b	0.001
M	2000
$R_{T,i}^*$	64 Kbps
MF_i	10 Kbps
$\left[R_{Min,i}^*, R_{Max,i}^*\right]$	$[54, 74]$ Kbps
R_i^{Max}	2.4 Mbps

Notice that the functions $T_i(R_i^*)$ selected in each user case do not only satisfy the five properties of the general throughput utility function (see section 2.4) but they are also in agreement with the definitions (1) and (2), which are summarized into: $T_i(R_i^*)=\begin{cases}\text{sigmoid}, \forall i\in L_{RT}\\ \text{concave}, \forall i\in L_{NRT}\end{cases}$. Moreover, the maximum permissible transmission power was set at 2 Watts (see section 2.1) as well as the initial power value used in the step (1) of the MTTPG algorithm: $p_{net,i}^{*(0)}=P_i^{Max}=2\text{ W}, \forall i\in L$ (since the proposed algorithm converges independently of the choice of the initial power value). Finally, the bandwidth of the CDMA system under consideration is $10^6\,Hz$, while the noise power (see equation (2)) was set equal to $5\cdot 10^{-16}W$.

4.2 Results

We will now present five case scenarios where various aspects of the Two-Tier Cellular Network under study are examined and analyzed. Before that, we have to decide on the best pricing factor (c_{best}) of the femto-users in order to use it on later simulations as a predefined parameter.

4.2.1 Finding the best pricing factor

In this section, using the Network Part of the MTTPG algorithm, we find the value c_{best} which is the femto-users' pricing factor that maximizes the network efficiency (which corresponds to a greater total utility of the system users). The network topology used in this case was as follows: 10 macro-users (5 voice users and 5 data users) randomly placed inside the macrocell and 3 FAPs (each one with two users as mentioned in section 2.1). The measurements made were the average power per user and the sum of all the network users' utility $\left(\sum_{\forall i \in L} U_i^{net}(\cdot)\right)$, for different values of the pricing factor c: $c = 10^1, 10^{1.5}, 10^2, 10^{2.5}, \ldots$

In order to better understand the users' interaction with the network – through the utility that they derive after using its resources and their degree of satisfaction in terms of QoS-aware performance – as well as the change of the average power per user through the change of the network's topology (since in the next scenarios we will test many different use cases), the previous measurements were repeated another three times by adding two new FAPs in the network each time (without changing the positions of the macro-users or the previously placed FAPs). Thus, in the last series of measurements (where the system has now $3 \times 2 = 6$ extra FAPs), the network topology is as in Figure 13:

Note: In all the next figures, unless otherwise indicated, we will use the red color to represent the data NRT users while with blue color we will represent the voice RT users. The circle "o" will denote the femto-users while we will use the "x" symbol for the macro-users. The MBS is located at the coordinates $(500, 500)$ and has a radius of $R_c = 500m$ (red circle) whereas for every femtocell the radius is $R_f = 50m$ (green circles).

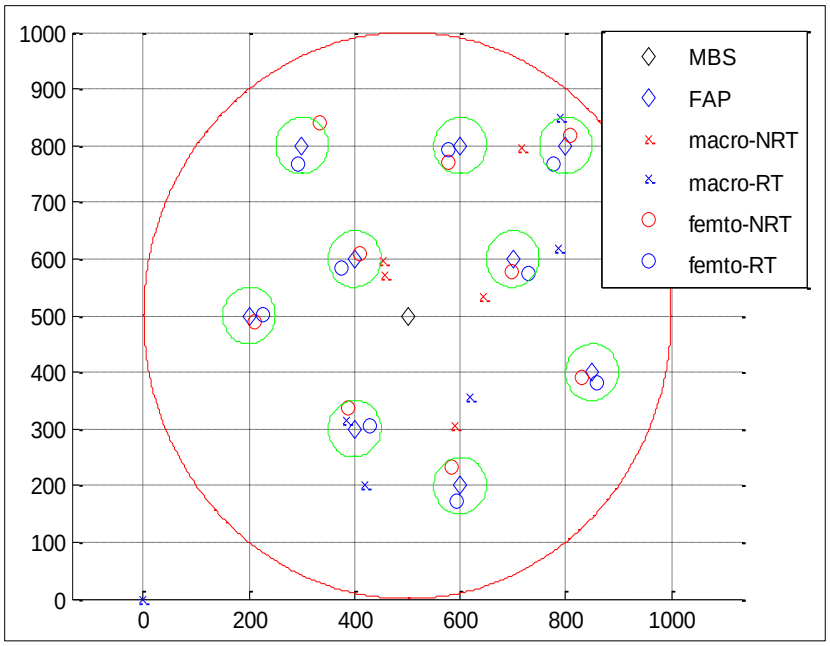

Figure 13: Network topology with 9 FAPs and 10 macro-users

By studying Figures 14 and 15, we conclude that the average power per user shows a small drop for values of the pricing factor larger than 10^8, which corresponds to an analogous increase in the total utility of the system. For values $c > 10^{10}$ the system stabilizes, i.e. there is no further decrease in the average power per user and thus the total utility remains unchangeable.

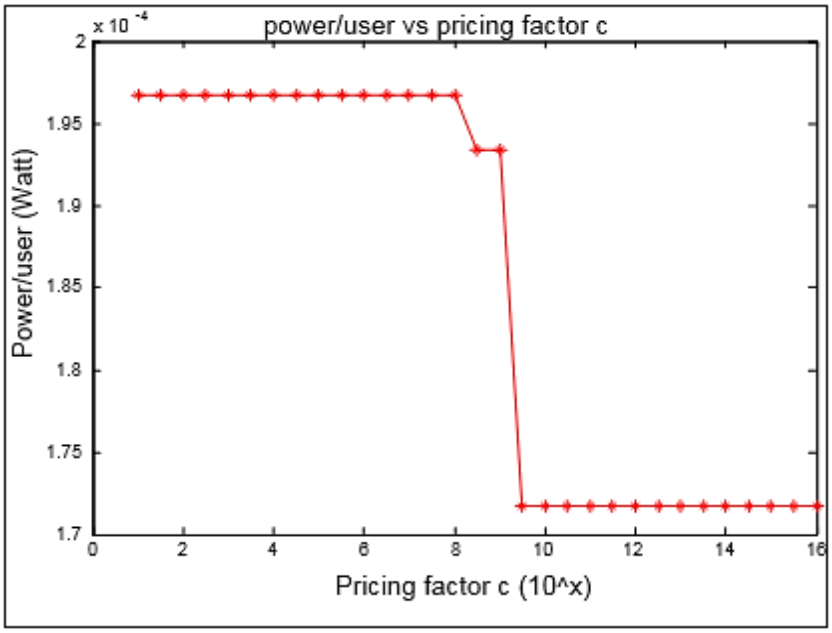

Figure 14: Average power per user for a network with 3 FAPs

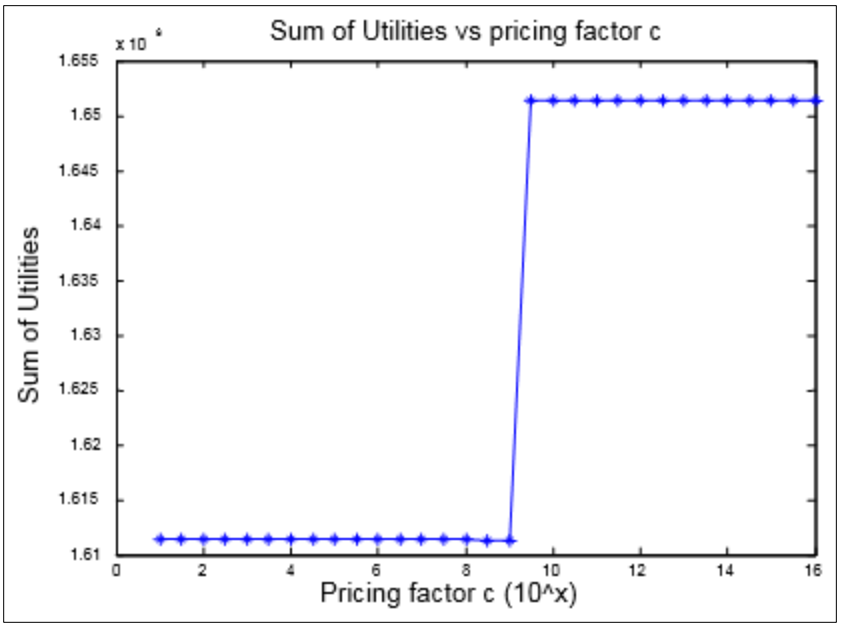

Figure 15: Total user Utility for a network with 3 FAPs

Continuing, in Figures 16 and 17, we observe that even though the topology of the network was changed (2 FAPs were added – so 4 new users), the graphing plots have the same form as before – the only difference being that now the total network user utility displays a peak and then stabilizes on a lower value.

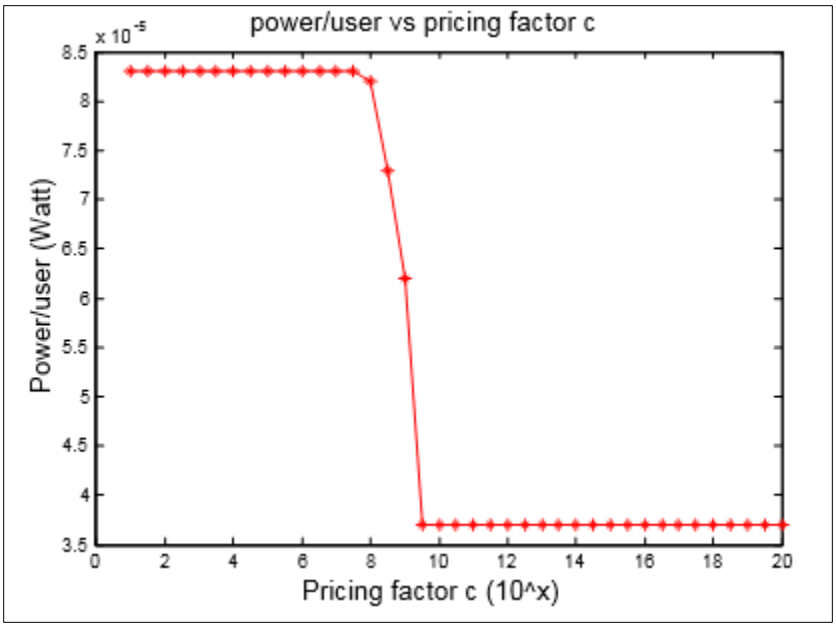

Figure 16: Average power per user for a network with 5 FAPs

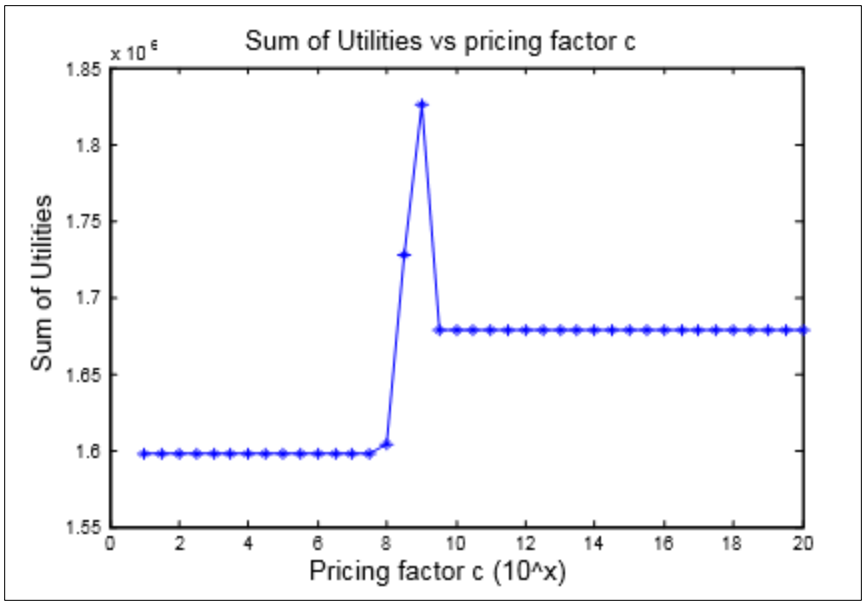

Figure 17: Total user Utility for a network with 5 FAPs

In Figures 18 and 19, we observe a normalization of the graphs (they become curvier) as well as a larger range of changes in the values of the examined quantities (in previous figures the changes were too small to draw meaningful conclusions).

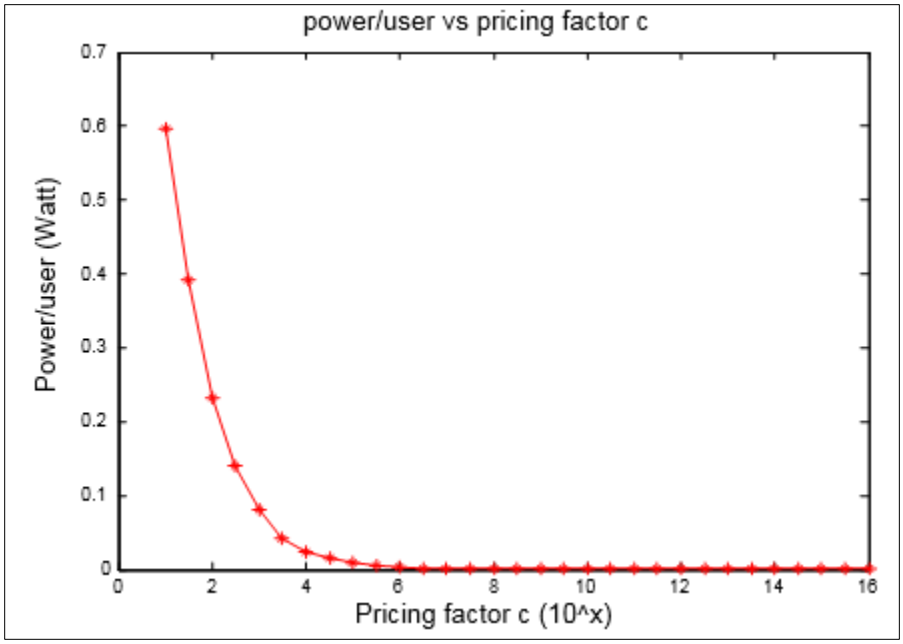

Figure 18: Average power per user for a network with 7 FAPs

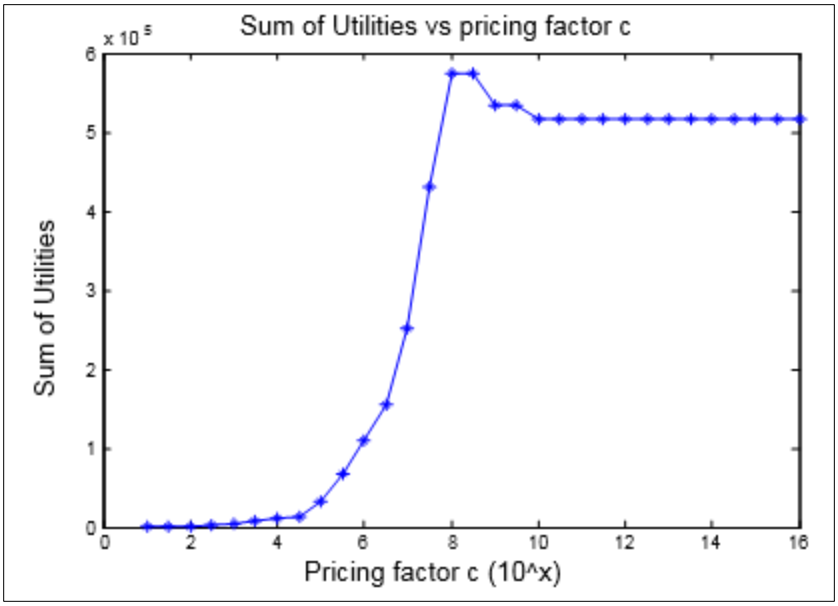

Figure 19: Total user Utility for a network with 7 FAPs

The main reason for the normalization observed in the previous graphs is the addition of more users to the network (the two new FAPs inside the macrocell). Specifically, in order to better understand the interaction between the femto and macro-users with regards to the pricing scheme imposed on the former, the new FAPs were placed in an area of the macrocell that had many macro-users nearby (see Figure 13) and so, since the macro-users were now next to or even inside the radius of the newly added FAPs, this allowed us to see the effect of a larger pricing factor c to the femto-users, which forces them to lower their respective transmission powers (making also the macro-users lower their own transmission powers since the interference was reduced). Thus, while with a non-pricing policy the users to have an average power of 0.6 Watts, with pricing this value reduces to the order of mW. Note that for values of c between 10^6 and 10^{10} the transmission power is further reduced but this change cannot be seen in Figure 18 because of the difference in the order of magnitude between the initial non-pricing-policy power value and the values for $c \geq 10^6$.

We observe a similar behavior in Figure 19, where because of the large interference between the femto-users and the macro-users that are near the corresponding FAPs, the total user utility has small values which nonetheless increase when we raise the value of c, since the average power consumption per user decreases. For $c = 10^8$ the total utility reaches its maximum value and stabilizes for $c \geq 10^{10}$. Finally, adding two more FAPs (9 in total – see Figure 13) the corresponding plots are similar to the ones discussed above (see Figures 20 and 21).

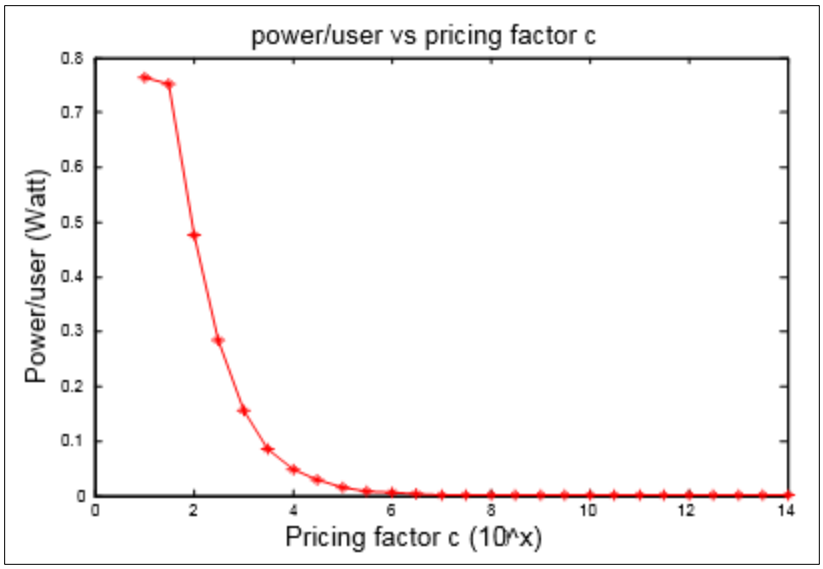

Figure 20: Average power per user for a network with 9 FAPs

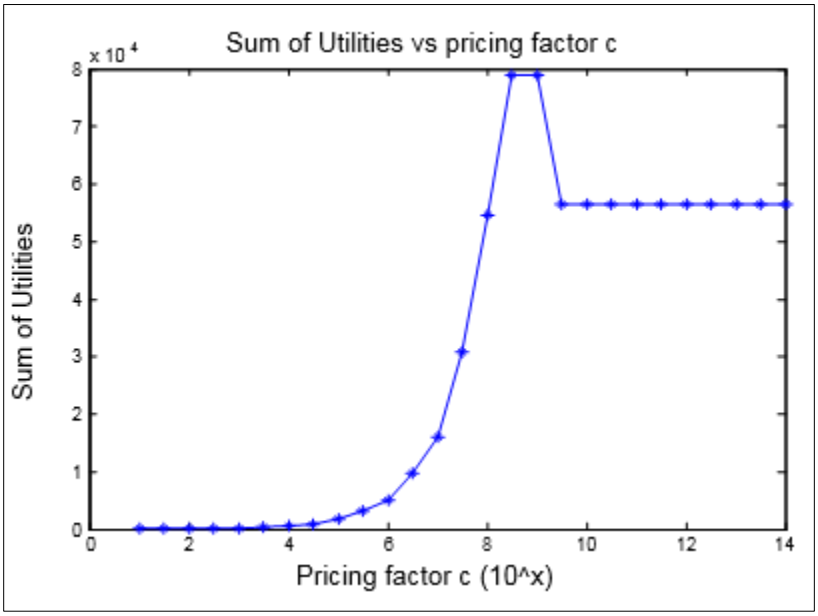

Figure 21: Total user Utility for a network with 9 FAPs

Concluding, we choose as the best pricing factor the value $c_{best} = 10^{10}$ and we will use it as a predetermined parameter in the next scenarios. The reason for choosing this value is simple: it is the one that brings the maximum possible efficiency to the system studied, in terms of maximum stabilized total user utility and minimum average power consumption (power being the most valuable resource in this work) as it was observed in the previous test cases. Practically, what happened was that by increasing the

pricing imposed on the femto-users, they had to reduce their transmission powers, thus allowing the macro-users to reach lower optimal transmission powers as well (since the interference was reduced) and in the end, the total network user utility was further increased. This also shows why imposing a pricing policy to the femto-users is a good strategy choice in order to protect and secure the quality of service of the higher priority macro-users (see section 2.6).

4.2.2 Scenario 1

In this case scenario, we study the behavior of the femto-users of 3 FAPs and one NRT macro-user who crosses the boundaries of one of these femtocells while getting further away from the MBS. The network topology of this particular scenario can be seen in Figure 22, where we have marked with blue color the path that this macro-user followed while passing through the femtocell whose center is at $(300, 500)$ and which we will call for the rest of this scenario the 1st FAP. The FAPs at the locations $(400, 300)$ and $(400, 600)$ are the 2nd and 3rd FAP respectively. We study the uplink power, data rate achieved as well as the total utility of the macro-user who goes through the 1st FAP, with respect to his distance from the MBS. Then we investigate how this macro-user movement affects the femto-users of the 1st FAP he passes through as well as the users of the other two FAPs.

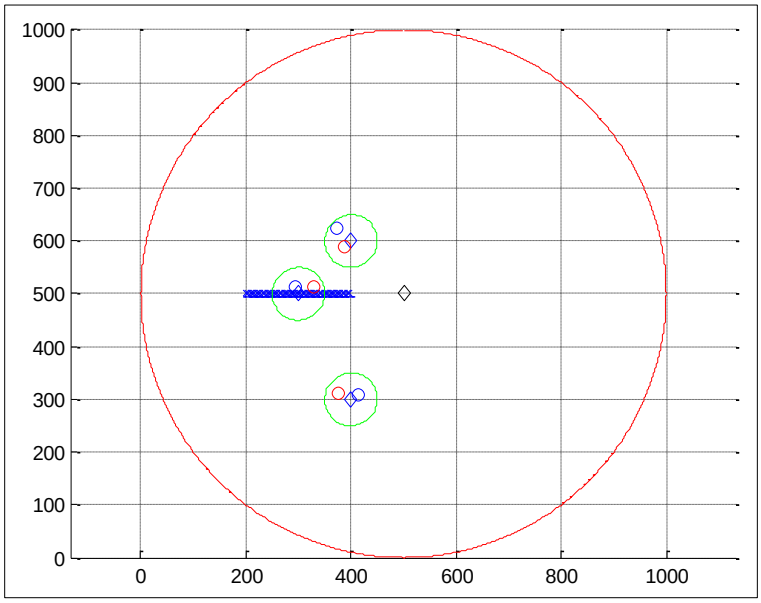

Figure 22: Network topology of the 1st Scenario with 3 FAPs and 1 NRT macro-user

In Figure 23, we can see that the macro-user transmits with very low power for as long as he is outside the radius of the 1st FAP, since the interference which is caused by the femto-users and is reaching the MBS is practically negligible. When he gets very close to the femtocell access point device ($d \leq 10m$), the interference that he causes to the femto-users of the 1st FAP is large enough to make them transmit with maximum power (2 Watt) in order to protect their quality of service (see Figure 24). Consequently, he also increases his transmission power (because of the interference caused by the higher transmission power of the femto-users), although it remains on low enough levels (~0.15 Watt).

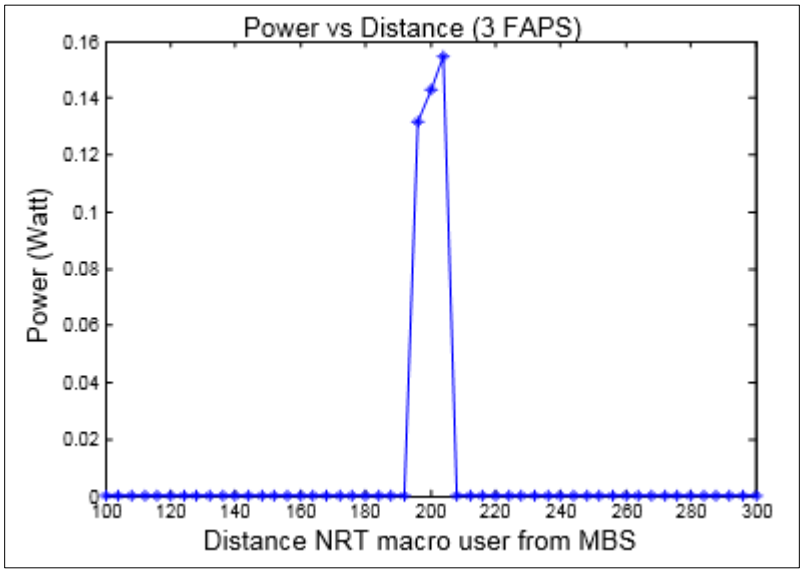

Figure 23: Macro-user power with respect to his distance from the MBS

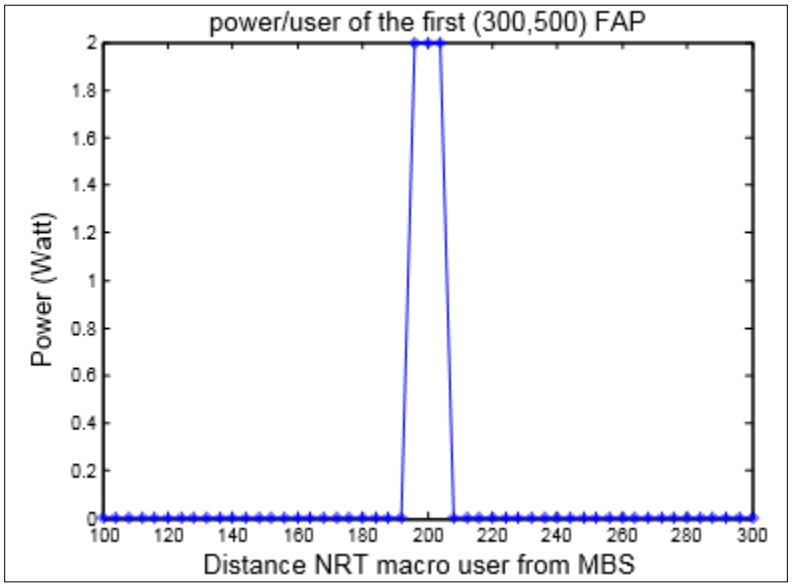

Figure 24: Average power per user of the 1st FAP with respect to the macro-user's distance from the MBS

Continuing, due to the macro-user intrusion into the 1st FAP and the increase of the femto-users' average power (see Figure 24), the average total utility per femto-user is significantly decreased (see Figure 25). When the macro-user exits the femtocell, the average utility per user returns to its initial values.

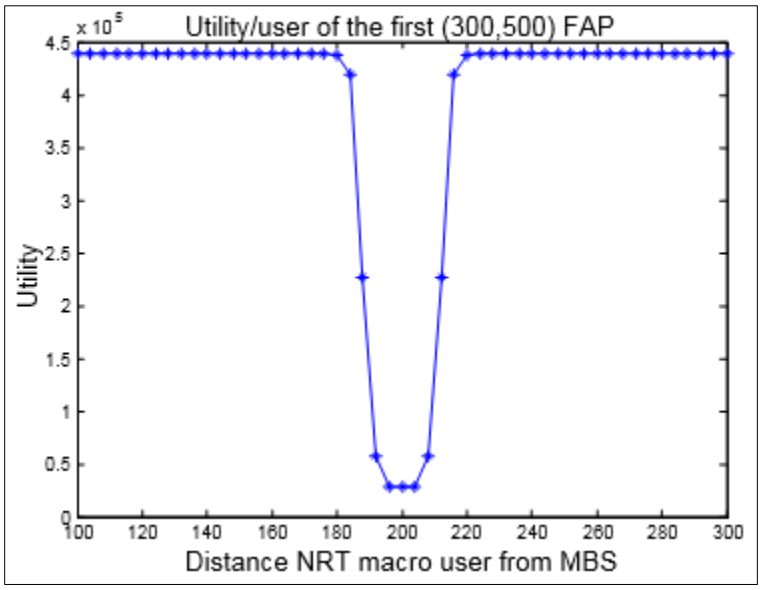

Figure 25: Average Utility per user of the 1st FAP with respect to the macro-user's distance from the MBS

In the next two figures, we represent the impact that the macro-user's movement through the 1st FAP has on his achieved data rate (or throughput) as well as his total utility.

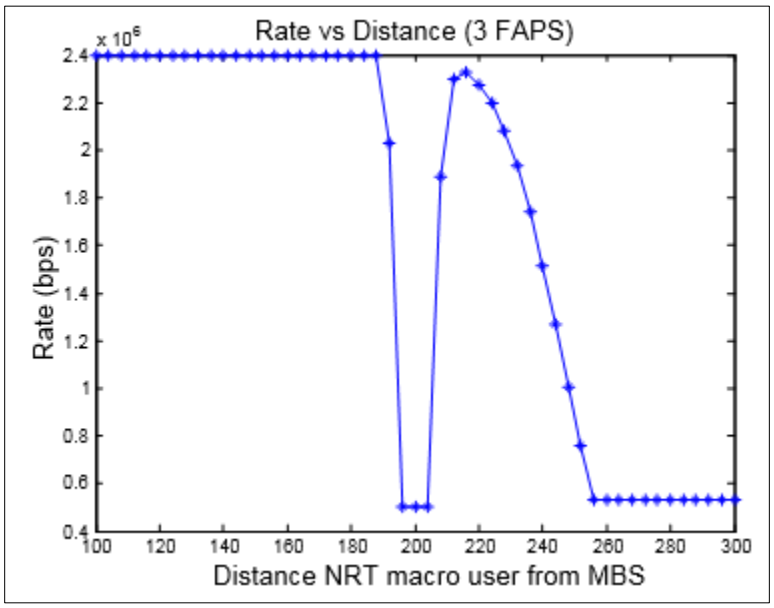

Figure 26: Macro-user's throughput with respect to his distance from the MBS

We observe that the macro-user's data rate decreases exponentially when he approaches the center of the 1st FAP (see Figure 26) whereas it returns to its initial levels when he goes further away from it (the macro-user achieves the highest possible data rate – 2.4 Mbps – when he is outside the range of the femtocell base station because of the negligible interference from the other users). Furthermore, since the distance between the macro-user and the MBS increases, his throughput steadily decreases – although in the end, it stabilizes at the satisfactory value of 0.5 Mbps (for a data user).

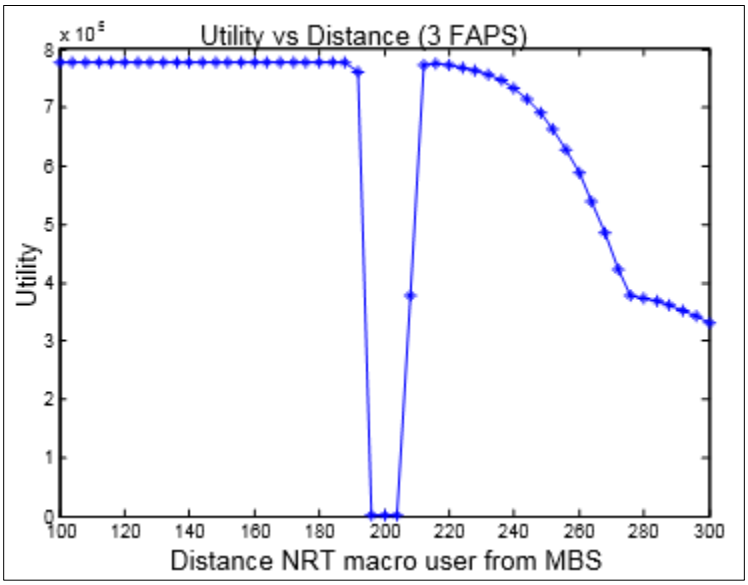

Figure 27: Macro-user's Utility with respect to his distance from the MBS

In Figure 27, we can see that the utility of the macro-user is lessened when he passes through the 1st FAP, since his throughput achieved was decreased (see Figure 26) while at the same time his transmission power was increased (see Figure 23). When the macro-user goes outside the radius of the femtocell, his utility levels return to the initial values and then they are steadily reduced due to the corresponding decreased throughput he achieves while getting further away from the MBS.

We will now study the impact that this intrusion of the NRT macro-user in the 1st FAP had on the femto-users of the other two FAPs in the network and we will compare the results between these two FAPs with respect to the distance of the macro-user from the MBS. We first compare the average power per user in each of the two FAPs:

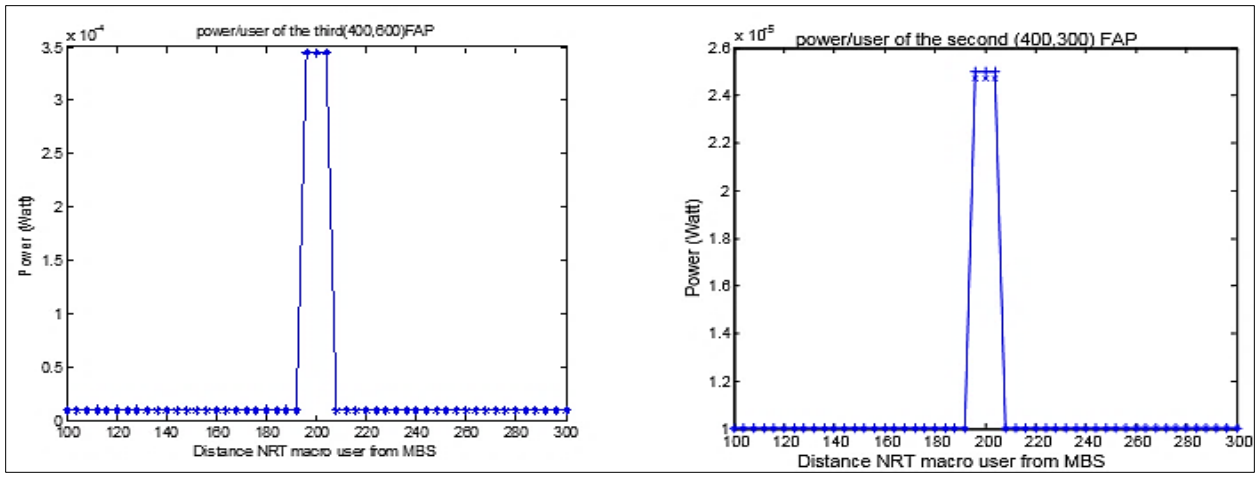

Figure 28: Average power per user of the 3rd and 2nd FAP with respect to the macro-user's distance from the MBS

Examining Figure 28, we conclude that just like the femto-users of the 1st FAP increased their transmission powers in order to protect their quality of service, the femto-users of the other two FAPs did so similarly – the difference is the larger distance between the macro-user and the 2nd and 3rd FAP which causes smaller interference and as such, the corresponding femto-users of the two distant FAPs are affected less (they transmit with lower power). Distance is the key here, since we can see that the 3rd FAP $(400, 600)$ is closer to the 1st FAP (and thus to the macro-user when he walks through it) and as a result it is affected more than the 2nd FAP $(400, 300)$ which is further away, since its users are forced to transmit with higher power levels than the users of the 2nd FAP whereas the average total utility per user is smaller for the users of the 3rd FAP as is shown in Figure 29:

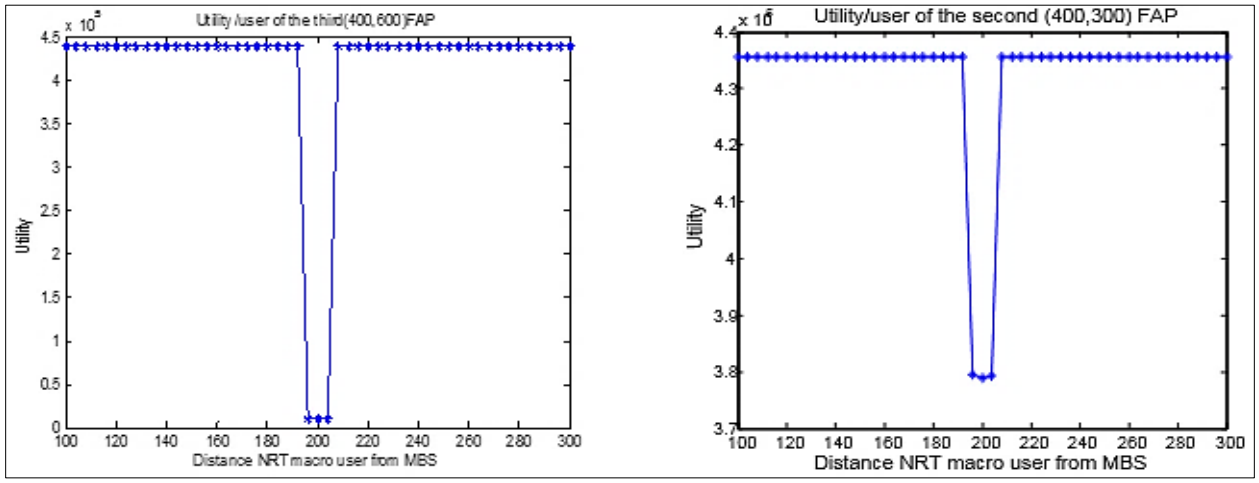

Figure 29: Average Utility per user of the 3rd and 2nd FAP with respect to the macro-user's distance from the MBS

Concluding, in the 1st use case scenario we studied the undesirable situation of a macro-user going through a femtocell – a situation which causes problems to him and to the nearby users of the network as well. We noticed that the femto-users of the FAP that the macro-user enters, are also the ones that are affected more: when the macro-user approaches to a distance $d \leq 10m$ from the femtocell access point device, the femto-users are forced to transmit with the maximum permissible power due to the strong interference caused by the intruding user, while their quality of service is kept at minimum levels (which is reflected by the very low average utility per user as seen in Figure 25). On the other hand, the macro-user is not affected much, since he keeps a relatively low transmission power while his throughput remains in satisfactory levels (even though his utility is somewhat reduced).

The situation described above is primarly caused by the access policy that was chosen for the system model in this thesis (the main access policies in femtocells were discussed in section 1.3). We chose to use the closed access policy which means that every FAP has a limited number of subscribers (two in our case) which are the exclusive users of the femtocell's resources and thus no other user can become a member of the femtocell's CSG (Closed Subscribed Group). Consequently, when another user happens to be near to a closed access femtocell, he will cause strong interference to its dedicated femto-users as is the case in Figure 4, where dead zones are created in the uplink scenario.

In order to avoid such undesirable situations, we advise to use an open or hybrid access policy, in which the macro-user would share the resources of the femtocell he was entering (he would be handovered to the corresponding FAP for as long as he was in its active service radius) and thus, by transmitting to the closer FAP and not the far away MBS, he would decrease the interference caused to a minimum, making the femto-users also lower their respective powers and achieve higher utility through the better management of the femtocell's resources. Consequently, both the macro-user and the femto-users would have a better quality of service (i.e. lower transmission power, larger achieved throughput/data rate and higher utility) while the network under consideration would reach a more balanced state and better overall efficiency/performance.

4.2.3 Scenario 2

In this case scenario, we study how the number of FAPs inside the macrocell affect different measured quantities such as the transmission power, the utility, the throughput achieved and the signal-to-interference-plus-noise ratio (SINR) per user. In each of the following figures we will present four graphs to match the four different classes of users (RT macro-users, NRT macro-users, RT femto-users and NRT femto-users – see section 2.1). Regarding the network topology, we put 8 macro-users in four zones which are essentially rings with a radius $r < R_c$ and 100m in thickness. The first's zone radius is 100m, the second's 200m, the third's 300m and the fourth's 400m. Furthermore, in each zone we have randomly placed two macro-users – one is a voice user (blue "x") and the other is a data user (red "x"). The number of the randomly placed FAPs inside the macrocell ranges from 0 to 100 (we add 10 FAPs in each simulation): in Figures 30 and 31 we can see the network topology with 10 and 100 FAPs respectively while the aforementioned ring zones and the fixed positions of the macro-users can also be seen.

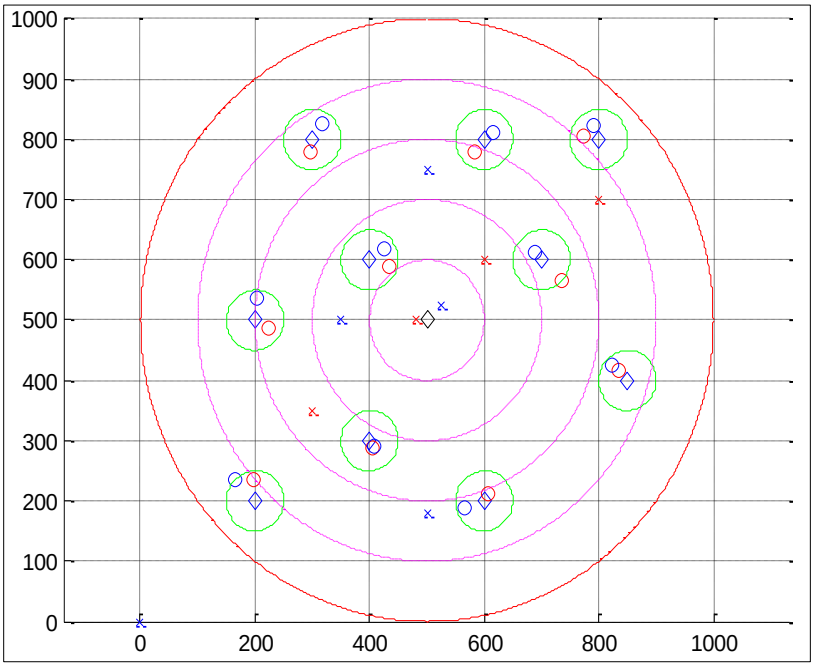

Figure 30: Network topology of the 2nd Scenario with 10 FAPs and 8 macro-users in zones

As we can see in Figure 31, a dense network where inside the macrocell there are over 100 FAPs deployed, could be a real-world scenario. A characteristic of such a mass deployment of femtocells in an

urban area is the creation of FAP *clusters*, which refers to a number of nearby femtocell stations which could be located either in neighboring houses or even in different apartments/floors of the same building.

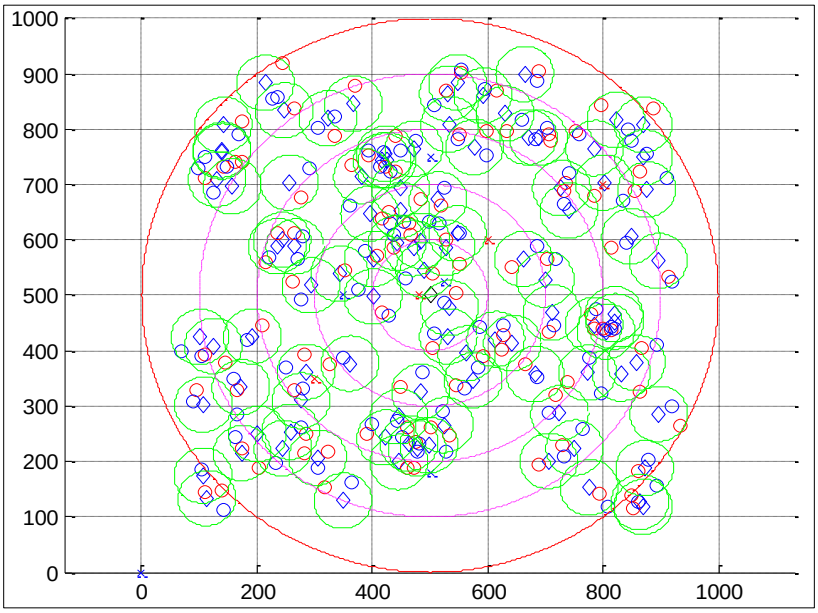

Figure 31: Network topology of the 2nd Scenario with 100 FAPs and 8 macro-users in zones

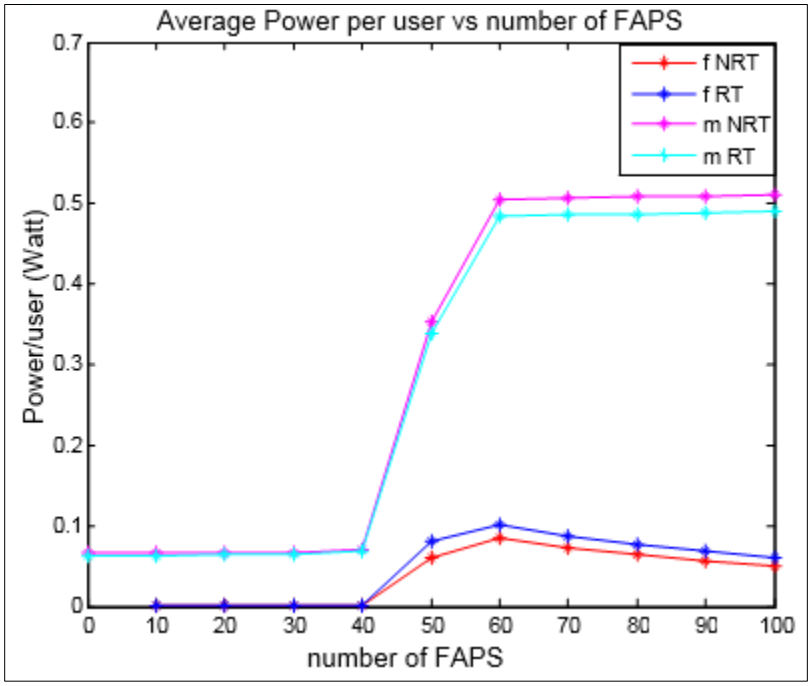

Figure 32: Average power per user class with respect to the number of FAPs in the network

In Figure 32, we can see that for $\#FAPs \leq 40$ (the meaning of the symbol "#" is "the number of") all the network users transmit at very low average power values. For $\#FAPs \geq 50$, since more users are added to the network, the total interference increases and thus the average power per user is also increased. At the end of the simulations, the macro-users' average power stabilizes near ~0.5 W while the femto-users never transmit with more than 100 mW on average (although there are cases of femto-users that transmit with the maximum permissible power, i.e. 2 Watt). Specifically, for $\#FAPs = 40$, the average power per femto-user is ~1 mW, while with the addition of more femtocells it increases to ~60 mW: this happened because the 10 FAPs that were added in the 6th repetition of the algorithm in this scenario's simulation, were placed near the 8 fixed-positioned macro-users and thus this caused strong cross-tier interference (like the case in Scenario 1). Consequently, the average transmission power of all nearby users (femto and macro) was increased. After the 7th repetition, we observe that the average power per femto-user is further decreased while the macro-users transmit at ~0.5 W even with 100 FAPs, which means that the newly added FAPs were placed far enough from the macro-users so as to not create strong interference that would otherwise affect the average power per network user. Also, since there are many new femto-users that transmit as low as possible, the average power consumption per femto-user is thus decreased.

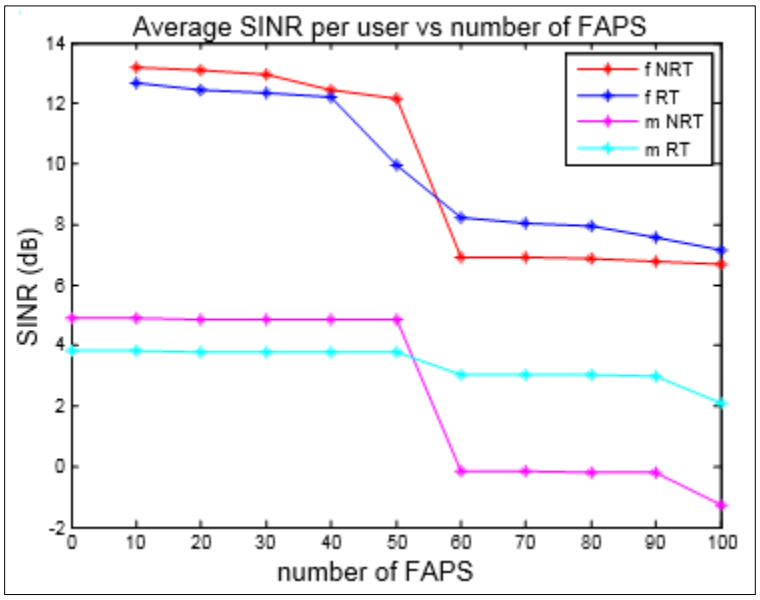

Figure 33: Average SINR per user class with respect to the number of FAPs in the network

In Figure 33, we observe that for $\#FAPs \leq 50$ the average SINR remains mostly stable for all users. The femto-users have larger SINR values than the macro-users, since the former have the base station closer and can thus transmit with better signal quality (also the interference is not strong enough to affect

their SINR). Continuing, for $\#FAPs > 50$, we observe a reduction in the SINR value for all users independently of the class they belong to, which is due to the increase of the total number of users in the network as well as the placement of newly added FAPs near the macro-users, where the strong cross-tier interference that is created causes the reduction in the SINR value.

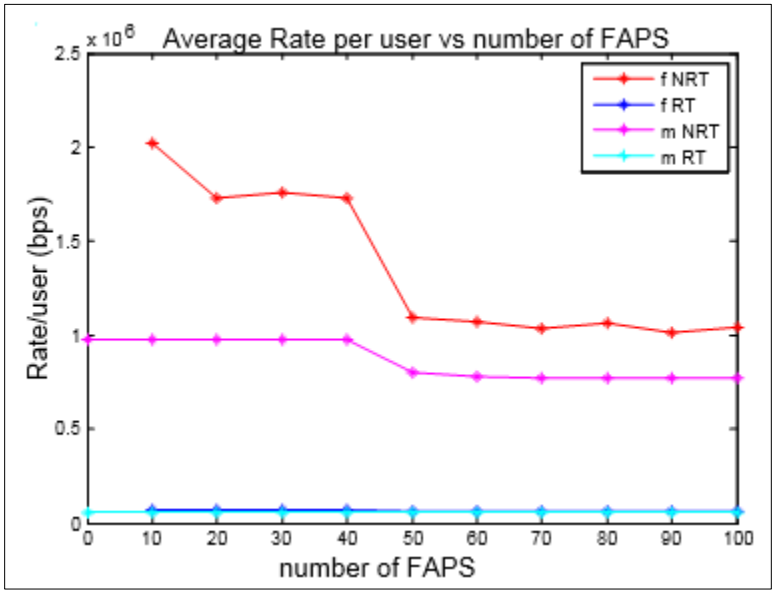

Figure 34: Average throughput per user class with respect to the number of FAPs in the network

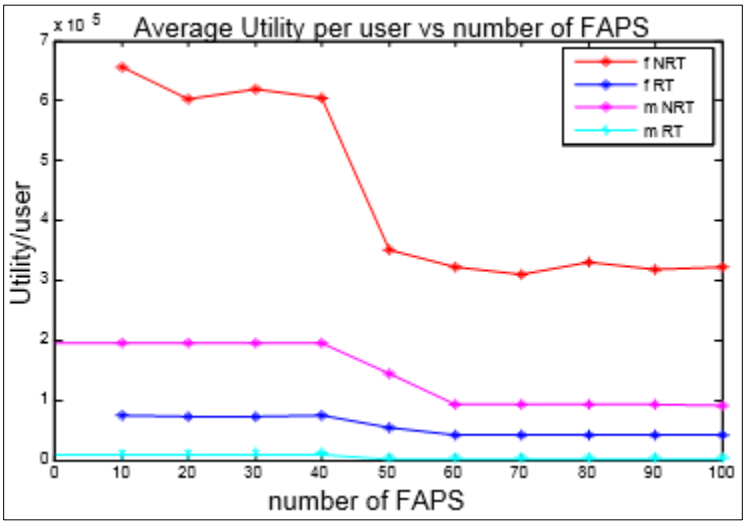

Figure 35: Average Utility per user class with respect to the number of FAPs in the network

Examining Figures 34 and 35, we conclude that for $\#FAPs < 50$, all the network users achieve satisfactory QoS in terms of achieved throughput and total utility. Specifically, the NRT femto-users achieve an average data rate ~1.5 Mbps while the NRT macro-users ~1 Mbps. On the other hand, the RT femto-users achieve a data rate ~70 Kbps (which is above the specified target rate) while the RT macro-users ~64 Kbps (the target rate). With the addition of further femtocells, the macro-users' throughput is reduced but nevertheless, at the end of the simulations it is stabilized at the satisfactory value of ~54 Kbps for voice services and ~0.75 Mbps for the respective data services – the corresponding utility graph shows a similar behavior of decline and normalization afterwards. Furthermore, the users that are affected more from the addition of FAPs in the network are the data users (independent of the tier they belong to) since they have a larger range of changes allowed in their respective measured quantities such as the throughput achieved. This is a result of the choice of the throughput function (strictly concave) which is more "flexible" regarding the value of R^*, meaning that as a variable, the actual data rate has a larger range of permitted values: $R^* \in [0, 2.4]$ Mbps, in contrast to the voice users whose permissible range is a lot smaller ($R^* \in [54, 74]$ Kbps) and is limited near the inflection point of the sigmoid function $T(R^*)$ (see definition (1) and Figure 8).

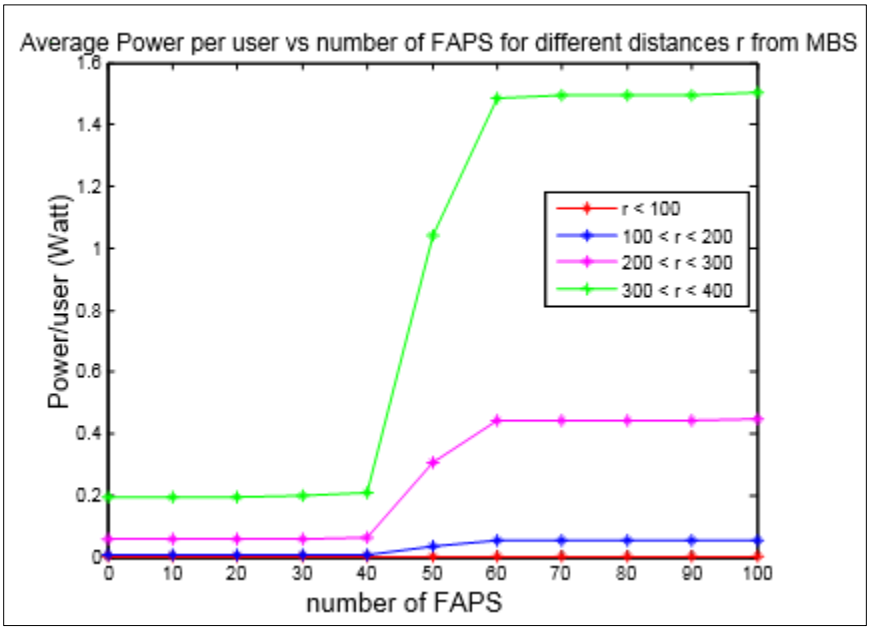

Figure 36: Macro-users' average power per zone with respect to the number of FAPs in the network

We will now analyze the behavior of the macro-users in the network based on the zone that they belong to. Figure 36 shows the average power consumption per macro-user zone and it is evident that the

more distant the zone from the MBS is, the larger the respective macro-users' average power is. The macro-users of the 4th zone which have a distance $r > 300$m from the MBS, transmit with high enough power (~1.5 W), while for $r < 300$m they achieve satisfactory low power values.

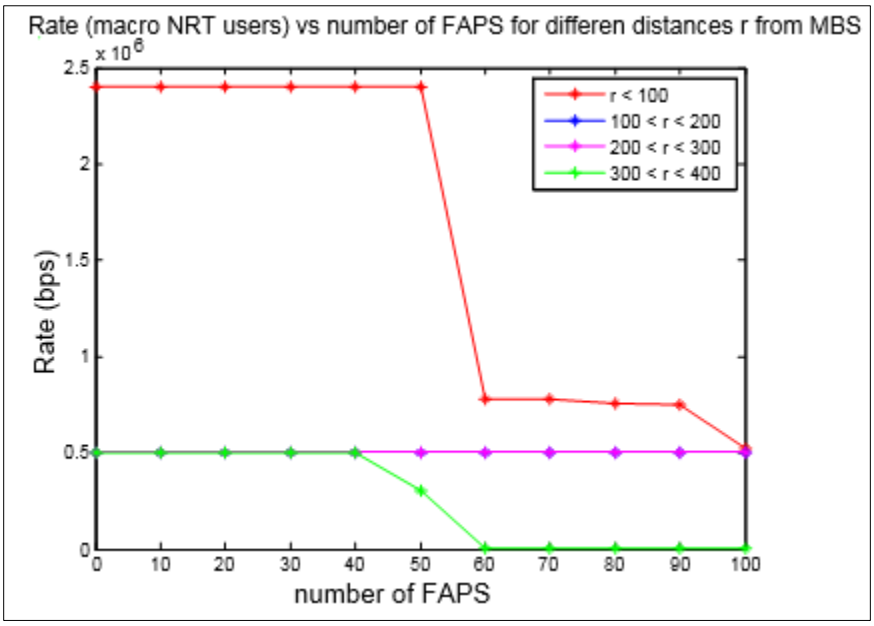

Figure 37: NRT macro-users' average data rate per zone with respect to the number of FAPs in the network

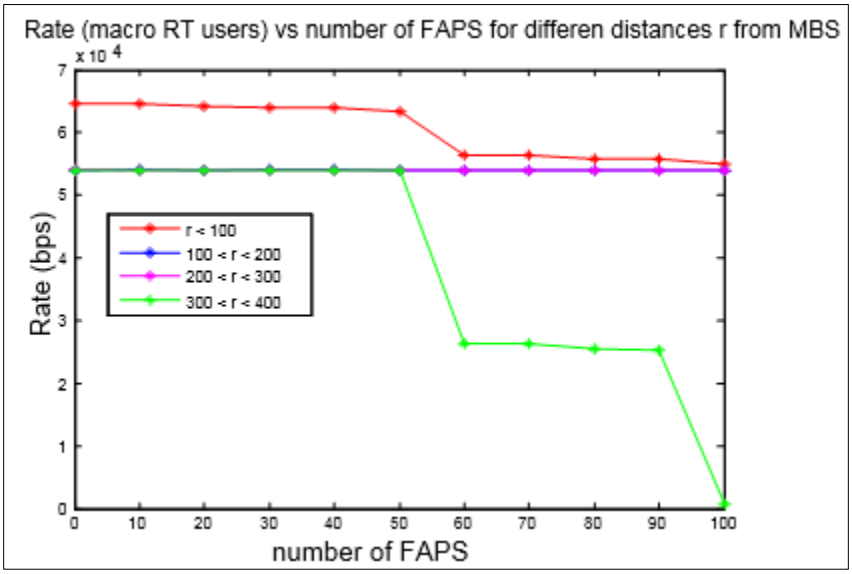

Figure 38: RT macro-users' average data rate per zone with respect to the number of FAPs in the network

Continuing, the Figures 37 and 38 show the macro-users' average achieved throughput per zone and per service classification (data and voice services respectively). The users of the 2nd zone (blue line) have similar behavior to the users of the 3rd zone (light purple line) and as a result, the two lines overlap in both figures. We observe that for $\#FAPs < 50$, all the macro-users (independent of the zone they belong to or the kind of service they want) achieve satisfactory throughput or at least the minimum requested through their QoS requirements (for the voice users this is the 54 Kbps and for the data users the value is around 0.5 Mbps) while adding more FAPs to the network results in poor data rate for the users of the last zone ($r > 300$m, see the green line in Figures 37 and 38). On the other hand, for $\#FAPs \geq 50$, the macro-users of the rest of the zones manage to sustain their quality of service in respectable levels with regards to the data transmission rate to the MBS.

To conclude, in order to design an efficient performance-wise Two-Tier Cellular network, there should be no more than 40-50 active femtocell stations inside one macrocell, because having more FAPs would affect the QoS of the macro-users which are located far away from the MBS ($r > 300$m). Such a mass deployment would force these macro-users to transmit with higher power values, increasing thus the interference caused to the nearby users, which would in turn increase their respective transmission power levels in order to attain more network resources and protect their quality of service. So, assuming that no more than 50 FAPs are placed inside the macrocell, the results of the above simulations show that all femto-users will achieve an excellent QoS which translates to low power values and high enough throughput (no matter the service class they belong to) while 8-12 macro-users will have a satisfactory data rate, great utility and low transmission power for a distance up to 300m from the MBS. If more distant macro-users exist in the network, they will meet their minimum QoS requirements for voice and data services, but they will have to transmit with power > 1.5 W and if they are close enough to the edge of the macrocell, even with 2 Watt (the maximum permissible power).

We now compare some of the previous results of the 2nd Scenario with the case where the femto-users are not under any pricing policy (so instead of $c_{best} = 10^{10}$ we will now have $c = 0$ and we will run the same simulations) in order to present the disadvantages of not having such a pricing scheme imposed on the femto-users of the proposed network system. In Figure 39, we observe an increase of the average transmission power of the femto-users as well as of the macro-users, in comparison to the results from Figure 32. In more detail, the femto-users stabilize in a larger power value than before (~200 mW – a 140% increase) since there is no pricing scheme to force them to decrease their power levels while the macro-users transmit with power equal to ~0.8 W (a 60% increase) due to the increased interference caused from the rest of the network users.

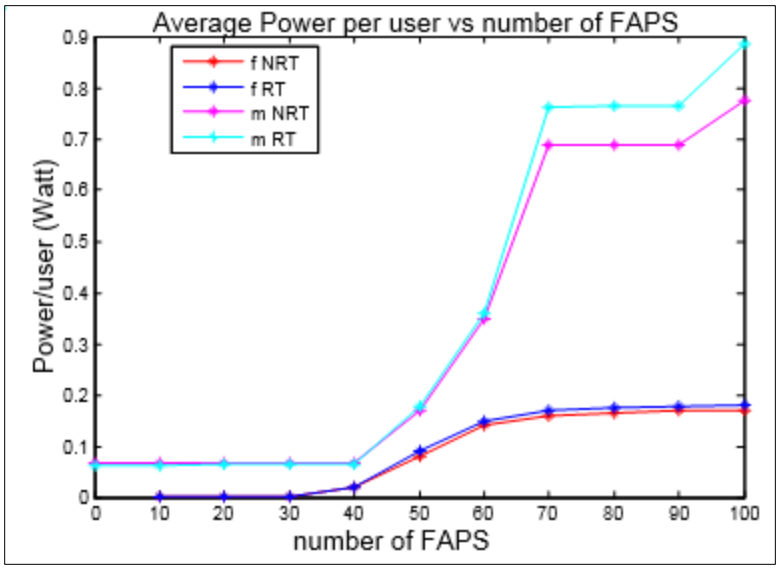

Figure 39: Average power per user class with respect to the number of FAPs in the network without femto-user pricing

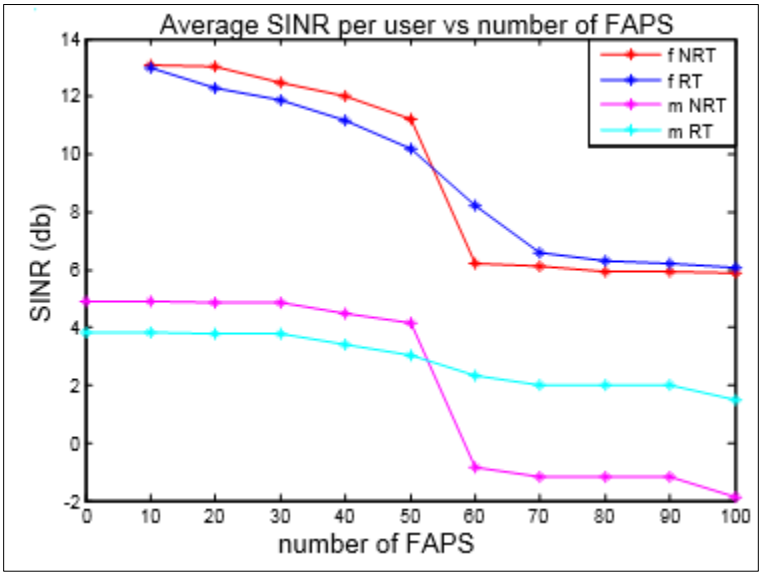

Figure 40: Average SINR per user class with respect to the number of FAPs in the network without femto-user pricing

Since all the network users increase their respective transmission powers, the interference that they cause will naturally also increase and so, the average changes of the SINR value will not be large enough to be distinguishable from the scenario which includes pricing (see that both the numerator and the denominator of equation (2) increase). In Figure 40, we observe that the SINR value of all users is decreased for $\#FAPs \geq 50$, which means that the interference takes precedence over the transmission power signal.

Overall, the difference between having and not having a pricing mechanism imposed to the femto-users is small enough with respect to the SINR value (in the order of 1-2 dB). Lastly, we observe that the SINR of the NRT macro-users takes negative values for $\#FAPs > 60$.

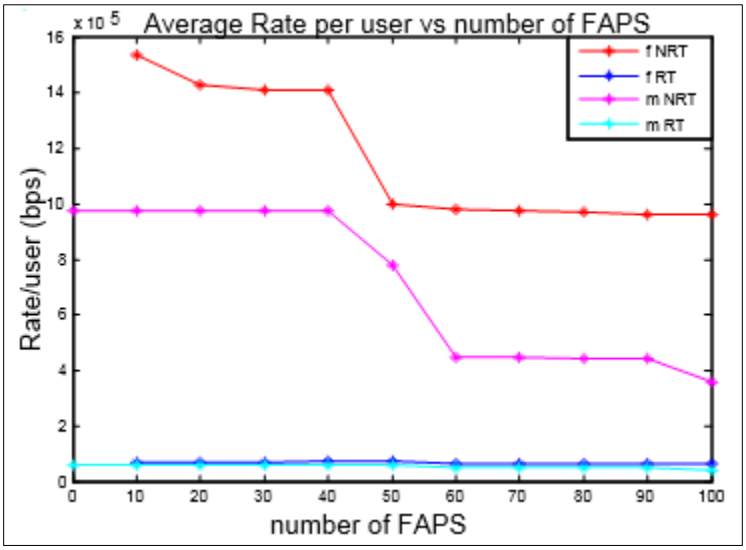

Figure 41: Average throughput per user class with respect to the number of FAPs in the network without femto-user pricing

In Figure 41, we can see how the different user classes are affected when there is no pricing scheme imposed on the femto-users. It is obvious that for $\#FAPs \geq 40$, the NRT users (femto and macro) are greatly affected since their corresponding achieved data rates are less than before (the NRT macro-users' average throughput is now lower than 0.5 Mbps while the NRT femto-users' average throughput is a little below 1 Mbps). Furthermore, we can see that the RT macro-users are affected even more than the data users for $\#FAPs > 50$, since their data rate is below the minimum QoS-aware acceptable value (the 54 Kbps) and as a result they attain close to zero utility (see light blue line in Figure 42). Also, comparing Figures 35 and 42, we can easily deduce that the macro-users are the ones that are affected more by the absence of a pricing mechanism to the femto-users, since the latter have to increase just a little their respective transmission power and will thus keep the same quality of service as before when they were under such a pricing scheme. On the other hand, in order to deal with the problem of a higher total interference in the network, the macro-users transmit with larger power values without though achieving satisfactory data rates according to their QoS requirements - as it can be seen from their attained average utility (see Figure 42).

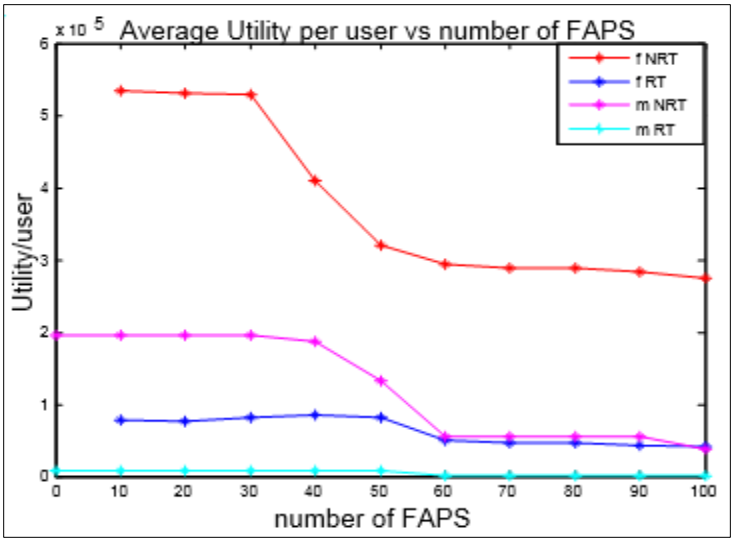

Figure 42: Average Utility per user class with respect to the number of FAPs in the network without femto-user pricing

Finally, in Figure 43 we observe an increase of more than 50% to the average transmission power of the macro-users between the scenario without the pricing mechanism and the one which included such a policy, mainly for the users of the 3rd and 4th zones, whose distance from the MBS is $r > 200$m. Also, it is evident that the macro-users of the 4th zone transmit with the maximum permissible power (2 Watt) but this does not guarantee though the maintenance of their QoS at acceptable levels as it was demonstrated previously (see Figure 41). Consequently, the use of a pricing scheme on the femto-users in order to protect and ensure the QoS of the macro-users is absolutely necessary in the system under consideration.

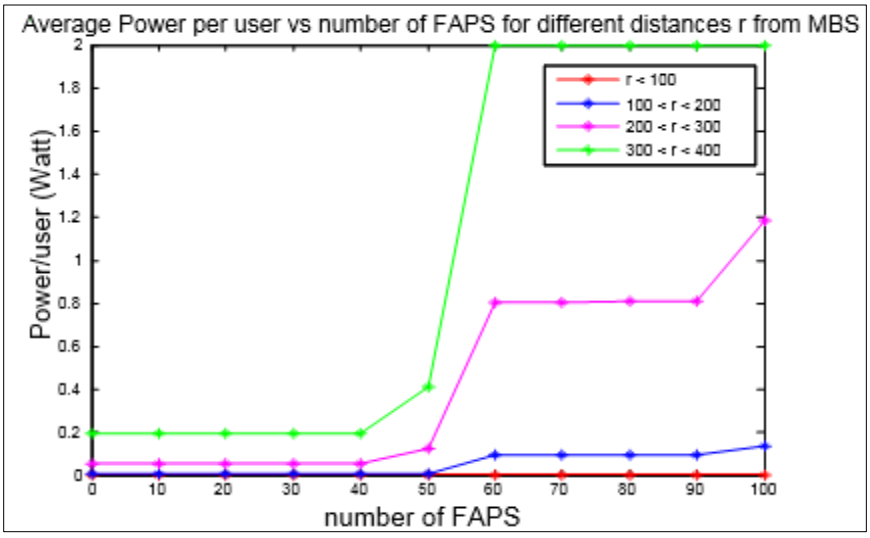

Figure 43: Macro-users' average power per zone with respect to the number of FAPs in the network without femto-user pricing

4.2.4 Scenario 3

This scenario is the complement of the previous one, in the sense that in Scenario 2 we proposed a design solution for the network under consideration regarding the number of the randomly placed FAPs (considering that the number of the macro-users was fixed as well as their position in the macrocell) whereas the main problem that we face in this scenario is how many randomly placed macro-users can the system support (i.e. how many can achieve a satisfactory quality of service) while having a constant number of FAPs.

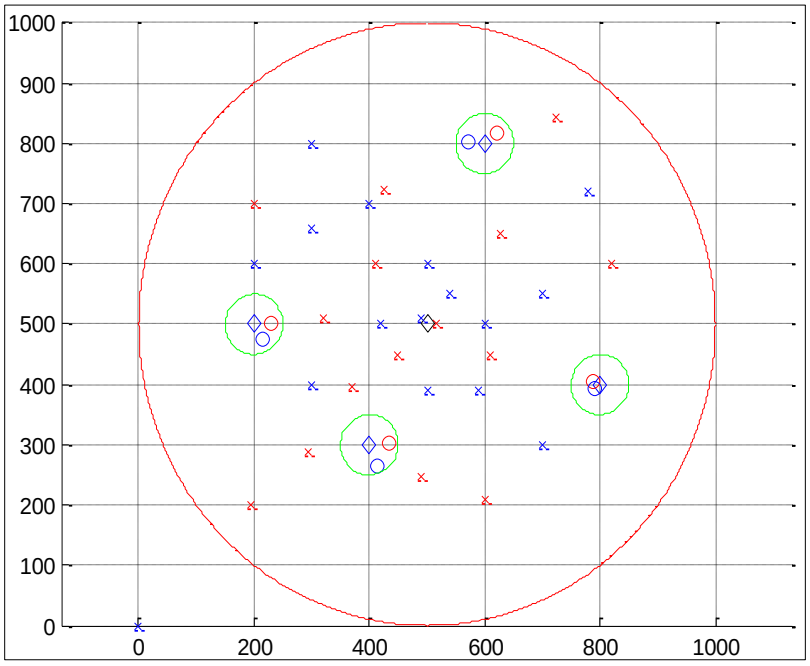

Figure 44: Network topology of the 3rd Scenario with 4 FAPs and 30 macro-users randomly placed inside the macrocell

In Figure 44 we can see the network topology of the last simulation of this scenario, in which we have 30 macro-users (split into 15 voice users and 15 data users). In every simulation, we added two macro-users, one in each service class, while keeping the positions of the previously placed macro-users fixed. The first simulation included just two macro-users (one was a voice user and the other a data user). The number of FAPs in every simulation was four, with the femto-users having fixed positions during the simulations, while the macro-users were deliberately placed away from the femtocells in order to avoid the cross-tier interference and dead zone problems that were studied in Scenario 1 and that would otherwise tamper with the results of this scenario. We measure the same quantities as in the 2nd Scenario: average power, throughput, SINR and utility per user with respect to the number of macro-users in the network.

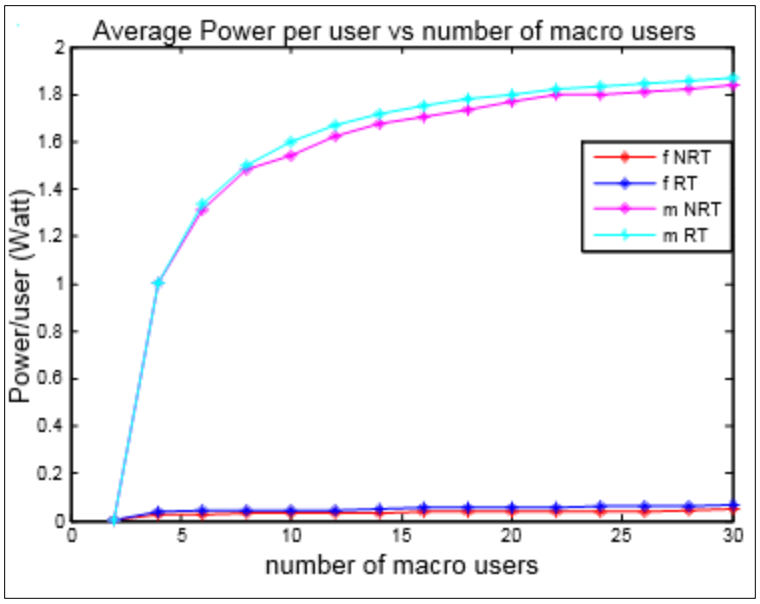

Figure 45: Average power per user class with respect to the number of macro-users in the network

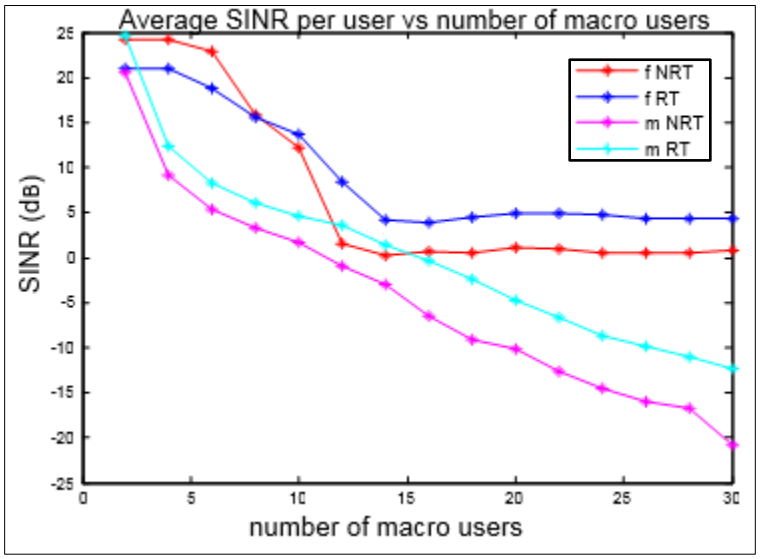

Figure 46: Average SINR per user class with respect to the number of macro-users in the network

Examining Figures 45 and 46, where the average transmission power and SINR per user class are shown, we observe that all the femto-users transmit with an average power < 100 mW independently of the number of macro-users while their SINR starts from very high values (which is explained by their shorter distance to their respective FAPs as well as the absence of strong interference in the network since the macro-users are relative few in number in the first simulations) and it stabilizes for a number of macro-users $m > 15$ to ~5 dB for the voice users and ~1 dB for the data users (see Figure 46). These results regarding the femto-users' achieved SINR in the later simulations are the product of the strong cross-tier

interference that exists in the network due to the increased average transmission power of the macro-users, as can be seen in Figure 45: their average power value is above 1.5 W for $m > 15$. Likewise, the average SINR of the macro-users is constantly decreasing during the course of the simulations since by adding more macro-users to the network system, the co-tier interference is greatly increased (the interference caused by the femto-users is negligible).

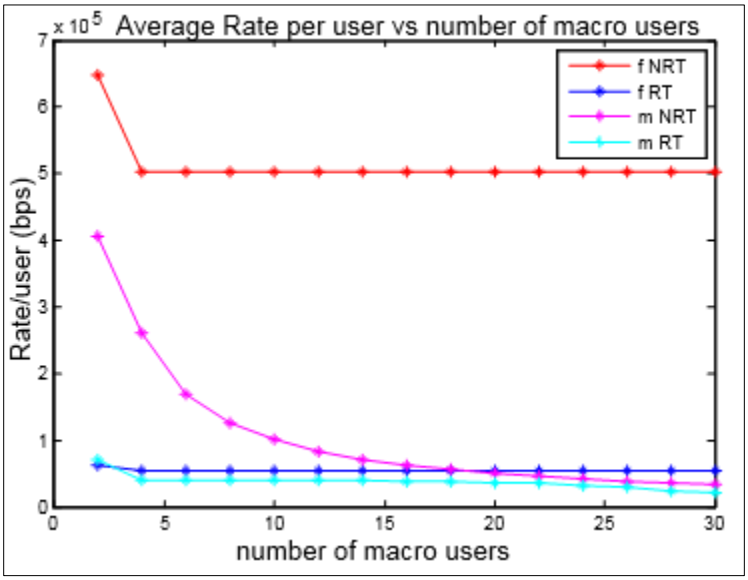

Figure 47: Average throughput per user class with respect to the number of macro-users in the network

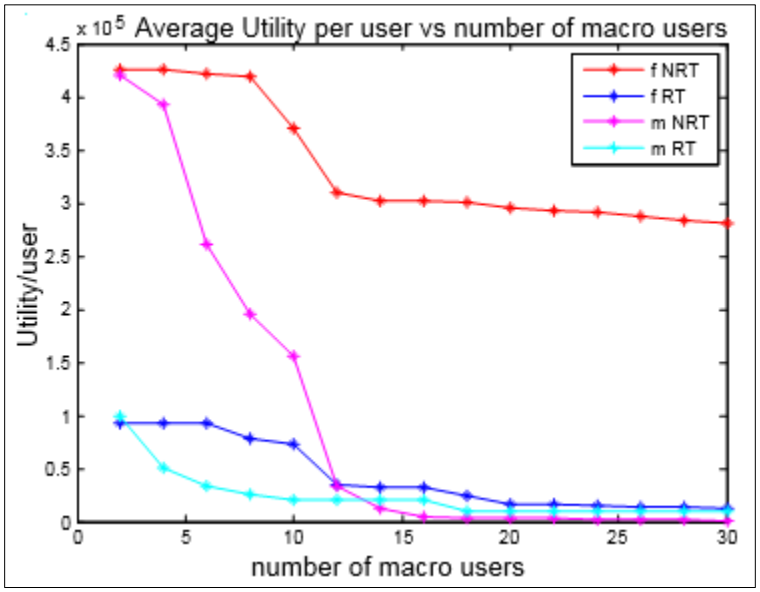

Figure 48: Average Utility per user class with respect to the number of macro-users in the network

In Figures 47 and 48, the average throughput and utility attained per user class in relation to the number m of macro-users in the network is shown. The femto-users manage to keep a stable and satisfactory quality of service in terms of achieved data rates and total utility from using the network's resources. On the other hand, we notice a decrease in the macro-users' throughput when their population increases – this observation applies to both the voice and data macro-users. Specifically, the RT macro-users transmit with an average data rate smaller than the minimum accepted rate (54 Kbps) while the NRT macro-users' throughput levels are even lower than 100 Kbps (see Figure 47) which is also reflected from the rapid decline of their utility in Figure 48 (the light purple line).

By adding the measurements and results of the 2nd and 3rd Scenario to our knowledge, we conclude that the system under study can support up to 12-15 macro-users, which means that wherever these users are placed inside the range of the macrocell, they will meet their minimum QoS requirements in terms of achieved throughput and will transmit with low to moderate power levels. We note that the distance of the macro-users from the MBS plays a significant role: e.g. in the 2nd Scenario, the macro-users of the 4th zone are far enough to transmit with low power levels but they achieve satisfactory QoS nonetheless, while the macro-users of the 1st zone, being close to the MBS, manage to reach the upper limits of their respective QoS requirements (which are 2.4 Mbps for the data users and 74 Kbps for the voice users) while transmitting with minimum power. Concluding, a further increase in the number of macro-users in the network will also cause an increase in the total interference (co-tier and cross-tier), decreasing thus the utilities of the network users and leading the system to undesirable efficiency levels.

4.2.5 Scenario 4

In this scenario, we study how the use of FAPs in the network can bring benefits to the system as a whole (maximize its performance) as well as to each user independently. The simulation consisted of two parts: at first, they were 10 randomly placed macro-users inside the macrocell (see Figure 49). At the second stage, 8 of these macro-users became the femto-users of the four new FAPs which were added to the network (this tier-related change kept the users' service orientation intact – meaning that the RT users remained RT users and the similar applied to the NRT users) – see Figure 50. In each simulation stage, we made measurements such as the average transmission power per user, the average throughput achieved per user and the total utility of all the users, while specifically for the second stage, we separately measured the aforementioned quantities for the macro-users that remained in the service of the macrocell as well as for the ones that became the femto-users of the newly added FAPs.

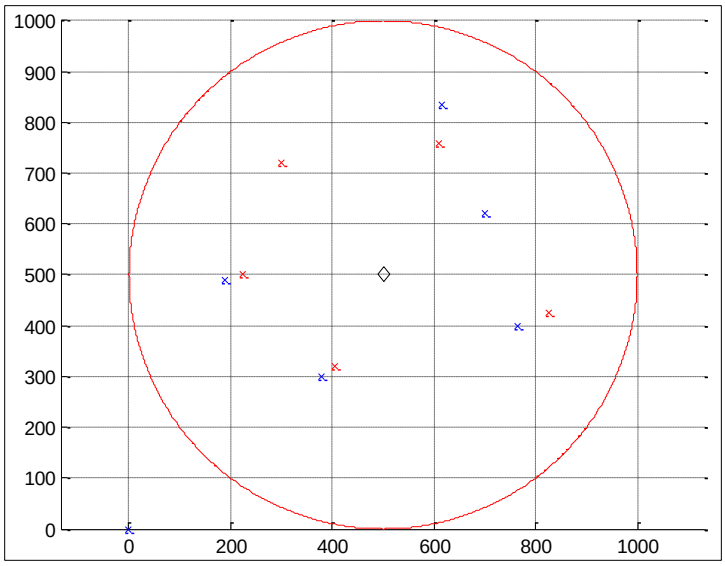

Figure 49: Network topology of the 4th Scenario before the deployment of the 4 FAPs – 10 macro-users

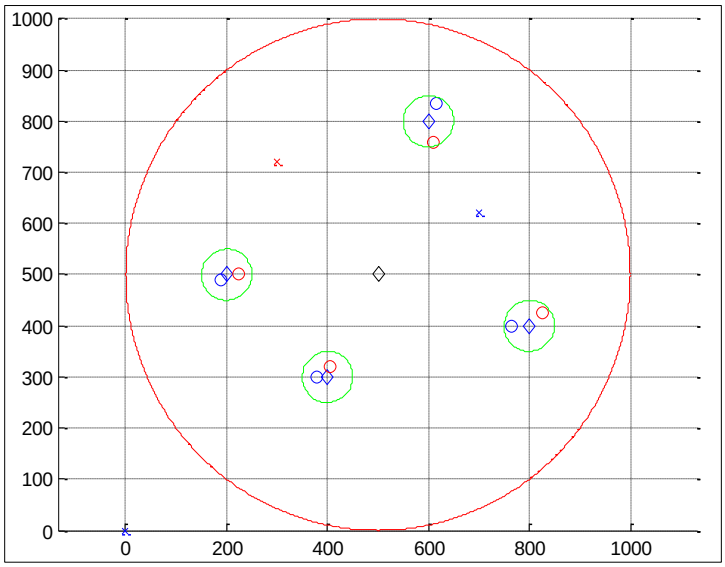

Figure 50: Network topology of the 4th Scenario after the deployment of the 4 FAPs – 2 macro-users and 8 femto-users

In Figures 51 and 52, the average transmission power per user and data rate achieved is shown, for both stages of the simulation (i.e. before and after the addition of the FAPs). We observe that with the utilization of the FAPs, the average power per user is decreased by 86% while the average throughput increases by 175%. Note that the macro-users already have small transmission power levels (see Figure 54), but by being served by the closer femtocell stations (which is the reason we put them at those positions), they manage to transmit in even lower power values, while simultaneously achieving larger average data

rates. Consequently, we observe an increase in the total users' utility by 388% (see Figure 53), which means that with the deployment of the four new FAPs, the total utility of the system under consideration was almost quadrupled.

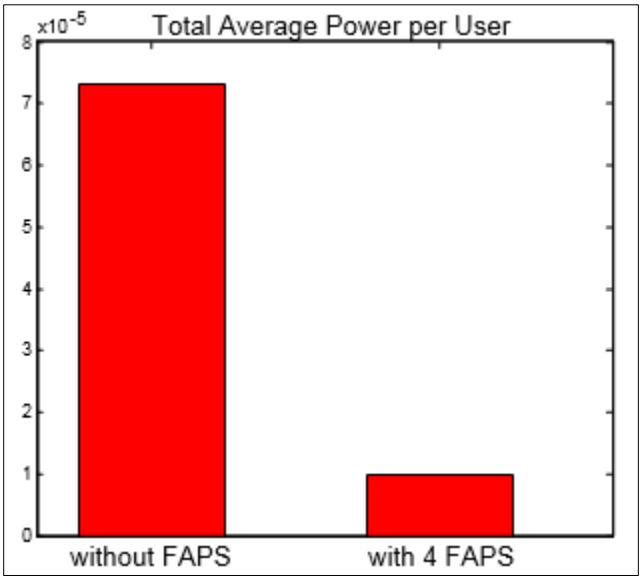

Figure 51: Average power per user before and after the deployment of the 4 FAPs

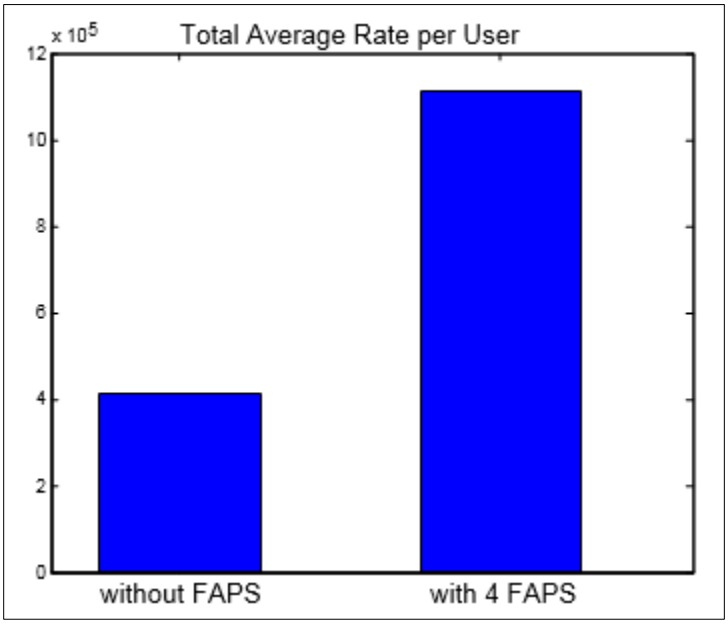

Figure 52: Average throughput per user before and after the deployment of the 4 FAPs

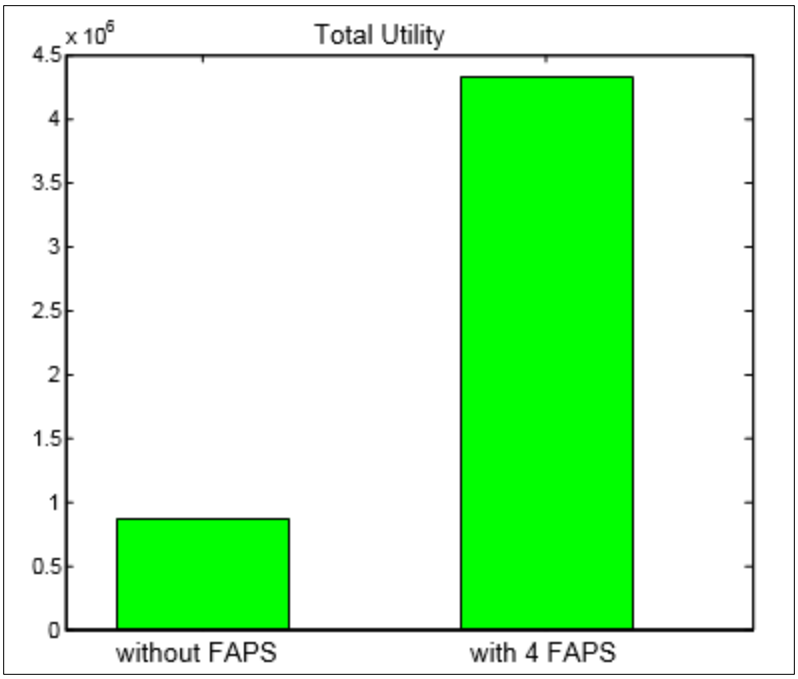

Figure 53: Total user Utility before and after the deployment of the 4 FAPs

Continuing, we separately study the behavior of the 2 macro-users that after the utilization of the four FAPs, remained in the service of the macrocell' s base station (MBS).

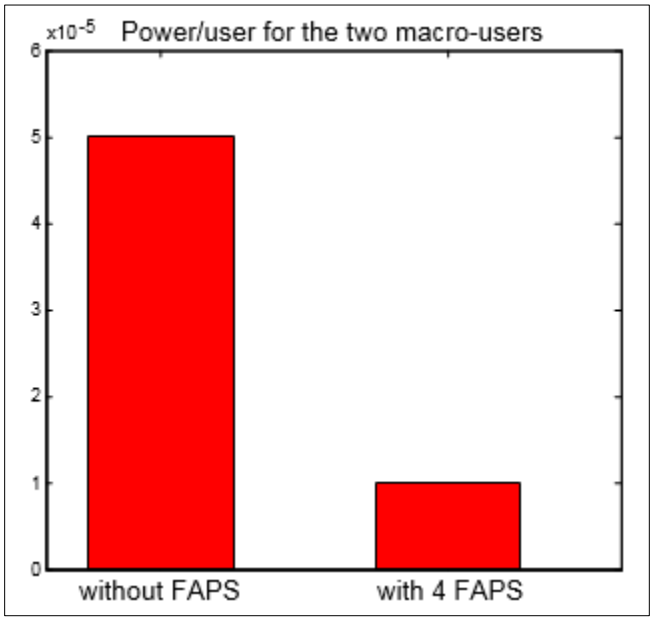

Figure 54: Average power per macro-user before and after the deployment of the 4 FAPs

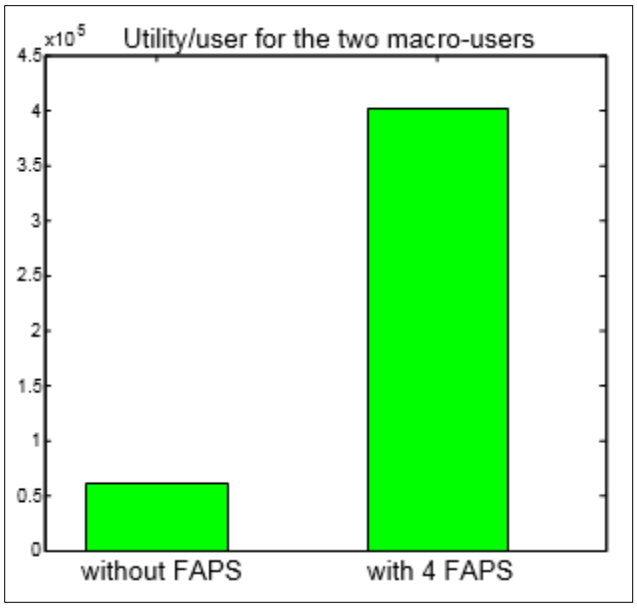

Figure 55: Average Utility per macro-user before and after the deployment of the 4 FAPs

Examining Figures 54 and 55, we can see that the average power per user decreases by 80%, while the average utility of the two macro-users increases by a staggering 566%. The cause of this outrageous increase in the macro-users' utility is the corresponding decrease in transmission power to just a fifth of the initial value. Also, during the second stage of the simulation, the co-tier interference that existed previously is not present since the macro-users that caused it changed to femto-users, which in turn create negligible cross-tier interference. So, the two macro-users do not suffer from any strong interference and can thus transmit with minimum power levels.

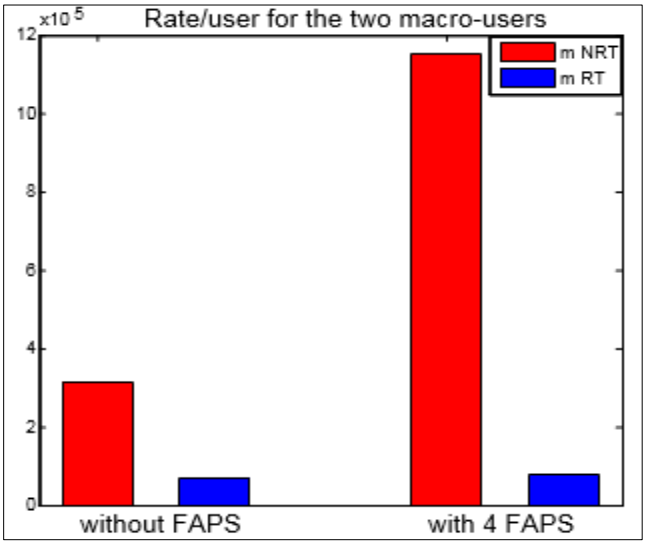

Figure 56: The two macro-users' data rates before and after the deployment of the 4 FAPs

In Figure 56, we can see how the throughput of each one of these two macro-users was affected with the deployment of the four femtocells in the network. We observe that the NRT macro-user had achieved throughput equal to 0.33 Mbps before but now he transmits with 1.15 Mbps (a 248% increase) while the RT macro-user from 55 Kbps can now, as a femto-user, transmit with 67 Kbps (a 22% increase).

Regarding the rest of the network users (which changed their respective base station to a FAP), the impact that the utilization of the new femtocells had to their performance can easily be seen from Figures 57, 58 and 59, where quantities such as the power, data rate and utility per user are depicted with regards to the type of service class the users belong to (data and voice users respectively). In Figure 57, we observe a reduction in the average transmission power of the NRT users by 80% and by 90% for the RT users. The former macro-users, due to the absence of strong interference inside the femtocells, now transmit with the minimum possible power value allowed in the simulation. Continuing, in Figure 58, we can see that there is an increase in the average data rates achieved by both user classes which results in an analogous increase of their utility. In more detail, the data users transmit with almost double the data rate, reaching the maximum value of 2.4 Mbps (200% increase), while the voice users transmit with 70 Kbps (from 60 Kbps which was the throughput when they were still macro-users – a 15% increase). Finally, a corresponding increasing behavior can also be seen in the graph of the users' total utility (see Figure 59).

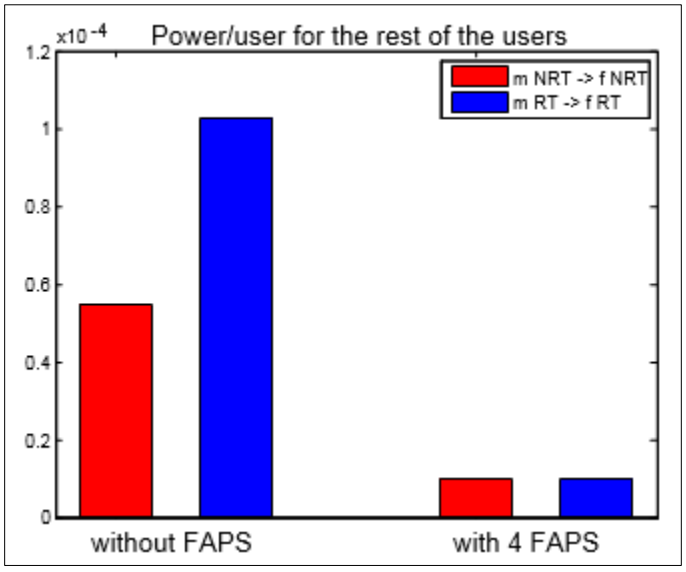

Figure 57: Average power per user and service class for the 8 users that changed base stations

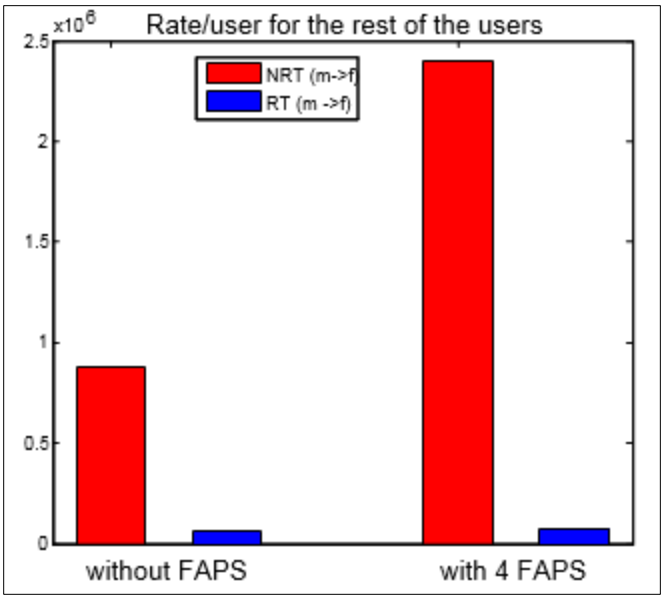

Figure 58: Average throughput per user and service class for the 8 users that changed base stations

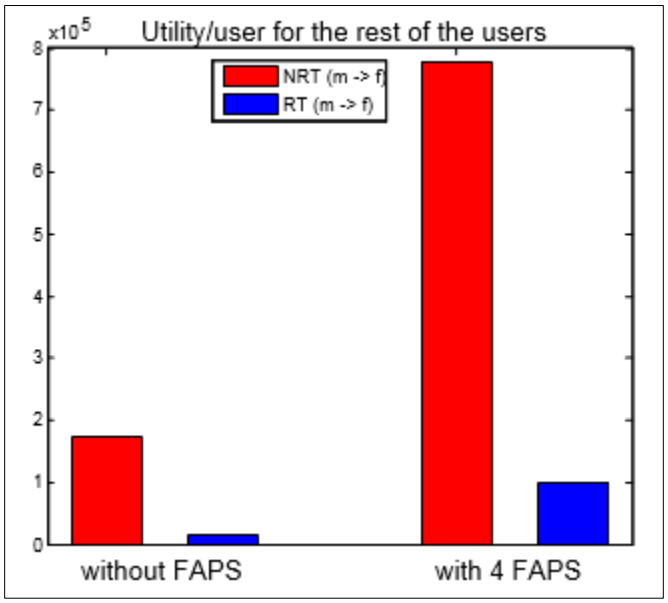

Figure 59: Average Utility per user and service class for the 8 users that changed base stations

The main conclusion of all the aforementioned results is that when the macro-users are being served by femtocells, this increases the whole system's efficiency, by better managing and allocating its resources to the network users, which in turn achieve larger data rates with less power consumption – independently of the base station they transmit to. Thus, the use of femtocell resources by users outside of its CSG, contributes to the decongestion of the macrocell network and so it is fairly advisable to choose an open or

hybrid type of access to femtocells against the closed access policy which was adopted in this thesis. All in all, the closed access policy, as studied in previous figures and in the 1st Scenario as well, has several drawbacks.

4.2.6 Scenario 5

In this scenario, we study the MTTPG algorithm's behavior with the help of two different network topologies of the Two-Tier Cellular system under consideration. In the first network topology, there are 30 randomly placed FAPs with their corresponding users and 10 macro-users positioned in a straight line, which alternatingly belong to a different service class (one is a NRT user, the next a RT user, etc.) – see Figure 60. The second network topology (see Figure 61), is almost the same as the first one with the difference being that the two more distant macro-users have now become the femto-users of a new FAP that was placed in the position $(975, 500)$ for exactly that purpose, thus reducing the number of macro-users in the network to 8. The main goal of this particular scenario is to find the dominant factors that affect the duration as well as the convergence speed of the MTTPG algorithm to the *NE* power vector of the corresponding game.

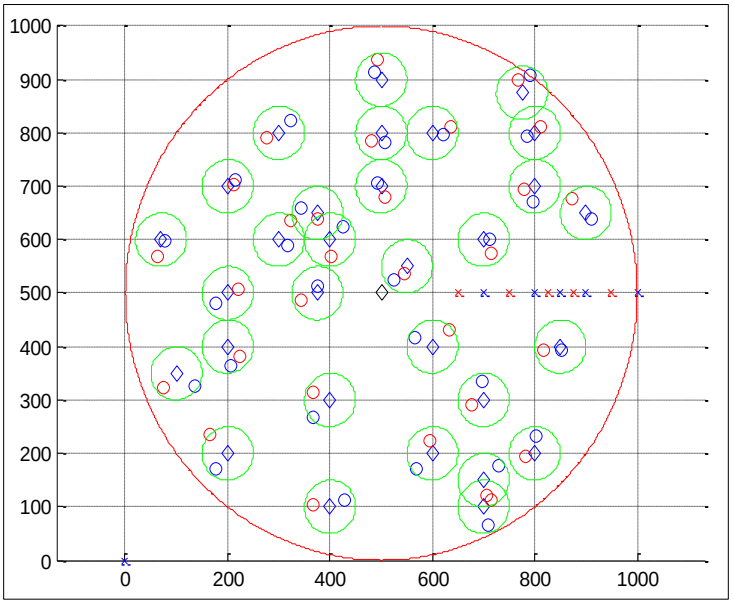

Figure 60: Network topology of the 5th Scenario (1st simulation) with 30 FAPs and 10 macro-users placed in a line

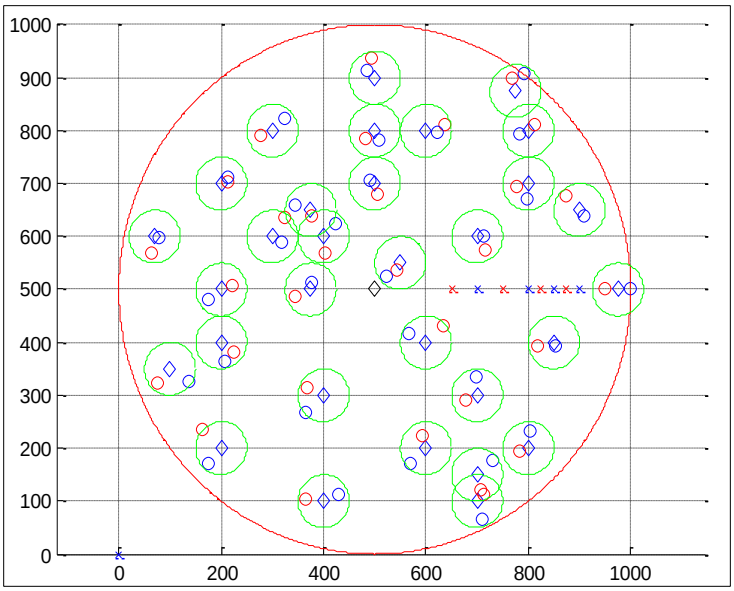

Figure 61: Network topology of the 5th Scenario (2nd simulation) with 31 FAPs and 8 macro-users placed in a line

In Figures 62 and 63, the convergence of the macro-users' powers to their equilibrium values is shown, for the first and second simulation respectively. We observe that a factor that affects the convergence speed of the proposed algorithm is the user's distance from his base station (in our case, since we are studying the macro-users' behavior, it's the MBS). In both Figures 62 and 63, the macro-users that are closer to the MBS converge to their optimal power values faster than the users that are further away and since the macro-users in this scenario were placed in a straight line, the convergence to the equilibrium powers is done in the order that they appear on this line: i.e. starting from the macro-user which is closer to the MBS and finishing with the one that is at the edge of the macrocell (thus the linear positioning of the macro-users translates to a uniform sequence-based convergence). We note that in the 1st simulation 50 repetitions of the algorithm were needed in order to find the *NE* power vector, while in the 2nd simulation around 25 repetitions. The main reason for this difference is the number of macro-users in the network: in the second simulation, the macro-users were decreased by two and as a result the algorithm duration was reduced to half in comparison to the first simulation.

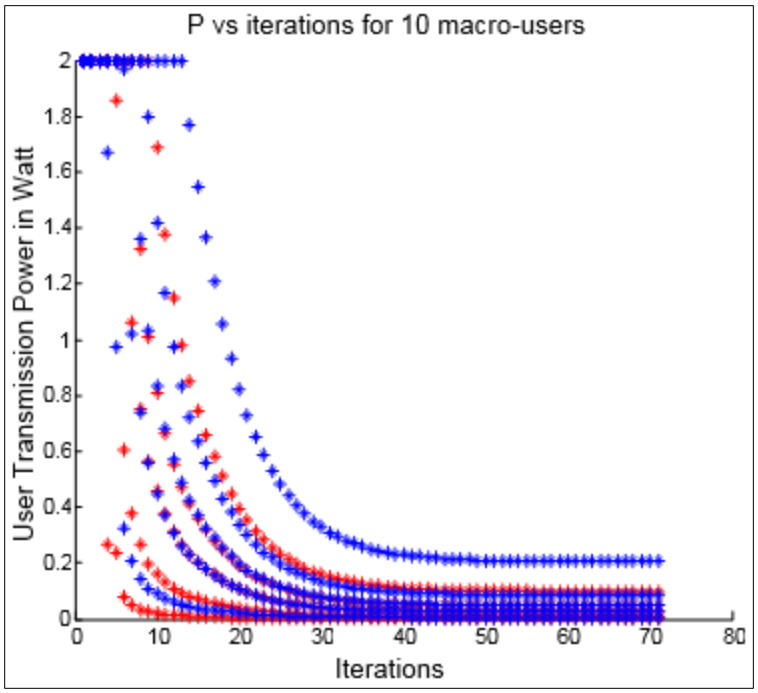

Figure 62: Convergence of the macro-users' powers for the 1st simulation

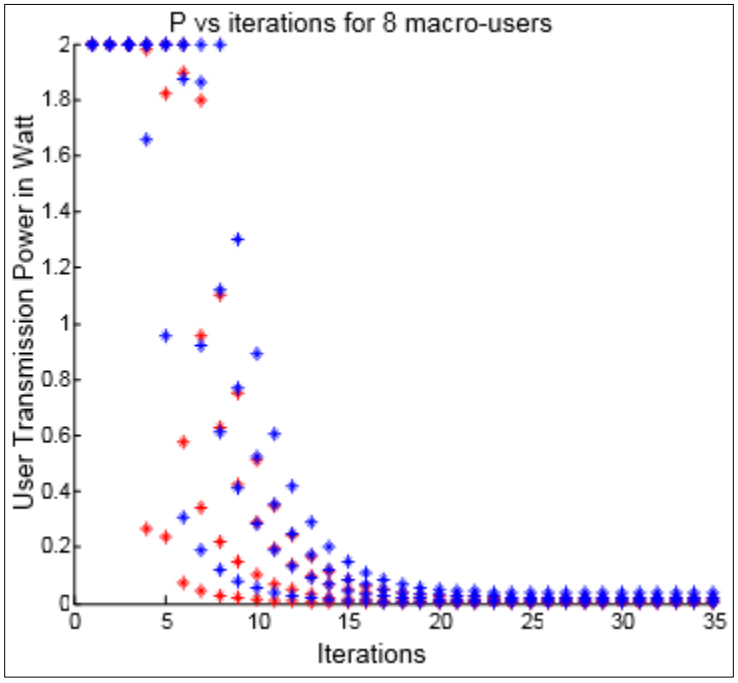

Figure 63: Convergence of the macro-users' powers for the 2nd simulation

Examining Figures 64 and 65, where the convergence of the femto-users' powers to their respective equilibrium values in both simulations is shown, we conclude that the number of femto-users in the network does not affect the algorithm's convergence speed, since in every case, the femto-users have their respective base stations so close to them ($r < R_f = 50m$) that the convergence to the equilibrium powers is always very fast (~5 repetitions are needed for every femto-user).

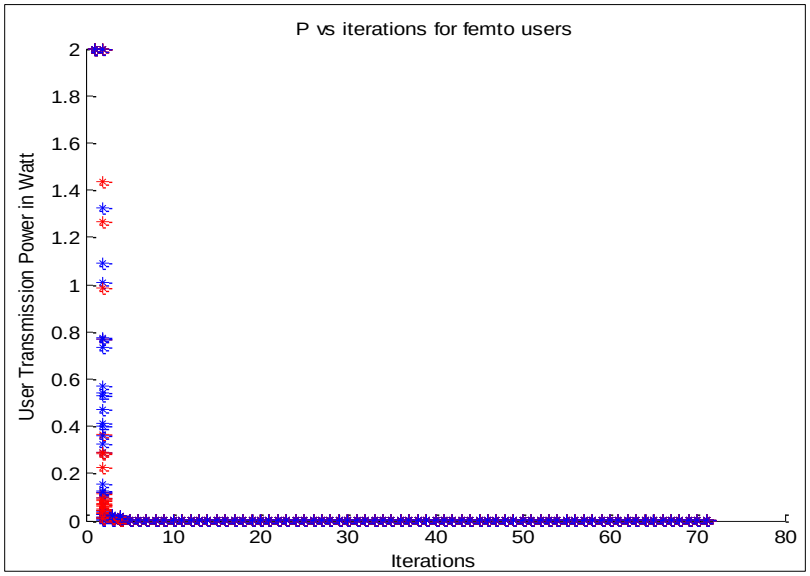

Figure 64: Convergence of the femto-users' powers for the 1st simulation

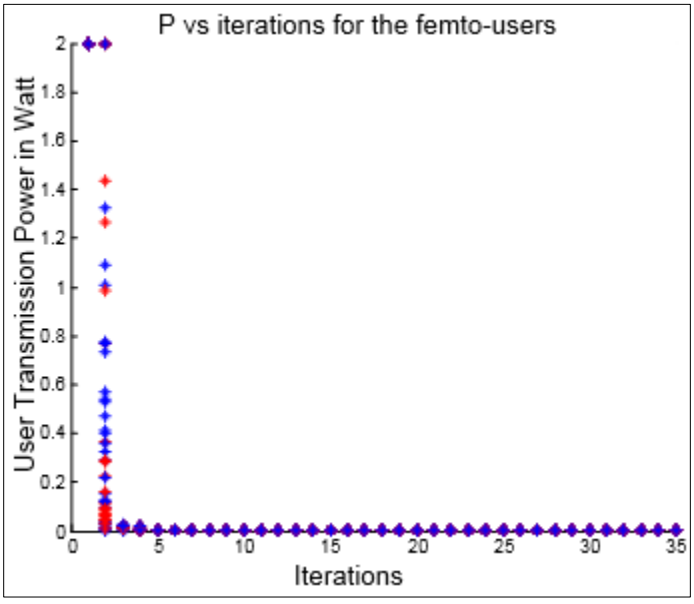

Figure 65: Convergence of the femto-users' powers for the 2nd simulation

Continuing, in Figure 66 we can see the *NE* powers of the 10 macro-users, before and after the deployment of the 31st FAP in the position $(975, 500)$, which "claimed" two of these macro-users as its own. Note that the distances of the linear placed macro-users from the MBS (the x–axis in the following diagrams) are: 150, 200, 250, 300, 325, 350, 375, 400, 450 and 500 meters respectively (see Figure 60). We observe that the transmission powers of the macro-users are reduced almost in half, since the co-tier interference is decreased by changing the number of macro-users from 10 to 8 (the cross-tier interference produced by the femto-users is negligible and note that it is the same in both simulations since the network topology does not change considerably). The last two macro-users which are the more distant from the MBS, have the largest transmission power levels during the 1st simulation whereas when they become the femto-users of the 31st FAP they transmit with minimum power values (which is also reflected from the huge increase in their utility in Figure 67). So, every macro-user's utility doubles (at least) because of the decrease in transmission power in the 2nd simulation, as it is shown in Figure 67. Note that this increase in utility is mainly due to the smaller transmission power and not because of the increased achieved throughput, which as we can see from Figure 68, does not change considerably with the addition of the 31st FAP (the 8 macro-users already had a satisfactory QoS). Only the NRT macro-user that becomes a femto-user in the second stage of the simulation shows a substantial increase in the throughput achieved, in particular from 0.5 Mbps to 1.9 Mbps. Finally, the voice macro-users transmitted with 54 Kbps at first (the minimum acceptable data rate) and with the utilization of the new FAP they reached the target throughput, which is 64 Kbps.

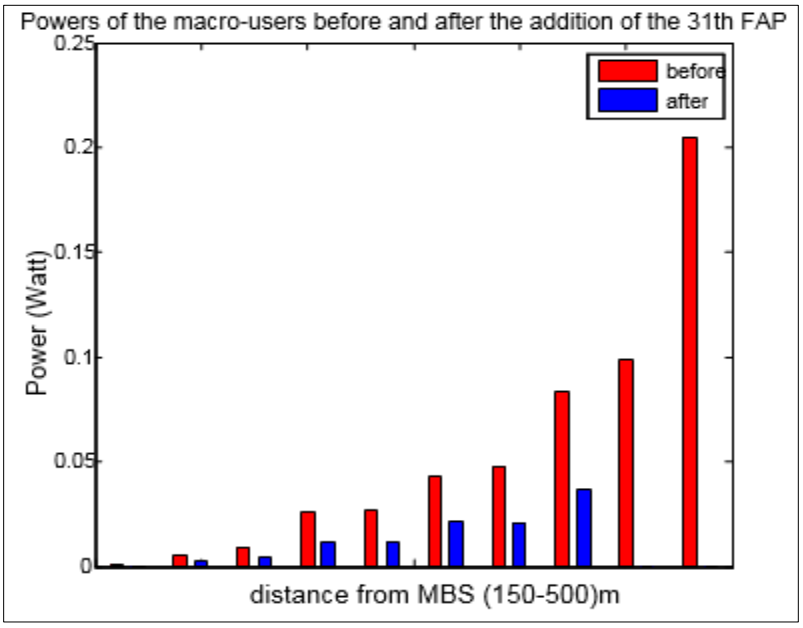

Figure 66: Macro-users' powers before and after the deployment of the 31st FAP with respect to the distance from the MBS

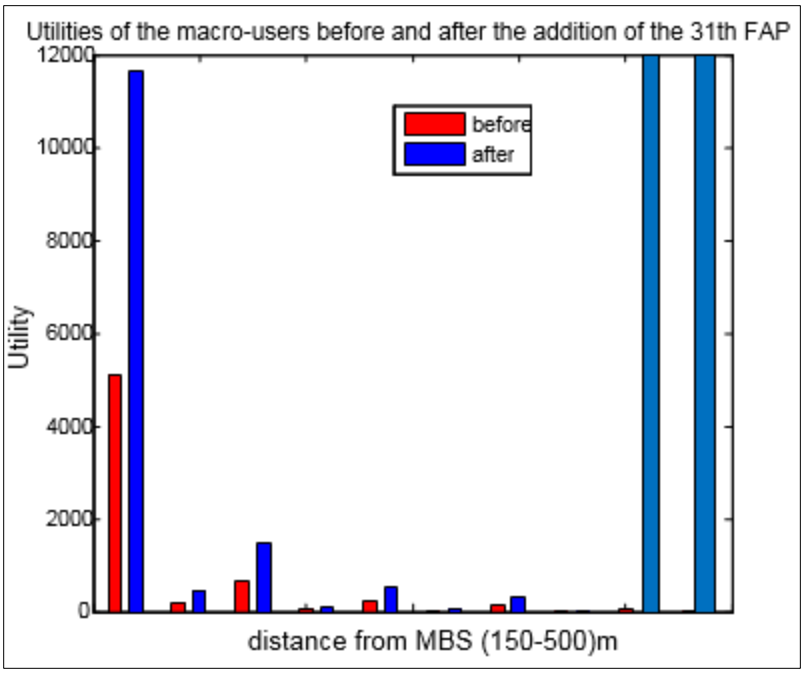

Figure 67: Macro-users' Utilities before and after the deployment of the 31st FAP with respect to the distance from the MBS

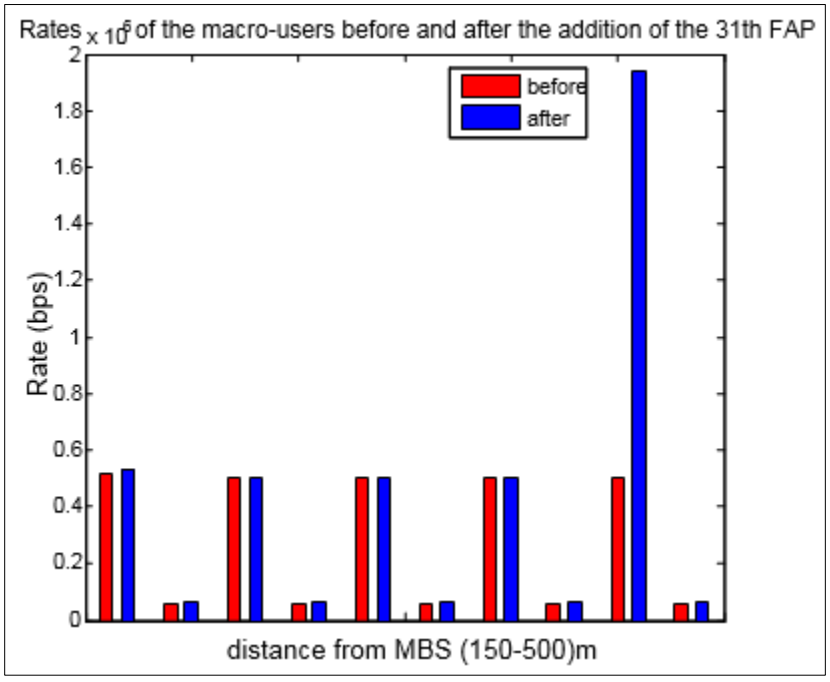

Figure 68: Macro-users' throughput before and after the deployment of the 31st FAP with respect to the distance from the MBS

Concluding, the convergence of the users' powers to the equilibrium optimal values is closely related to the distance from their respective base stations (MBS, FAPs). Consequently, when executing the MTTPG algorithm in a Two-Tier femtocell network, the first users for whom the power will reach its equilibrium state are the femto-users since they are generally closer to their base stations (FAPs) in comparison to the other users. Then, the macro-users' power convergence will follow, in the order of their respective distances from the MBS (i.e. the closer the macro-user is to the MBS, the fewer repetitions are needed by the algorithm to reach its *NE* power).

Furthermore, as it was observed in the above results, a key factor that affects the convergence speed of the MTTPG algorithm is the number of macro-users in the network: more macro-users will result in longer running time for the algorithm to find the *NE* power vector. Lastly, this scenario provided another advantage for the adoption of an open or hybrid access policy to the network's femtocells: such a policy, not only contributes to the decongestion of the macrocell (see Scenario 4), but it also results in the faster convergence of the users' powers to the *NE* vector (since the macro-users are reduced by transmitting to the closer femtocell stations) which in turn translates to less required computational power by the user's device for the execution of the proposed distributed algorithm in each time slot and thus to increased battery life of the user's mobile phone.

5. Conclusions and future work

In this chapter, we firstly present the most important results from this thesis – which were analyzed extensively in the previous section – and we conclude by proposing some directions for further research on the subject at hand.

5.1 Conclusions

1. The use of knowledge from Game Theory (Utility function, Nash Equilibrium) was crucial for the solution of the main problem presented in this thesis – which was the maximization of the network users' utilities. The use of Economics Theory to tackle optimization problems in the theory of Wireless Networks is not new, since it offers flexibility, generalization, solving methods and other useful tools that help us prove lemmas and theorems which would be extremely difficult to prove otherwise, e.g. with the use of other (mathematical) theories that do not have all the properties listed above or are not suitable enough to solve similar optimization problems.
2. Through our simulations in Scenario 4, we showed that the use of femtocells has a positive effect in the system's performance. As it was observed, with the use of FAPs, the total network user utility increases since the femtocells can give their resources to nearby macro-users and thus contribute to the decongestion of the macrocell. This results in better quality of service (QoS) for all the users of the cellular network and consequently, to an increase of the total utility. Similar results were found for the average throughput achieved per user, while the average power decreases to minimum levels when the users transmit to the nearby femtocell base stations.
3. Through our simulations in Scenario 2, we showed the importance of the use of a pricing policy for the femto-users in order to protect and ensure the macro-users' QoS (which are the main users of the radio spectrum) and to allocate as best as possible the network's resources to its users. The users' power, which is one of the most important resources of the network, should be efficiently allocated and the use of a pricing scheme helps in that direction, since it lessens the cross-tier interference towards the macro-users and it also increases the utility of all the users – making thus the system more efficient. Looking back at the results of Scenario 2, we note the negative impact that the absence of a pricing mechanism for the femto-users has on the macro-users' performance.

4. Regarding the design of a Two-Tier Cellular Network, using the results from the scenarios 2 and 3, we propose (considering a radius of $R_c = 500m$ for the macrocell and $R_f = 50m$ for the femtocells, as well as a closed access policy to the FAPs) a network topology consisting of no more than 40-50 FAPs – randomly placed inside the macrocell – and 12-15 macro-users (which can be anywhere inside the macrocell but their position must be fixed since the mobility of the users is not considered in this thesis), with the macro-users staying far away from the FAPs to avoid creating interference problems. Given such a network topology within our system model, all the users of the network (regardless of the type of service they want to satisfy – voice or data services) will achieve a satisfactory QoS which translates to at least 54 Kbps for the RT users and to 0.5 Mbps for the NRT users, while transmitting with low enough power values – with respect to their distance from the base station they transmit to.
5. The reason why it is not desirable to have a macro-user near a femtocell base station in the previously proposed network design is the huge cross-tier interference that the macro-user causes to the femto-users of that particular FAP, resulting in the rapid drop of their quality of service (see Scenario 1). Consequently, in the uplink case, the adoption of a closed access policy to the femtocells (meaning that only their respective subscribers can use their resources) would bring catastrophic results to the femto-users' QoS in a situation where a macro-user is transmitting very close to their FAP (e.g. consider the case where the macro-user is inside a building and there is an apartment with a FAP deployed near him). It is therefore critical to jointly examine in such a Two-Tier Cellular Network the resource allocation mechanisms that help users maximize their utility as well as the call admission control policies.
6. Finally, the results of the simulations of the 5th Scenario gave helpful insights regarding the power control algorithm's behavior in the network under consideration as well as the factors that affect this behavior. Specifically, the most crucial factor is the user's distance from its respective base station: a shorter distance translates to faster convergence to the *NE* power and that's why the femto-users are the first for whom we find the equilibrium power values in our simulations. Furthermore, the number of macro-users in the network is also a key factor since the more they are, the longer it will take for the proposed algorithm to converge and finish its execution.

5.2 Directions for further research

1. **Downlink Case:** This thesis was focused on the study of power control in the uplink scenario, while it is also possible (with the use of appropriate utility functions) to analyze the downlink of a Two-Tier Cellular Network.
2. **User Mobility:** In this thesis, we assumed that all the users had fixed positions during the execution of the power control scheme that was implemented. If the users were mobile, we could study issues regarding handovers or generally how a power control algorithm could be realized when the network users constantly change positions or the base stations they transmit to.
3. **The use of another access policy:** In this thesis, we adopted a closed access policy in femtocells, which has several drawbacks as we verified from our simulations. So, it would be interesting to combine our previous study methodology with an open or hybrid access policy, which represents a more balanced solution between managing interference and system performance.
4. **The use of another spectrum assignment policy:** The thesis's system model included a shared spectrum policy in which the macrocell shared the same bandwidth with the femtocells. It would be interesting to study a different spectrum assignment policy, e.g. the partially shared spectrum, where the macrocell has access to all the spectrum while the femtocells operate only on a subset of it. Such a policy would have the advantages discussed in section 1.2.
5. **The use of another pricing function:** The authors of (Tsiropoulou, Katsinis, & Papavassiliou, 2012) have proven that an exponential convex pricing function (such as the one we used in our simulations) results in better system efficiency than a usage-based pricing mechanism that is a linear scheme of the users' transmission power. On the other hand, we have seen a case (Chandrasekhar, Muharemovic, Shen, Andrews, & Gatherer, 2009) where an entirely different pricing function was used, one that takes into account the total interference received by a femtocell from all the network users. In such a case, the femtocells that receive more interference, are priced less. All in all, there exist various pricing policies that could be used in conjunction with the work from this thesis, such as flatrate, access-based, usage-based, priority-based, etc.
6. **A larger CSG:** We could extent the results of this thesis to include cases where the closed subscriber group (CSG) of the femtocells included more than just two femto-users, e.g. four or five femto-users with randomly chosen QoS prerequisites (either voice or data services). It would be interesting to combine this larger subscriber pool with a hybrid access policy in order to study how many more users can a femtocell give access to while guaranteeing their QoS requirements and how much the system's efficiency would improve.

6. References

Abdulrahman, A., & Ahmad, M. A. (2012, March). Interference Management in Femtocells. *Journal of Advanced Computer Science and Technology Research.*

Andrews, J. G., Claussen, H., Dohler, M., Rangan, S., & Reed, M. C. (2012, April). Femtocells: Past, Present, and Future. *IEEE journal on Selected Areas In Communications, 30*(3), pp. 497-508.

Chandrasekhar, V., & Andrews, J. G. (2008, Sempteber). Femtocell Networks: A Survey. *IEEE Communications Magazine*.

Chandrasekhar, V., & Andrews, J. G. (2009, August). Uplink Capacity and Interference Avoidance for Two-Tier Femtocell Networks. *IEEE Transactions on Wireless Communications, 8*(8), 4316-4328.

Chandrasekhar, V., Muharemovic, T., Shen, Z., Andrews, J. G., & Gatherer, A. (2009, July). Power Control in Two-Tier Femtocell Networks. *IEEE Transactions on Wireless Communications, 8*(7), 3498-3509.

Choi, D., Monajemi, P., Kang, S., & Villasenor, J. (2008). Dealing with loud neighbors: the benefits and tradeoffs of adaptive femtocell access. *IEEE Global Telecommunications Conference*, (pp. 1-5).

D. T. Ngo, D. T., Le, L. B., Le-Ngoc, T., Hossain, E., & Kim, D. I. (2012, March). Distributed interference management in femtocell networks. *IEEE Trans. Wireless Communications, 11*(3), 979–989.

Goffman, C. (1971). *The Calculus: An Introduction.* . Harper & Row.

Jin, M. S., Chae, S. A., & Kim, D. I. (2011). Per Cluster Based Opportunistic Power Control for Heterogeneous Networks. *Vehicular Technology Conference (VTC Spring)* (pp. 1-5). IEEE.

Jo, H. S., C. Mun, C., Moon, J., & Yook, J. G. (2009, October). Interference mitigation using uplink power control for two-tier femtocell networks. *IEEE Transactions on Wireless Communications, 8*(10), 4906-4910.

Mesodiakaki, A. I. (2011). *Service-oriented utility-based uplink power control in two-tier femtocells networks.*

Ngo, D. T., Le, L. B., & Le-Ngoc, T. (2012, October). Distributed Pareto-Optimal Power Control for Utility Maximization in Femtocell Networks. *IEEE Transactions on Wireless Communications, 11*(10), pp. 3434-3446.

Roche, G., Valcarce, A., Lopez-Perez, D., & Zhang, J. (2010, January). Access Control Mechanisms for Femtocells. *IEEE Communications Magazine, 48*(1), pp. 33-39.

Rodriguez, V. (2003). An analytical foundation for resource management in wireless communication. *GLOBECOM '03, 2*, pp. 898-902.

Saraydar, C. U., Mandayam, N. B., & Goodman, D. J. (2002, February). Efficient power control via pricing in wireless data networks. *IEEE Transactions on Communications, 50*, 291–303.

Ta-Sung, L., & Wei-Sheng, L. (2012, May). A Distributed Cluster-Based Self-Organizing Approach to Resource Allocation in Femtocell Networks. *Vehicular Technology Conference (VTC Spring)* (pp. 1-5). IEEE.

Tsiropoulou, E. E., Kastrinogiannis, T., & Papavassiliou, S. (2009, October). QoS-Driven Uplink Power Control in Multi-Service CDMA Wireless Networks - A Game Theoretic Framework. *J. Comm., 4*(9), 654-668.

Tsiropoulou, E. E., Katsinis, G. K., & Papavassiliou, S. (2012, January). Distributed Uplink Power Control in Multiservice Wireless Networks via a Game Theoretic Approach with Convex Pricing. *IEEE Trans. on Parallel and Distributed Systems, 23*(1).

Xin, K., Liang, Y.-C., & Garg, H. K. (2011). Distributed Power Control for Spectrum-Sharing Femtocell Networks Using Stackelberg Game. *IEEE International Conference in Communications (ICC)*, (pp. 1-5).

Yates, R. D. (1995). A framework for uplink power control in cellular radio systems. *IEEE Journal on Selected Areas in Communications, 13*, 1341–1347.